Ecology of a polymetallic nodule occurrence gradient: implications for deep-sea mining

Abstract:	Abyssal polymetallic nodule fields constitute an unusual deep-sea habitat. The mix of soft sediment and the hard substratum provided by nodules increases the complexity of these environments. Hard substrata typically support a very distinct fauna to that of seabed sediments, and its presence can play a major role in the structuring of benthic assemblages. We assessed the influence of seafloor nodule cover on the megabenthic ecology of a marine conservation area (Area of Particular Environmental Interest 6, APEI6) in the Clarion Clipperton Zone (3950-4250 m water depth) using extensive photographic surveys from an autonomous underwater vehicle. Variations in nodule cover (1-20%) appeared to exert statistically significant differences in faunal standing stocks, some biological diversity attributes, faunal composition, functional group composition, and the distribution of individual species along the nodule cover gradient. The standing stock of both the metazoan fauna and the giant protists (xenophyophores) doubled with a very modest initial increase in nodule cover (from 1 to 3%). Notably, faunal density determined by sample-based rarefaction, was positively correlated with nodule cover, while taxon richness, determined by individual-based rarefaction, was invariant (c. 60 taxa among 500 individuals). Faunal composition varied continuously along the nodule cover gradient. We discuss these results in the context of potential seabed-mining operations and the associated sustainable management and conservation plans. We note in particular that successful conservation actions will likely require the preservation of areas comprising the full range of nodule cover and not just the low cover areas that are least attractive to mining.

1   **Ecology of a polymetallic nodule occurrence gradient: implications**

2   **for deep-sea mining**

3   Erik Simon-Lledó[1, 2], Timm Schoening[3], Noelie M.A. Benoist[1,2], Brian J. Bett[1], Veerle A. I.

4   Huvenne[1], Daniel O. B. Jones[1]

5

6   [1] National Oceanography Centre, University of Southampton Waterfront Campus, European Way,

7   Southampton, UK

8   [2] Ocean and Earth Science, University of Southampton, National Oceanography Centre,

9   University of Southampton Waterfront   Campus, European Way, Southampton, UK

10   [3] GEOMAR Helmholtz Centre for Ocean Research, Wischhofstraße 1-3, Kiel, Germany

11

12

14

15

16

17

18

19

20

21

1

Abstract

Abyssal polymetallic nodule fields constitute an unusual deep-sea habitat. The mix of soft

sediment and the hard substratum provided by nodules increases the complexity of these

environments. Hard substrata typically support a very distinct fauna to that of seabed sediments,

and its presence can play a major role in the structuring of benthic assemblages. We assessed the

influence of seafloor nodule cover on the megabenthic ecology of a marine conservation area

(Area of Particular Environmental Interest 6, APEI6) in the Clarion Clipperton Zone (3950-4250

m water depth) using extensive photographic surveys from an autonomous underwater vehicle.

Variations in nodule cover (1-20%) appeared to exert statistically significant differences in faunal

standing stocks, some biological diversity attributes, faunal composition, functional group

composition, and the distribution of individual species along the nodule cover gradient. The

standing stock of both the metazoan fauna and the giant protists (xenophyophores) doubled with a

very modest initial increase in nodule cover (from 1 to 3%). Notably, faunal density determined

by sample-based rarefaction, was positively correlated with nodule cover, while taxon richness,

determined by individual-based rarefaction, was invariant (c. 60 taxa among 500 individuals).

Faunal composition varied continuously along the nodule cover gradient. We discuss these results

in the context of potential seabed-mining operations and the associated sustainable management

and conservation plans. We note in particular that successful conservation actions will likely

require the preservation of areas comprising the full range of nodule cover and not just the low

cover areas that are least attractive to mining.

Introduction

44

45   Abyssal polymetallic nodule fields represent a unique deep-sea habitat (Radziejewska

46   2014). The hard substratum provided by the nodules combined with the background soft sediment

47   seabed acts to increase habitat complexity, and is thought to promote the occurrence of some of

48   the most biologically diverse seafloor assemblages in the abyss (Amon et al. 2016, Gooday et al.

49   2017). This unusual and diverse habitat is potentially subject to imminent large-scale human

50   impacts in the form of seafloor mining (Gollner et al. 2017, Kuhn et al. 2017). Mining

51   disturbances are likely to extend over extremely large seafloor areas (Aleynik et al. 2017) and

52   have a clear potential to drive major changes in the resident fauna (Jones et al. 2017). Predicting

53   the nature of such changes remains difficult; the ecology of this remote habitat is poorly

54   understood, in particular, very little is known of the biodiversity associated with nodules

55   (Veillette et al. 2007, Vanreusel et al. 2016).

56   The presence of hard substratum is thought to be a key factor in structuring heterogeneous

57   deep-sea habitats (Buhl-Mortensen et al. 2010, Bell et al. 2016). For example, modest variations

58   in the availability and the composition of hard surfaces can influence the larval settlement

59   processes of the seafloor fauna (Van Dover et al. 1988, Roberts et al. 2006). Substratum

60   selectivity is commonly exhibited by many deep-sea species, including soft corals (Sun et al.

61   2011), sponges (Lim et al. 2017), and foraminifera (Gooday et al. 2015). The presence and extent

62   of hard substratum is therefore expected to exert a significant control on the composition of deep-

63   sea benthic assemblages (Levin et al. 2001, Smith and Demopoulos 2003). Seafloor environments

64   in the deep sea with extensive hard substratum range in nature from landscape-scale features such

65   as seamounts (Clark et al. 2010) and canyons (De Leo et al. 2010), to widely dispersed pebbles,

66   cobbles, and boulders referred to as iceberg drop-stones (Meyer et al. 2016), and the similar

67   human artefact habitat produced by steamship clinker (Ramirez-Llodra et al. 2011). While

68   individual polymetallic nodules are generally small, 1-20 cm in diameter, nodule fields can

69   extend over extremely large areas, many hundreds of km^2, as occurs in the Clarion Clipperton

70   Zone (CCZ) of the central Pacific Ocean (Kuhn et al. 2017).

71   Polymetallic nodules in the CCZ are thought to support a specialised fauna that differs

72   from that of nodule-free sediment areas (Thiel et al. 1993, Gooday et al. 2015). Nodule-dwelling

73   meiofauna such as nematodes, tardigrades, harpacticoids, and foraminifera inhabit the crevices

74   (Veillette et al. 2007, Miljutina et al. 2010), while sessile macro- and megafauna such as

75   polychaetes, sponges, cnidarians and xenophyophores are commonly found attached to nodule

76   surfaces (Gooday et al. 2015, Amon et al. 2016). Consequently, nodule occurrence has been

77   linked with variations in faunal standing stocks and distributions (Amon et al. 2016, Vanreusel et

78   al. 2016). However, logistic constrains have limited the detailed monitoring of nodule cover

79   (Vanreusel et al. 2016, Tilot et al. 2018), restricting the assessment of seafloor ecology along

80   nodule occurrence gradients.

81   Recent advances in large-scale seafloor visual imaging (Durden et al. 2016), coupled with

82   automated nodule-detection algorithms (Schoening et al. 2016, Schoening et al. 2017) now make

83   such studies possible. Here, we combine extensive nodule coverage and faunal data obtained by

84   photography from an autonomous underwater vehicle (AUV) to examine the effect of nodule

85   occurrence on the ecology of megafauna in the CCZ. We include protozoan, invertebrate, and

86   fish species that can be distinguished in photographs, having body length-scales > 1 cm, as

87   members of the megafauna. In particular, we consider variations in their standing stock,

88   biological diversity, and faunal composition along a nodule cover gradient. This work is carried

89   out within an 'Area of Particular Environmental Interest' (APEI), a form of marine protected area

90   designed as a conservation measure in response to potential future seabed mining in the region

91   (ISA 2012). Consequently, we also cast our results in the context of the sustainable management

92   and conservation of this unusual abyssal habitat.

93

94   4

Methods

Study area

Our initial study area was a 5500 km^2 rectangular region of seafloor centred on 122° 55'

W 17° 16' N within the APEI6 region (Fig. 1). This location was selected to have similar

topographic relief to mining contract areas in the central CCZ. Water depth ranged 3950-4250 m,

and the seafloor landscape comprised a succession of crenulated ridges and shallow troughs

oriented north-south between dispersed level-bottom (<3° slope) areas. General seafloor

conditions were described by Simon-Lledo et al. (submitted) and are only briefly summarised

here. Surface sediments (0-1 cm) were homogenous across the study area, dominated by very fine

silt and clay particles (58-68% <7.8 μm diameter), and having a very low content of total organic

carbon (TOC, 0.44 ± SD 0.05 %). The polymetallic nodules present were of a flattened,

ellipsoidal form with smooth surfaces. The seafloor exposed mean individual nodule area was 2.5

cm^2, with most nodules <5 cm^2 (90%), and very few >10 cm^2 (1%). In individual seafloor

photographs, average nodule cover was 6.4% and ranged from nodule-free to 37%. Nodule cover

was patchy, with extremes of variation occurring at metre-scales (Fig. 1). All results reported

here were acquired April-May 2015, during RRS *James Cook* cruise JC120; additional

supporting technical detail is provided by Jones (2015).

Data collection and processing

Seafloor images were collected using a digital camera (FLIR Integrated Imaging

Solutions Inc. *Grasshopper2*; 2448 x 2048 pixels) mounted vertically beneath the AUV

Autosub6000 (Morris et al. 2014). The AUV was programmed for a target altitude of 3 m above

the seafloor, a speed of 1.2 m s^{-1}, and a photographic interval of 850 milliseconds. At the target

altitude, individual vertical photographs imaged 1.71 m^2 of seabed. Three landscape types (Ridge,

Flat, and Trough), delimited by objective analysis of bathymetric data, were surveyed using zig-

120   zag designs with random start points (Strindberg and Buckland 2004) as detailed by Simon-Lledó

121   et al. (submitted). A total of 40 individual image transects were surveyed in each landscape-type.

122   Images taken as the vehicle changed course, i.e. junctions between transects, were removed. In

123   the remaining straight-line sections, every second image was removed to avoid overlap between

124   consecutive images and to prevent double counting. To ensure consistency in specimen and

125   nodule detection, images outside the altitude range 2-4 m were also removed. Four transects were

126   randomly selected from each landscape-type for subsequent analysis. The full resultant dataset

127   was composed of data from 10052 non-overlapping images, representing a seafloor area of 18580

128   m^2.

129   All images were colour corrected, as described by Morris et al. (2014), before manual and

130   automated analyses were performed to obtain biological and environmental data. Nodule cover

131   (%) was quantified using the Compact-Morphology-based poly-metallic Nodule Delineation

132   method (CoMoNoD, Schoening et al. 2017). The CoMoNoD algorithm calculates the size of each

133   nodule (i.e. seafloor exposed area size) detected in an image, enabling the calculation of

134   descriptive nodule statistics. Megafauna specimens were identified to the lowest taxonomic level

135   possible, and their physical dimension measured, using BIIGLE 2.0 (Langenkämper et al. 2017).

136   Each specimen was assigned to a 'nodule-attached' (NA) or 'nodule-free-living' (NFL) life-habit

137   category. The biovolume of individual metazoan specimen was estimated as a proxy for biomass,

138   using the generalised volumetric method described by Benoist et al. (submitted).

139   To ensure consistency in specimen identification, a CCZ-standardised megafauna

140   morphospecies catalogue was developed upon the taxonomic compilation developed by the

141   International Seabed Authority (available online: http://ccfzatlas.com), which we further

142   expanded in consultation with international taxonomic experts and by reference to existing

143   literature (Dahlgren et al. 2016, Glover et al. 2016, Amon et al. 2017, Kersken et al. 2018). The

144   likely feeding behaviour of each morphospecies was inferred from similar organisms described in

145 the literature (Iken et al. 2001). The full dataset comprised 7837 metazoan specimens across 133

146 morphospecies, and 47133 giant foraminifera (xenophyophores) specimens across 22

147 morphospecies.

148

149 **Data analysis**

150 To perform an initial broad assessment of the potential influence of seafloor nodule cover on the

151 ecological characteristics of the megafauna, all images from the three landscape types were

152 pooled. This total image set was ordered by estimated nodule cover, and then divided into ten

153 subsets at nodule-cover breakpoints chosen to yield approximately equal numbers of megafaunal

154 observations in each image subset. Metazoan and xenophyophore data were processed separately

155 on the basis that it was not possible to determine whether the latter were living from the images

156 (Hughes and Gooday 2004). Across the ten resultant nodule-cover classes, metazoan megafauna

157 counts ranged 784-787, and xenophyophore counts 4714-4719. To establish measures of

158 variability in ecological characteristics within the nodule-cover classes, the corresponding image

159 subsets were resampled using a modified form of bootstrapping (Davison and Hinkley 1997).

160 Each image subset was randomly resampled with replacement until a minimum of 500 specimens

161 were encountered, and that process was repeated 1000 times for each nodule-cover class. This

162 resampling process yielded bootstrap-like samples that ranged in metazoan specimen counts 500-

163 565, and xenophyophore counts 500-587. We adopted these specimen-count based methods to

164 recognise and control the impact of specimen number on the estimation of biological diversity

165 and faunal composition parameters (Sanders 1968, Forcino et al. 2015, Simon-Lledo et al.

166 submitted).

167 A range of ecological parameters was calculated for each of the 10×1000 bootstrap-like

168 samples, including metazoan and xenophyophore numerical density (ind m^{-2}) and metazoan

169 biovolume density (ml m^{-2} ≈ g fresh wet weight m^{-2}). To examine the range of diversity

170 characteristics, Hill's diversity numbers of order 0, 1, and 2 (Jost 2006) were calculated as

171 metazoan morphospecies richness (S_N), the exponential form of the Shannon index (Exp H'), and

172 the inverse form of Simpson's index (1/D). We also calculated morphospecies density (S_A),

173 based on an additional set of bootstrap-like samples generated following the same procedure, but

174 with a controlled minimum seabed area encompassed by each sample, that was set to the smallest

175 seabed area (c. >700 m^2) obtained in the specimen-controlled set of bootstrap-like samples used

176 to calculate the rest of parameters. Variation in metazoan community composition was assessed

177 by 2d non-metric multidimensional scaling (nMDS) ordination of all 10000 bootstrap-like

178 samples, based on square-root transformed faunal density and use of the Bray-Curtis dissimilarity

179 measure (Clarke 1993). The resultant dimension 1 scores (MDS-d1) were used as a univariate

180 measure of faunal composition.

181   Mean (median in the case of biovolume assessment) values of these various parameters

182 were calculated from each bootstrap-like sample set, together with corresponding 95 %

183 confidence intervals based on the simple percentile method (Davison and Hinkley 1997). Data

184 processing and analyses described above were performed using a custom R (R Core Team, 2014)

185 script incorporating multiple functions of the 'vegan' package (Oksanen et al. 2018).

186   In addition to the general analyses of ecological responses to the nodule cover gradient,

187 we considered landscape-type-related variations in those responses by undertaking a separate

188 analysis within each landscape-type. This material is provided in Appendix 1.

189

190

191 **Results**

192 **Standing stocks**

193   Metazoan and xenophyophore density were significantly and substantially lower in the

194 lowest nodule-cover class (Fig. 2a). We found no significant correlation between density and

195 nodule availability (Table 1); density variation of both groups across the nodule gradient

196 described a rapid asymptote, stabilising in cover levels >2-3%. In contrast, metazoan biomass

197 density showed a high dispersion rate and no significant variations along the nodule cover

198 gradient (Fig. 2a).

199 **Biological diversity**

200   Diversity measures calculated with controlled number of individuals exhibited no

201 significant correlation with nodule cover (Table 1). Morphospecies richness (S_N) was near

202 constant across nodule-cover classes with no indication of any significant difference between any

203 pair of classes (Fig 2b). Exp *H'* was more variable across classes, but exhibited no coherent

204 substantive change across the nodule gradient. In contrast, 1/D showed a significantly lower

205 value in the lowest nodule class. On the other hand, morphospecies density (S_A; calculated with

206 controlled seabed area) was significantly correlated with nodule cover (Table 1). S_A was

207 consistently lower than S_N across the nodule gradient, though marginally (confidence intervals

208 overlapped), except in the lowest nodule class, where S_A was significantly and substantially

209 lower than S_N.

210 **Faunal composition**

211 **Assemblage**

212   Two-dimensional MDS ordination of bootstrap-like samples showed that metazoan

213 assemblages progressively differed across the nodule gradient (Fig. 3a); the lowest and the

214 highest nodule-cover classes yield the largest dissimilarity rates. MDS-d1 was strongly and

215 significantly correlated with nodule cover (Table 1). MDS-d1 score in the lowest nodule class

216 was substantially and significantly different from all other cover classes (Fig. 3b).

217 **Functional groups**

218   Neither nodule-attached (NA) nor nodule-free-living (NFL) faunal density was

219 significantly correlated with nodule cover (Table 1). However, in both cases density in the lowest

220 nodule-cover class was significantly lower than in any other class (Fig. 4a). Both deposit-feeder

221 and suspension-feeder faunal density was significantly and substantially lower in the lowest

222 nodule-cover class, while predator and scavenger density showed no significant variations across

223 the nodule cover gradient (Appendix 2; Fig. B1). Variation in suspension and deposit-feeder

224 density across the nodule gradient described a rapid asymptote, yet none of the three functional

225 groups densities exhibited a significant correlation with nodule cover (Appendix 2; Table B1).

226 **Taxonomic groups**

227   Among the 15 most abundant morphospecies (Appendix 2: Fig B3) a graded series of

228 distributions across nodule-cover classes was apparent (Appendix 2: Fig B4; Table B1). For

229 example (Fig. 4b): (i) negative monotonic, Porifera msp-5, strong and statistically significant

230 correlation with nodule cover (Table 1); (ii) unimodal, *C.* cf *bayeri*, statistically significant

231 difference between tails (classes 1, 8-10) and centre (classes 2-6) of the distribution; (iii) positive

232 unimodal, *Lepidisis* msp, strong and statistically significant correlation with nodule cover (Table

233 1). The density of Polychaete msp-5 and Actinia msp-18 was significantly and substantially lower

234 in the lowest nodule-cover class, while density of *Ophiosphalma* sp., Columnella msp, and

235 Irregularia msp-1 was also lower in the lowest nodule-cover class, though marginally (Appendix

236 2: Fig B4). Among major taxa levels (i.e. most dominant phyla) a graded series of distributions

237 across nodule-cover classes was also apparent (Appendix 2: Fig B2 and Table B1).

238

10

Discussion

We found substantial and statistically significant variations in megafaunal standing stock,

biological diversity, and faunal composition along a gradient of seafloor nodule cover. These

responses were generally graded with nodule cover. However, in many cases the magnitude of

change between the first two cover classes was particularly marked. Both of these observations

are of direct relevance to sustainable management and conservation concerns in relation to seabed

mining in the CCZ and similar environments elsewhere.

Standings stocks

Differences in metazoan density across the nodule cover gradient were predominately

driven by variations in suspension feeder abundance, particularly anthozoans living attached to

nodules; the abundance of which was substantially and statistically significantly reduced in the

lowest nodule class (Appendix 2: Fig. B1; Fig. B2b). Hard substrata provide a stable anchor point

for suspension feeders and enable the placement of food-catching structures into faster off-bottom

currents (Wildish and Kristmanson 2005). Enhanced densities of hard substratum attached fauna

has been observed on bedrock in seamounts or canyons (Clark et al. 2010, Baker et al. 2012,

Jones et al. 2013), in areas with drop-stones (Jones et al. 2007, Meyer et al. 2016), and in

polymetallic nodule fields (Amon et al. 2016, Vanreusel et al. 2016). Our results provide

additional detail that suggests a non-linear, asymptotic relationship between standing stock and

nodule cover (Fig. 2a). This response may be simply explained by resource limitation (Tilman

1982), i.e. hard substratum is initially limiting, but food resource (i.e. advecting organic particles)

becomes limiting as attached suspension feeder density increases (Jeffreys et al. 2009). Variation

in suspension-feeder density at the landscape-type scale sustains this hypothesis and suggest that

the transition between limiting resources (i.e. from nodules to food) occurs at nodule cover > 2-

3% (Fig. 5a).

264   Xenophyophore density showed a rapid asymptotic relationship with nodule cover in the

265   broad assessment but a different pattern in each area when investigated at the landscape-type

266   level, with a clearly higher abundance in the Ridge (Fig. 5b). Other studies have documented

267   enhanced xenophyophore density on elevated terrain, e.g. seamounts (Levin and Thomas 1988,

268   Wishner et al. 1990) and abyssal hills (Stefanoudis et al. 2016), and their dominance in the

269   megafauna and high taxonomic diversity in the CCZ (Amon et al. 2016, Gooday et al. 2017).

270   Although sediment-dwelling species are well-known, nodules clearly represent a very important

271   habitat for xenophyophores (Gooday et al. 2015, Kamenskaya et al. 2015). While the specific

272   feeding modes of xenophyophores remain uncertain (Gooday et al. 1993, Laureillard et al. 2004),

273   the nodule-attached forms are most likely suspension feeders, and the sediment-dwellers most

274   likely deposit feeders (Gooday et al. 2017). Yet our results suggest that, although nodule resource

275   may limit the development of a part of the xenophyophore fraction (i.e. suspension feeder forms),

276   geomorphological variations are a stronger control on the overall xenophyophore standing stock.

277

Biological diversity

279   Variation between morphospecies richness and morphospecies density was evident in the lowest

280   nodule class (Fig. 2b), suggesting either a lower faunal density and/or a lower evenness between

281   taxa abundances where nodule resource is limiting, yet no reduced taxa richness, as previous

282   CCZ megafauna assessments suggested (Amon et al. 2016, Vanreusel et al. 2016, Tilot et al.

283   2018). However, previous studies typically used fixed-area samples, in fact reporting taxa

284   density. For instance, Tilot et al. (2018) compared richness between areas with varying nodule

285   abundance based on subsample units with fixed seabed areal cover, yet ranging in size from ~150

286   to ~450 individuals, which possibly generated strong biases in richness estimations as these are

287   highly sensitive to the number of individuals surveyed (Gotelli and Colwell 2001). Distinction

288   between morphospecies richness and density becomes particularly relevant in the assessment of

289 nodule-field communities, as the lower megafaunal density characteristic of areas with low

290 nodule cover can lead to the underestimation of taxonomic richness. In turn, if richness appears to

291 be essentially invariant with respect to nodule cover, indices more sensitive to the variation in

292 taxa evenness (i.e. heterogeneity diversity) may consequently be more appropriate monitoring

293 targets.

294 Heterogeneity diversity measures indicated a clearly reduced diversity in the lowest nodule class,

295 markedly so in the case of 1/D index (Fig. 2b). Our results concur with Amon et al. (2016) that

296 nodule availability does not need to be high to promote higher megafauna diversity (although not

297 necessarily richness), and with Vanreusel et al. (2016) that suspension feeder abundance

298 distribution appears to lead (most) of this variation. Lower diversity in the lowest nodule class

299 was predominantly generated by two combined factors: (i) general reduction in the abundance of

300 almost all suspension feeder taxa, and (ii) extremely high numerical dominance of one taxon

301 (Porifera msp-5), possibly better adapted to the environmental conditions in the lowest nodule

302 class. On the other hand, landscape-type level analyses showed a clearly higher diversity in the

303 Ridge compared to the Trough in areas with low nodule cover (2-3%; Appendix 1: Fig. A2e-f),

304 possibly resulting from a more balanced taxa evenness, generated by the higher deposit feeder

305 taxa abundance within the Ridge (Simon-Lledo et al. submitted). Structurally more complex

306 habitats can provide a wider range of niches and diverse ways of exploiting the environmental

307 resources, promoting species coexistence in the deep-sea benthos (Levin et al. 2001). Hence, our

308 results suggest that nodules may act as 'keystone structures' (Tews et al. 2004) in the regulation

309 of habitat complexity at fine scales (tens of meters), while geomorphological variations

310 presumably modulating bottom water flows and deposition patterns (Mewes et al. 2014, Peukert

311 et al. 2018), may play an important role at larger scales (few kilometres) (Simon-Lledó et al.

312 submitted).

313   **Faunal composition**

314   Our data suggest that faunal composition changes continuously with nodule cover across the full

315   spectrum of the gradient studied. The first step on that gradient (from nodule class 1 to 2) was,

316   however, substantially greater than those that followed (Fig. 3). This initial 'jump' is consistent

317   with the change from an overwhelmingly background sedimentary habitat to a mosaic habitat

318   with a varying admixture of nodule hard substrata to that sediment background. A higher

319   dissimilarity of the lowest nodule-class assemblage was somewhat expected, since most of the

320   APEI6 megafaunal community (70% of taxa richness) were nodule-dwelling taxa (Simon-Lledo

321   et al. submitted) with reduced abundance in the lowest nodule class (Appendix B: Fig. B4). These

322   populations may simply not find enough suitable substratum to develop where nodules are

323   limited, as typically occurs in the smaller-sized meio- and macrofaunal communities (Mullineaux

324   1987, Veillette et al. 2007). This first, sharply defined, faunal composition change numerically

325   supports that even subtle increases in nodule availability can drive substantial variations in

326   megafaunal communities (Amon et al. 2016). Yet the following, rather continuous variations,

327   suggest a potential diversification of habitats along the nodule gradient beyond the simple

328   presence or absence of a minimum nodule resource level.

329   We found a clear shift in dominance from sponges (predominantly Porifera msp-5) in the lowest

330   nodule class to cnidarians in the remaining classes, and within the latter, an alternation of

331   dominance between primnoid soft corals, anemones, and bamboo corals with increasing nodule

332   cover. This suggests that other environmental drivers may potentially co-vary along the nodule

333   cover gradient. For instance, nodule size was positively linearly correlated with nodule cover

334   (r_p=0.72, p<0.001), with mean surface areas of nodules found in the lowest cover class (median:

335   1.66 cm^2; IQR: 0.44) being almost half the size of those in areas with the highest coverage

336   (median: 2.87 cm^2; IQR: 0.42). Such comparably larger nodule sizes are commonly found in

337   areas with lower sediment accumulation rates and relatively stronger bottom-current speeds

338   (Skornyakova and Murdmaa 1992, Mewes et al. 2014). Variable development of particular deep-

14

339 sea suspension feeder populations can be regulated by bottom current speeds (Thistle et al. 1985,

340 Smith and Demopoulos 2003), and also by the size of the available hard structures (Meyer et al.

341 2016), especially in soft corals (Watanabe et al. 2009). Areas with larger and hence potentially

342 more physically stable nodules possibly provide a more suitable long-term anchoring point for

343 bamboo coral taxa, enabling their greater final colony height compared to, for example, primnoid

344 soft corals (Lapointe and Watling 2015, Cairns 2016). In turn, the presumably stronger bottom

345 current speeds in areas with large nodule size perhaps limits the development of primnoids,

346 which appear to find a suitable habitat in areas with comparably lower nodule availability (4-6%).

347 Therefore, we hypothesise that factors interrelated with nodule availability, like nodule size or

348 bottom current speeds possibly act as environmental filters, ultimately controlling population

349 recruitment rates.

350

Conclusions

Sustainable management and conservation

353 Our results suggest that areas less likely to be exploited by deep-sea mining (i.e. low to

354 intermediate nodule-cover classes) would not serve the preservation of the full range of taxa that

355 live in polymetallic nodule fields. Although these may act as source populations of taxa that also

356 lives in high nodule abundance areas (i.e. actinians or bryozoans), our results show that these

357 cannot support abundant populations of the fauna found in high nodule cover areas (i.e. bamboo

358 corals). Moreover, the potential deposition of sediment plumes in non-directly exploited areas

359 (Aleynik et al. 2017) may also compromise the preservation of source populations for most

360 suspension feeder taxa (Bluhm 2001), that represent the vast majority of the metazoan standing

361 stock at the CCZ (Amon et al. 2016, Vanreusel et al. 2016), and appear to be the most sensitive

362 fauna to variations in nodule cover (i.e. this study). This suggests that the combined effects of

363 nodule removal and sediment plume deposition are likely to generate biodiversity and standing

364   stock losses at the landscape scale, with the corresponding loss in rate processes and ecosystem

365   services provided by the megafauna.

366   Simplistically, a nodule field could be considered as two habitats: (a) the background sedimentary

367   habitat, and (b) the hard substratum environment of the nodules. More realistically, and certainly

368   at the physical scales inhabited by megafauna, the nodule field is likely better considered as a

369   mosaic habitat comprising those two components. However, our results make clear that the

370   mosaic habitat does not support a single biotope, nor indeed two biotopes; within the limits of the

371   nodule cover gradient that we have been able to study, faunal composition exhibits continuous

372   variation. Equally, it is also clear that we do not yet fully understand the drivers of ecological

373   variation along the nodule cover gradient. Consequently, sustainable management and

374   conservation plans (Levin et al. 2016, Durden et al. 2017), together with the monitoring

375   programmes that support them, must recognise this complexity and uncertainty if they are to be

376   effective.

377   In closing, we should note that our primary analyses have concerned a broad assessment of

378   nodule cover using data drawn from three distinct abyssal landscape types. These landscape-scale

379   variations in environmental and ecological characteristics (Simon-Lledo et al. submitted,

380   Supplementary material Appendix 1) add an additional layer of complexity that can be expected

381   to operate at the physical scale of individual conservation areas (Area of Particular

382   Environmental Interest in the CCZ) and potential mining operation areas.

383

384

385

386

387

Acknowledgements

398

399

400

401

402

403

404

405

406

407

408

409

410

References

Aleynik, D., M. E. Inall, A. Dale, and A. Vink. 2017. Impact of remotely generated eddies on plume dispersion at abyssal mining sites in the Pacific. Scientific Reports **7**:16959.

Amon, D., A. Ziegler, J. Drazen, A. Grischenko, A. Leitner, D. Lindsay, J. Voight, M. Wicksten, C. Young, and C. Smith. 2017. Megafauna of the UKSRL exploration contract area and eastern Clarion-Clipperton Zone in the Pacific Ocean: Annelida, Arthropoda, Bryozoa, Chordata, Ctenophora, Mollusca. Biodiversity Data Journal **5**:e14598.

Amon, D. J., A. F. Ziegler, T. G. Dahlgren, A. G. Glover, A. Goineau, A. J. Gooday, H. Wiklund, and C. R. Smith. 2016. Insights into the abundance and diversity of abyssal megafauna in a polymetallic-nodule region in the eastern Clarion-Clipperton Zone. Sci Rep **6**:30492.

Baker, K. D., V. E. Wareham, P. V. R. Snelgrove, R. L. Haedrich, D. A. Fifield, E. N. Edinger, and K. D. Gilkinson. 2012. Distributional patterns of deep-sea coral assemblages in three submarine canyons off Newfoundland, Canada. Marine Ecology Progress Series **445**:235-249.

Bell, J. B., C. H. S. Alt, and D. O. B. Jones. 2016. Benthic megafauna on steep slopes at the Northern Mid-Atlantic Ridge. Marine Ecology **37**:1290-1302.

Benoist, N. M., B. J. Bett, K. J. Morris, and H. A. Ruhl. submitted. A generalised method to estimate the biomass of photographically surveyed benthic megafauna. Limnology & Oceanography: Methods.

Bluhm, H. 2001. Re-establishment of an abyssal megabenthic community after experimental physical disturbance of the seafloor. Deep Sea Research Part II: Topical Studies in Oceanography **48**:3841-3868.

Buhl-Mortensen, L., A. Vanreusel, A. J. Gooday, L. A. Levin, I. G. Priede, P. Buhl-Mortensen, H. Gheerardyn, N. J. King, and M. Raes. 2010. Biological structures as a source of habitat heterogeneity and biodiversity on the deep ocean margins. Marine Ecology **31**:21-50.

436 Cairns, S. D. 2016. New abyssal Primnoidae (Anthozoa: Octocorallia) from the Clarion-

437   Clipperton Fracture Zone, equatorial northeastern Pacific. Marine Biodiversity **46**:141-

438   150.

439 Clark, M. R., A. A. Rowden, T. Schlacher, A. Williams, M. Consalvey, K. I. Stocks, A. D.

440   Rogers, T. D. O'Hara, M. White, T. M. Shank, and J. M. Hall-Spencer. 2010. The ecology

441   of seamounts: structure, function, and human impacts. Ann Rev Mar Sci **2**:253-278.

442 Clarke, K. R. 1993. Non-parametric multivariate analyses of changes in community structure.

443   Australian Journal of Ecology **18**:117-143.

444 Dahlgren, T. G., H. Wiklund, M. Rabone, D. J. Amon, C. Ikebe, L. Watling, C. R. Smith, and A.

445   G. Glover. 2016. Abyssal fauna of the UK-1 polymetallic nodule exploration area,

446   Clarion-Clipperton Zone, central Pacific Ocean: Cnidaria. Biodivers Data J:e9277.

447 Davison, A. C., and D. V. Hinkley. 1997. Bootstrap Methods and their Application. Cambridge

448   University Press, Cambridge.

449 De Leo, F. C., C. R. Smith, A. A. Rowden, D. A. Bowden, and M. R. Clark. 2010. Submarine

450   canyons: hotspots of benthic biomass and productivity in the deep sea. Proc Biol Sci

451   **277**:2783-2792.

452 Durden, J. M., K. Murphy, A. Jaeckel, C. L. Van Dover, S. Christiansen, K. Gjerde, A. Ortega,

453   and D. O. B. Jones. 2017. A procedural framework for robust environmental management

454   of deep-sea mining projects using a conceptual model. Marine Policy **84**:193-201.

455 Durden, J. M., T. Schoening, F. Althaus, A. Friedman, R. Garcia, A. G. Glover, J. Greinert, N.

456   Jacobsen Stout, D. O. B. Jones, A. Jordt, J. Kaeli, K. Köser, L. A. Kuhnz, D. Lindsay, K.

457   J. Morris, T. W. Nattkemper, J. Osterloff, H. A. Ruhl, H. Singh, M. Tran, and B. J. Bett

458   2016. Perspectives in visual imaging for marine biology and ecology: from acquisition to

459   understanding. — In: R. N. Hughes, D. J. Hughes, I. P. Smith, and A. C. Dale (eds),

460   Oceanography and Marine Biology: An Annual Review, Vol. 54. CRC Press, pp. 1-72.

19

461 Forcino, F. L., L. R. Leighton, P. Twerdy, and J. F. Cahill. 2015. Reexamining Sample Size

462   Requirements for Multivariate, Abundance-Based Community Research: When Resources

463   are Limited, the Research Does Not Have to Be. PLoS One **10**:e0128379.

464 Glover, A. G., H. Wiklund, M. Rabone, D. J. Amon, C. R. Smith, T. O'Hara, C. L. Mah, and T.

465   G. Dahlgren. 2016. Abyssal fauna of the UK-1 polymetallic nodule exploration claim,

466   Clarion-Clipperton Zone, central Pacific Ocean: Echinodermata. Biodiversity Data

467   Journal:e7251.

468 Gollner, S., S. Kaiser, L. Menzel, D. O. B. Jones, A. Brown, N. C. Mestre, D. van Oevelen, L.

469   Menot, A. Colaco, M. Canals, D. Cuvelier, J. M. Durden, A. Gebruk, G. A. Egho, M.

470   Haeckel, Y. Marcon, L. Mevenkamp, T. Morato, C. K. Pham, A. Purser, A. Sanchez-

471   Vidal, A. Vanreusel, A. Vink, and P. Martinez Arbizu. 2017. Resilience of benthic deep-

472   sea fauna to mining activities. Marine Environmental Research **129**:76-101.

473 Gooday, A. J., B. J. Bett, and D. N. Pratt. 1993. Direct observation of episodic growth in an

474   abyssal xenophyophore (Protista). Deep Sea Research Part I: Oceanographic Research

475   Papers **40**:2131-2143.

476 Gooday, A. J., A. Goineau, and I. Voltski. 2015. Abyssal foraminifera attached to polymetallic

477   nodules from the eastern Clarion Clipperton Fracture Zone: a preliminary description and

478   comparison with North Atlantic dropstone assemblages. Marine Biodiversity **45**:391-412.

479 Gooday, A. J., M. Holzmann, C. Caulle, A. Goineau, O. Kamenskaya, A. A. T. Weber, and J.

480   Pawlowski. 2017. Giant protists (xenophyophores, Foraminifera) are exceptionally

481   diverse in parts of the abyssal eastern Pacific licensed for polymetallic nodule exploration.

482   Biological Conservation **207**:106-116.

483 Gotelli, N. J., and R. K. Colwell. 2001. Quantifying biodiversity: procedures and pitfalls in the

484   measurement and comparison of species richness. Ecology Letters **4**:379-391.

485 Iken, K., T. Brey, U. Wand, J. Voigt, and P. Junghans. 2001. Food web structure of the benthic

486   community at the Porcupine Abyssal Plain (NE Atlantic): a stable isotope analysis.

487   Progress in Oceanography **50**:383-405.

488 ISA, International Seabed Authority. 2012. Decision of the Council relating to an environmental

489   management plan for the Clarion-Clipperton Zone. ISBA/18/C/22. Kingston, Jamaica.

490 Jeffreys, R. M., G. A. Wolff, and G. L. Cowie. 2009. Influence of oxygen on heterotrophic

491   reworking of sedimentary lipids at the Pakistan margin. Deep Sea Research Part II:

492   Topical Studies in Oceanography **56**:358-375.

493 Jones, D. O., S. Kaiser, A. K. Sweetman, C. R. Smith, L. Menot, A. Vink, D. Trueblood, J.

494   Greinert, D. S. Billett, P. M. Arbizu, T. Radziejewska, R. Singh, B. Ingole, T. Stratmann,

495   E. Simon-Lledo, J. M. Durden, and M. R. Clark. 2017. Biological responses to

496   disturbance from simulated deep-sea polymetallic nodule mining. PLoS One

497   **12**:e0171750, doi:10.1371/journal.pone.0171750

498 Jones, D. O. B. 2015. RRS James Cook Cruise JC120 15 Apr - 19 May 2015. Manzanillo to

499   Manzanillo, Mexico. Managing Impacts of Deep-seA resource exploitation (MIDAS):

500   Clarion-Clipperton Zone North Eastern Area of Particular Environmental Interest.

501   Southampton, National Oceanography Centre, 117pp.

502 Jones, D. O. B., B. J. Bett, and P. A. Tyler. 2007. Megabenthic ecology of the deep Faroe–

503   Shetland channel: A photographic study. Deep Sea Research Part I: Oceanographic

504   Research Papers **54**:1111-1128.

505 Jones, D. O. B., C. O. Mrabure, and A. R. Gates. 2013. Changes in deep-water epibenthic

506   megafaunal assemblages in relation to seabed slope on the Nigerian margin. Deep Sea

507   Research Part I: Oceanographic Research Papers **78**:49-57.

508 Jost, L. 2006. Entropy and diversity. Oikos **113**:363-375.

509   Kamenskaya, O. E., A. J. Gooday, O. S. Tendal, and V. F. Melnik. 2015. Xenophyophores

510   (Protista, Foraminifera) from the Clarion-Clipperton Fracture Zone with description of

511   three new species. Marine Biodiversity **45**:581-593.

512   Kersken, D., D. Janussen, and P. Martínez Arbizu. 2018. Deep-sea glass sponges (Hexactinellida)

513   from polymetallic nodule fields in the Clarion-Clipperton Fracture Zone (CCFZ),

514   northeastern Pacific: Part I – Amphidiscophora. Marine Biodiversity **48**:545-573.

515   Kuhn, T., A. Wegorzewski, C. Rühlemann, and A. Vink 2017. Composition, Formation, and

516   Occurrence of Polymetallic Nodules. — In: R. Sharma (ed), Deep-Sea Mining: Resource

517   Potential, Technical and Environmental Considerations. Springer International Publishing,

518   pp. 23-63.

519   Lapointe, A., and L. Watling. 2015. Bamboo corals from the abyssal Pacific: Bathygorgia.

520   Proceedings of the Biological Society of Washington **128**:125-136.

521   Laureillard, J., xe, L. janelle, and M. Sibuet. 2004. Use of lipids to study the trophic ecology of

522   deep-sea xenophyophores. Marine Ecology Progress Series **270**:129-140.

523   Levin, L. A., R. J. Etter, M. A. Rex, A. J. Gooday, C. R. Smith, J. Pineda, C. T. Stuart, R. R.

524   Hessler, and D. Pawson. 2001. Environmental Influences on Regional Deep-Sea Species

525   Diversity. Annual Review of Ecology and Systematics **32**:51-93.

526   Levin, L. A., K. Mengerink, K. M. Gjerde, A. A. Rowden, C. L. Van Dover, M. R. Clark, E.

527   Ramirez-Llodra, B. Currie, C. R. Smith, K. N. Sato, N. Gallo, A. K. Sweetman, H. Lily,

528   C. W. Armstrong, and J. Brider. 2016. Defining "serious harm" to the marine

529   environment in the context of deep-seabed mining. Marine Policy **74**:245-259.

530   Levin, L. A., and C. L. Thomas. 1988. The ecology of xenophyophores (Protista) on eastern

531   Pacific seamounts. Deep Sea Research Part A. Oceanographic Research Papers **35**:2003-

532   2027.

533 Lim, S.-C., H. Wiklund, A. G. Glover, T. G. Dahlgren, and K.-S. Tan. 2017. A new genus and

534   species of abyssal sponge commonly encrusting polymetallic nodules in the Clarion-

535   Clipperton Zone, East Pacific Ocean. Systematics and Biodiversity **15**:507-519.

536 Mewes, K., J. M. Mogollón, A. Picard, C. Rühlemann, T. Kuhn, K. Nöthen, and S. Kasten. 2014.

537   Impact of depositional and biogeochemical processes on small scale variations in nodule

538   abundance in the Clarion-Clipperton Fracture Zone. Deep Sea Research Part I:

539   Oceanographic Research Papers **91**:125-141.

540 Meyer, K. S., C. M. Young, A. K. Sweetman, J. Taylor, T. Soltwedel, and M. Bergmann. 2016.

541   Rocky islands in a sea of mud: biotic and abiotic factors structuring deep-sea dropstone

542   communities. Marine Ecology Progress Series **556**:45-57.

543 Miljutina, M. A., D. M. Miljutin, R. Mahatma, and J. Galéron. 2010. Deep-sea nematode

544   assemblages of the Clarion-Clipperton Nodule Province (Tropical North-Eastern Pacific).

545   Marine Biodiversity **40**:1-15.

546 Morris, K. J., B. J. Bett, J. M. Durden, V. A. I. Huvenne, R. Milligan, D. O. B. Jones, S. McPhail,

547   K. Robert, D. M. Bailey, and H. A. Ruhl. 2014. A new method for ecological surveying of

548   the abyss using autonomous underwater vehicle photography. Limnology and

549   Oceanography: Methods **12**:795-809.

550 Mullineaux, L. S. 1987. Organisms living on manganese nodules and crusts: distribution and

551   abundance at three North Pacific sites. Deep Sea Research Part A. Oceanographic

552   Research Papers **34**:165-184.

553 Oksanen, J., F. Guillaume Blanchet, M. Friendly, R. Kindt, P. Legendre, D. McGlinn, P. R.

554   Minchin, R. B. O'Hara, G. L. Simpson, P. Solymos, M. H. H. Stevens, E. Szoecs, and H.

555   Wagner. 2018. vegan: Community Ecology Package. R package version 2.4-6.

556   https://CRAN.R-project.org/package=vegan.

557 Peukert, A., T. Schoening, E. Alevizos, K. Köser, T. Kwasnitschka, and J. Greinert. 2018.

558   Understanding Mn-nodule distribution and evaluation of related deep-sea mining impacts

559   using AUV-based hydroacoustic and optical data. Biogeosciences **15**:2525-2549.

560 Radziejewska, T. 2014. Characteristics of the Sub-equatorial North-Eastern Pacific Ocean's

561   Abyss, with a Particular Reference to the Clarion-Clipperton Fracture Zone. -In:

562   Meiobenthos in the Sub-equatorial Pacific Abyss: A Proxy in Anthropogenic Impact

563   Evaluation. Springer, pp. 13-28.

564 Ramirez-Llodra, E., P. A. Tyler, M. C. Baker, O. A. Bergstad, M. R. Clark, E. Escobar, L. A.

565   Levin, L. Menot, A. A. Rowden, C. R. Smith, and C. L. Van Dover. 2011. Man and the

566   last great wilderness: human impact on the deep sea. PLoS One **6**:e22588.

567   doi:10.1371/journal.pone.0022588

568 Roberts, J. M., A. J. Wheeler, and A. Freiwald. 2006. Reefs of the deep: the biology and geology

569   of cold-water coral ecosystems. science **312**:543-547.

570 Sanders, H. L. 1968. Marine benthic diversity: a comparative study. American naturalist **102**:243-

571   282.

572 Schoening, T., D. O. B. Jones, and J. Greinert. 2017. Compact-Morphology-based poly-metallic

573   Nodule Delineation. Scientific Reports **7**:13338.

574 Schoening, T., T. Kuhn, D. O. B. Jones, E. Simon-Lledo, and T. W. Nattkemper. 2016. Fully

575   automated image segmentation for benthic resource assessment of poly-metallic nodules.

576   Methods in Oceanography **15-16**:78-89.

577 Simon-Lledo, E., J. M. Durden, R. M. Jeffreys, N. M. Benoist, T. Schoening, B. J. Bett, V. A. I.

578   Huvenne, and D. O. B. Jones. submitted. Megafaunal variation in the abyssal landscape of

579   the Clarion Clipperton Zone. Progress in Oceanography.

580 Skornyakova, N. S., and I. O. Murdmaa. 1992. Local variations in distribution and composition

581   of ferromanganese nodules in the Clarion-Clipperton Nodule Province. Marine Geology

582   **103**:381-405.

583   Smith, C. R., and A. W. J. Demopoulos 2003. Ecology of the deep Pacific Ocean floor. — In: P.

584   A. Tyler (ed), Ecosystems of the World: Ecosystems of the Deep Ocean. Elsevier, pp.

585   179-218.

586   Stefanoudis, P. V., B. J. Bett, and A. J. Gooday. 2016. Abyssal hills: Influence of topography on

587   benthic foraminiferal assemblages. Progress in Oceanography **148**:44-55.

588   Strindberg, S., and S. T. Buckland. 2004. Zigzag survey designs in line transect sampling. Journal

589   of Agricultural, Biological, and Environmental Statistics **9**:443-461.

590   Sun, Z., J.-F. Hamel, and A. Mercier. 2011. Planulation, larval biology, and early growth of the

591   deep-sea soft corals Gersemia fruticosa and Duva florida (Octocorallia: Alcyonacea).

592   Invertebrate Biology **130**:91-99.

593   Tews, J., U. Brose, V. Grimm, K. Tielbörger, M. C. Wichmann, M. Schwager, and F. Jeltsch.

594   2004. Animal species diversity driven by habitat heterogeneity/diversity: the importance

595   of keystone structures. Journal of Biogeography **31**:79-92.

596   Thiel, H., G. Schriever, C. Bussau, and C. Borowski. 1993. Manganese nodule crevice fauna.

597   Deep Sea Research Part I: Oceanographic Research Papers **40**:419-423.

598   Thistle, D., J. Y. Yingst, and K. Fauchald. 1985. A deep-sea benthic community exposed to

599   strong near-bottom currents on the Scotian Rise (western Atlantic). Marine Geology

600   **66**:91-112.

601   Tilman, D. 1982. Resource competition and community structure. Monogr Popul Biol **17**:1-296.

602   Tilot, V., R. Ormond, J. Moreno Navas, and T. S. Catalá. 2018. The Benthic Megafaunal

603   Assemblages of the CCZ (Eastern Pacific) and an Approach to their Management in the

604   Face of Threatened Anthropogenic Impacts. Frontiers in Marine Science **5**,

605   doi:10.3389/fmars.2018.00007

606   Van Dover, C. L., C. J. Berg, and R. D. Turner. 1988. Recruitment of marine invertebrates to

607   hard substrates at deep-sea hydrothermal vents on the East Pacific Rise and Galapagos

608   spreading center. Deep Sea Research Part A. Oceanographic Research Papers **35**:1833-

609   1849.

610 Vanreusel, A., A. Hilario, P. A. Ribeiro, L. Menot, and P. M. Arbizu. 2016. Threatened by

611   mining, polymetallic nodules are required to preserve abyssal epifauna. Sci Rep **6**:26808.

612 Veillette, J., J. Sarrazin, A. J. Gooday, J. Galéron, J.-C. Caprais, A. Vangriesheim, J. Étoubleau,

613   J. R. Christian, and S. Kim Juniper. 2007. Ferromanganese nodule fauna in the Tropical

614   North Pacific Ocean: Species richness, faunal cover and spatial distribution. Deep Sea

615   Research Part I: Oceanographic Research Papers **54**:1912-1935.

616 Wildish, D., and D. Kristmanson. 2005. Benthic suspension feeders and flow. Cambridge

617   University Press, Cambridge.

618 Wishner, K., L. Levin, M. Gowing, and L. Mullineaux. 1990. Involvement of the oxygen

619   minimum in benthic zonation on a deep seamount. Nature **346**:57.

620

621

622

623

624

625

626

627

628

629

630

631

632

Figures (legends)

Figure 1. Study area location and sampling operations within the APEI6 of the CCZ (North

Pacific Ocean). (a) Bathymetric survey chart of the study location. Landscape types depicted in

dark lines (left to right: Flat, Ridge, and Trough). White rectangles indicate AUV sampling areas

targeted within each landscape. (b) Map of the eastern CCZ showing contractor areas, Areas of

Particular Environmental Interest, and study location. (c) to (e) Full AUV imagery dataset

collected at each landscape type. Colour of survey tracks represents the nodule coverage level of

the seabed, obtained from automatic detection in survey images using the CoMoNoD algorithm

(Schoening et al. 2017). (c) Flat survey. (d) Ridge survey. (e) Trough survey.

Figure 2. Variation in (a) standing stock and (b) diversity with nodule cover at the APEI6

seafloor. Points indicate mean (median for metazoan biomass) values of each parameter

calculated from each nodule-cover class bootstrap-like sample set. Error bars represent 95%

confidence intervals. (a) Density of metazoans and xenophyophores (left y-axis), metazoan

biomass density (right y-axis). (b) Metazoan diversity: morphospecies richness (SN),

morphospecies density (S_A), Exponential Shannon index (Exp *H'*), and Inverse Simpson index

(1/D).

Figure 3. Variation in community composition with nodule cover at the APEI6 seafloor. (a)

nMDS plot describing 2D ordination of dissimilarity (distance) between the assemblages of each

bootstrap-like sample. Ellipses represent 95% confidence intervals for each nodule-cover class

bootstrap-like sample set. (b) Variation of nMDS dimension-1 with nodule cover. Data are mean

values of the parameter as calculated from each nodule-cover class bootstrap-like sample set.

Error bars represent 95% confidence intervals.

657 **Figure 4.** Variation in metazoan density (a) life modes and (b) selected morphospecies (sponge:

658 Porifera msp-5; primnoid soft-coral: *Callozostron* cf *bayeri*; bamboo soft-coral: *Lepidisis* msp),

659 with nodule cover. Data are mean values of the parameter as calculated from each nodule-cover

660 class bootstrap-like sample set. Error bars represent 95% confidence intervals.

661

662 **Figure 5**. Example of landscape-type variation in faunal response to nodule cover. Variation in

663 the density of (a) suspension-feeder metazoans and (b) xenophyophores with nodule cover. Data

664 are mean density values as calculated from each nodule-cover class bootstrap-like sample set for

665 each separate landscape-type analysis (Flat, Ridge, Trough). Error bars represent 95% confidence

666 intervals.

667

668

669

670

671

672

673

674

675

676

677

678

679 **Tables**

680 **Table 1.** Spearman's rank correlations of ecological parameters with nodule cover. Summary

681 results of tests performed between mean (median for metazoan biomass density) values of each

682 parameter calculated from each nodule-cover class bootstrap-like sample set, with detail of

683 significant differences between nodule class 1 (mean cover = 1.1%) and the rest of classes (cover

684 >2%). Distinct class 1: no overlap of the confidence interval of the lowest nodule-cover class

685 with any other class. Note that correlation approach fails to detect significance in the variation of

686 unimodal responses.

	Distinct	Correlations	
	class 1	r_s	p-value
Standing stock			
Xenophyophores (ind m^{-2})	**yes**	-0.297	0.404
Metazoans (ind m^{-2})	**yes**	0.345	0.328
Metazoan biomass (g fwwt m^{-2})	no	0.624	0.053
NA metazoa (ind m^{-2})	**yes**	0.466	0.174
NFL metazoa (ind m^{-2})	**yes**	0.224	0.533
Porifera msp-5 (ind m^{-2})	no	-0.976	**<0.001***
C. cf *bayeri* (ind m^{-2})	no	-0.6	0.067
Lepidisis msp (ind m^{-2})	no	0.952	**<0.001***
Diversity and composition			
Morphospecies richness (S_N)	no	0.248	0.405
Morphospecies density (S_A)	no	0.721	**0.018***
Exponential Shannon (Exp *H'*)	no	0.478	0.161
Inverse Simpson (1/D)	**yes**	0.345	0.328
MDS-dimension 1	**yes**	0.891	**0.001****

687

Mean nodule
size (cm)
- 1.1
- 2.7
- 3.5
- 4
- 5
- 5.8
- 7.3
- 9.8
- 12.5
- 19.5

NA
NFL
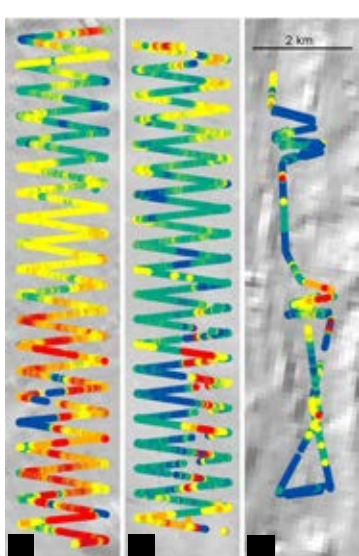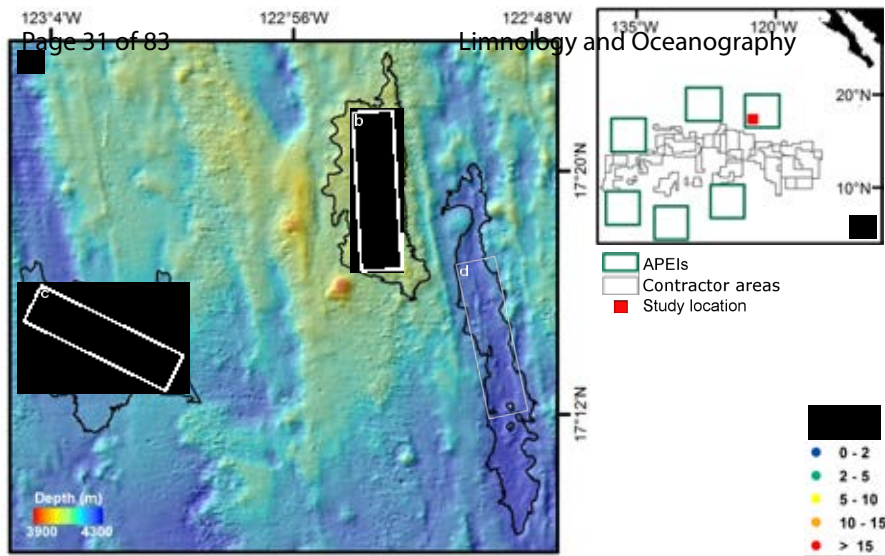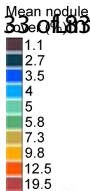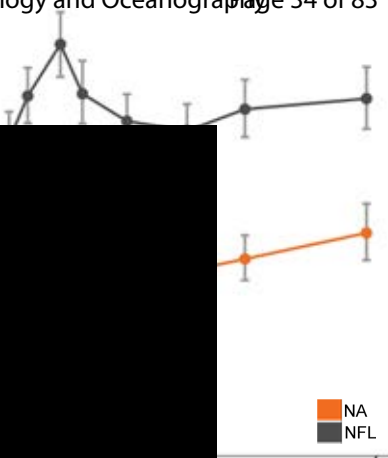
Porifera msp-5
C. cf *bayeri*
Lepidisis msp

P

Supplementary material

Appendix 1: Additional analyses within landscape type

The dataset was collected in three landscape types (LT), 'Flat', 'Ridge', and 'Trough' (main text, Fig. 1). To assess the potential influence of LT on ecological responses to the nodule cover gradient, we additionally carried out separate analyses within each LT. As in our broad analysis, images were ordered by nodule cover and divided into nine cover classes at breakpoints to yield an approximately equal number of megafauna specimens in each class. Megafauna data from each cover class, in each LT, was then subjected to a boostrap-like resampling procedure to produce 1000 targeting a minimum of 250 specimens per sample. Faunal density and diversity measures (as in main text) were calculated for each boostrap-like subsample, and 95% confidence intervals derived by the simple percentile method (see main text).
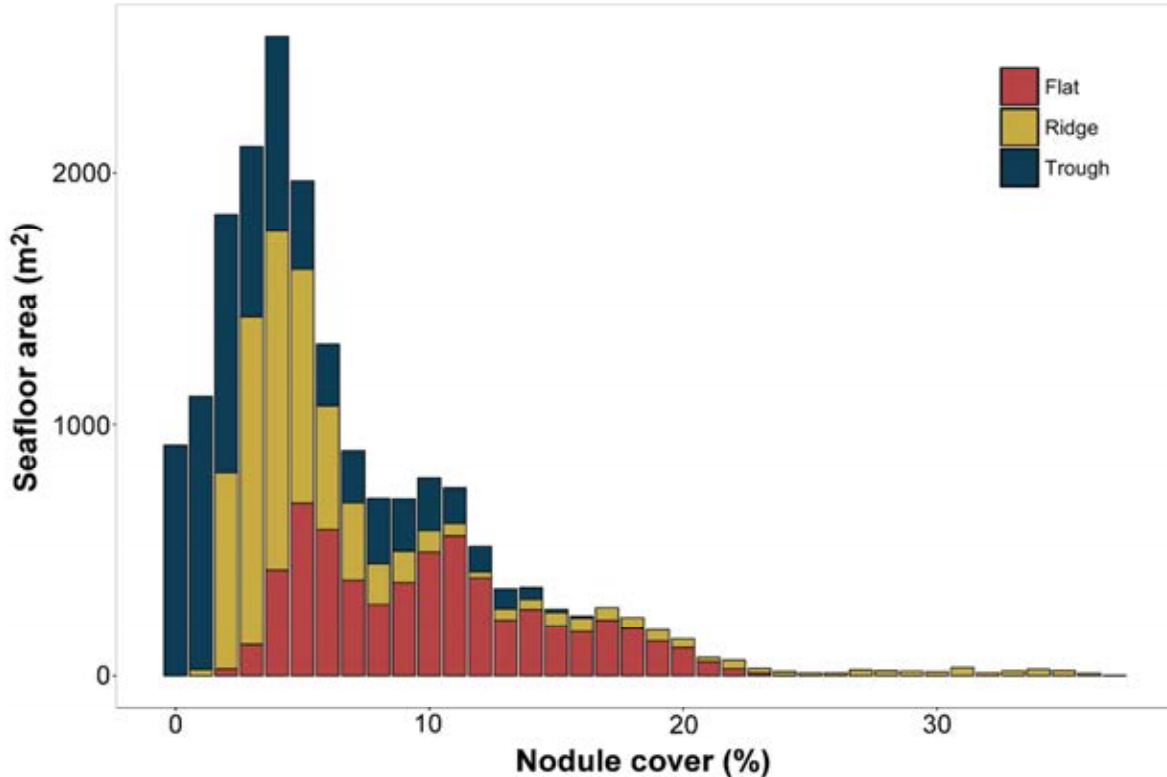
Figure A1. Areal distribution of nodule cover within each landscape type.
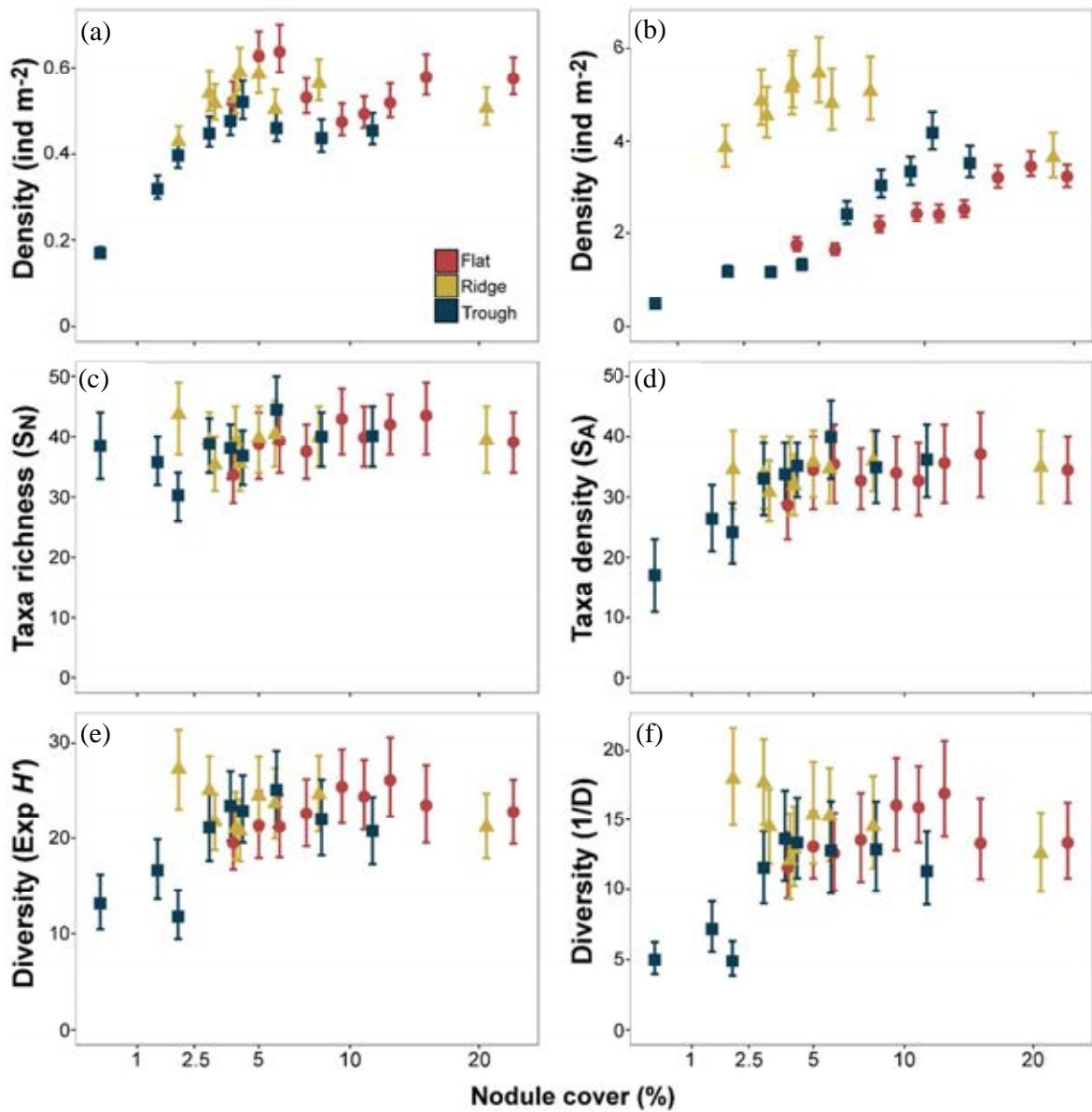
Figure A2. Variation of different ecological parameters across the nodule coverage gradient of each different APEI6 landscape type. Data are mean values of each parameter as calculated from each nodule cover class bootstrap-like sample set. Error bars represent 95% confidence. **(a)** Metazoan density. **(b)** Xenophyophore test density. **(c)** Morphospecies richness. **(d)** Morphospecies density. **(e)** Exponential Shannon index. **(f)** Inverse-Simpson index.

Appendix 2: Additional results of broad ecological assessment
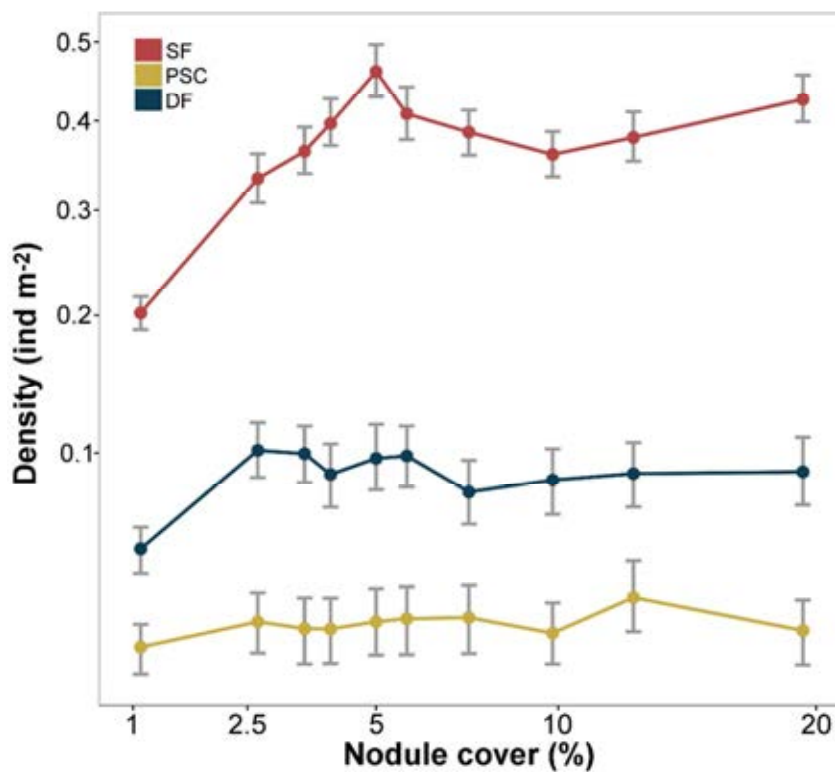
Figure B1. Variation in the density of three functional groups with nodule cover at the APEI6 seafloor. Data are mean density values of different metazoan types (SF: suspension feeders; PSC: predators and scavengers; DF: deposit feeders) calculated from each nodule cover class bootstrap-like sample set. Error bars represent 95% confidence intervals.
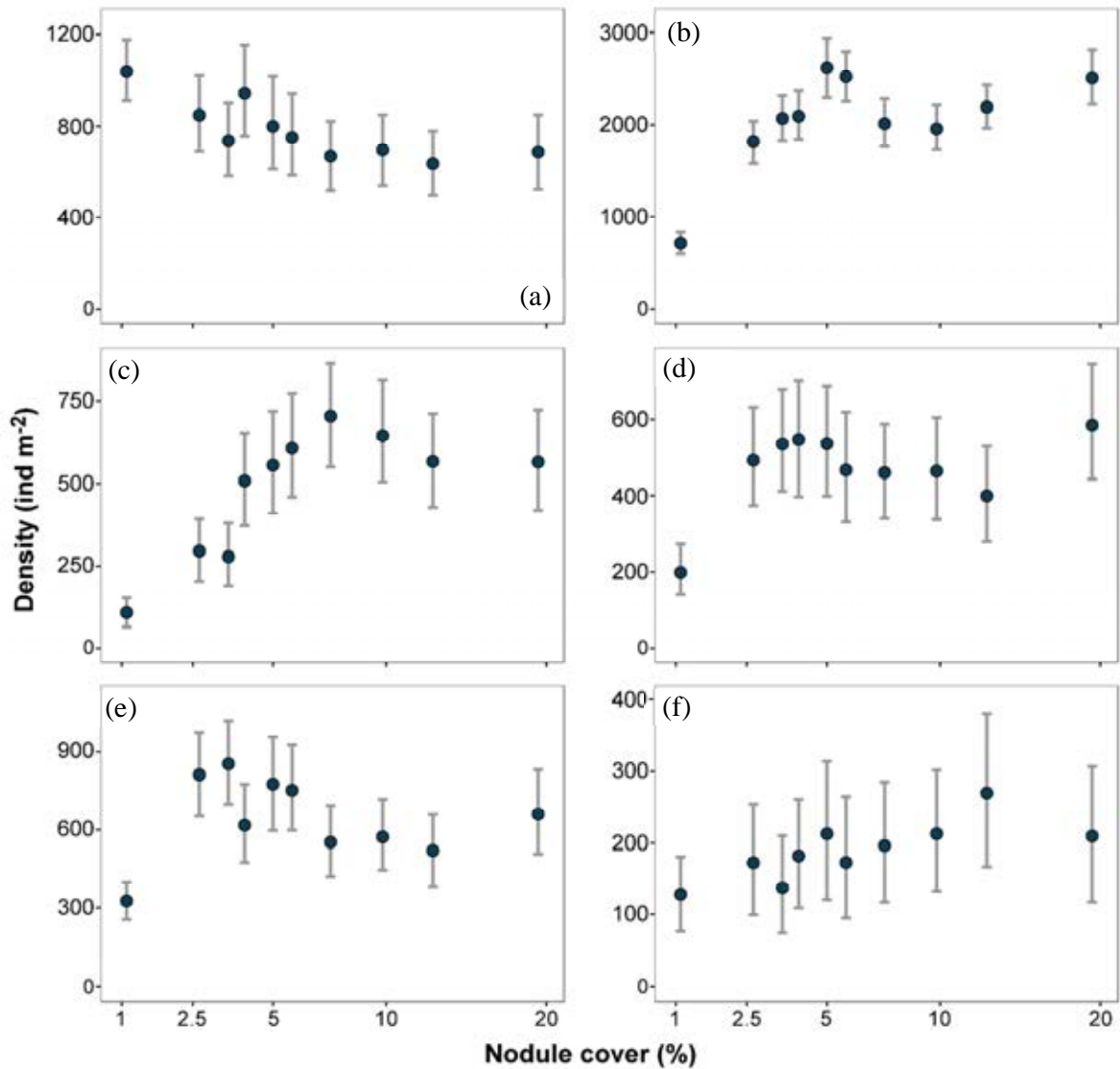
Figure B2. Variation in the density of taxonomical groups with nodule cover at the APEI6 seafloor. Data are mean density values of the six most dominant metazoan phyla as calculated from each nodule-cover class bootstrap-like sample set. Error bars represent 95% confidence intervals. **(a)** Sponges. **(b)** Cnidarians. **(c)** Bryozoans. **(d)** Annelids. **(e)** Echinoderms. **(f)** Arthropods: crustaceans.
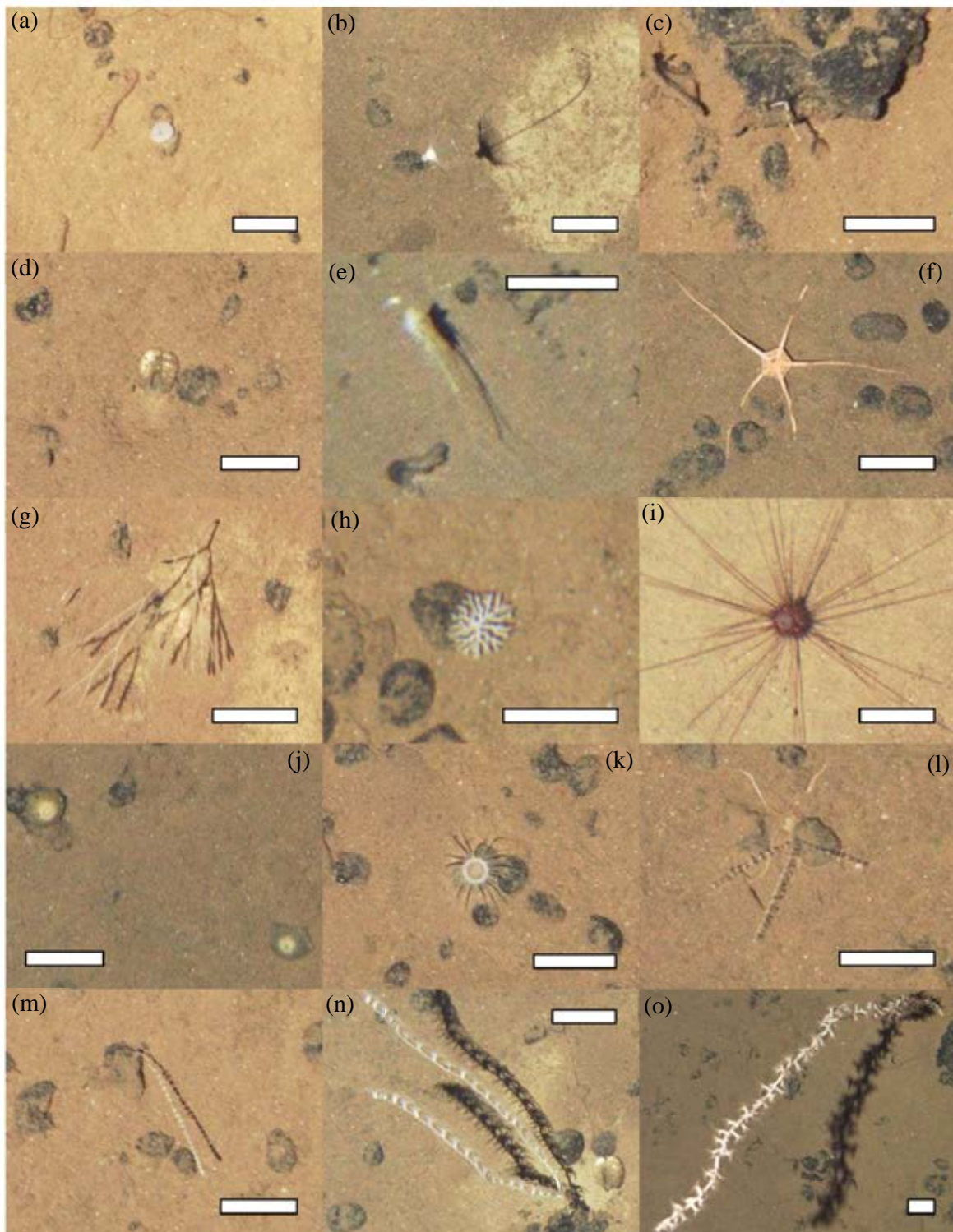
Figure B3. Top-15 most abundant metazoan morphospecies recorded at the APEI6 seafloor during JC120 AUV survey. Scale bars indicate 50 mm. **(a)** Porifera msp-5. **(b)** *Cladorhiza* cf *mexicana*. **(c)** Polychaete msp-5. **(d)** Irregularia msp-1. **(e)** *Mastigoteuthis* sp. **(f)** *Ophiosphalma* sp. **(g)** Columnella msp (Bryozoa). **(h)** Smithsonius msp (Bryozoa). **(i)** Aspidodiadematidae msp. **(j)** Actinia msp-18. **(k)** Actinia msp-22. **(l)** *Callozostron* cf *bayeri*. **(m)** *Calyptrophora* cf *persephone*. **(n)** *Bathygorgia* cf *profunda*. **(o)** *Lepidisis* msp.
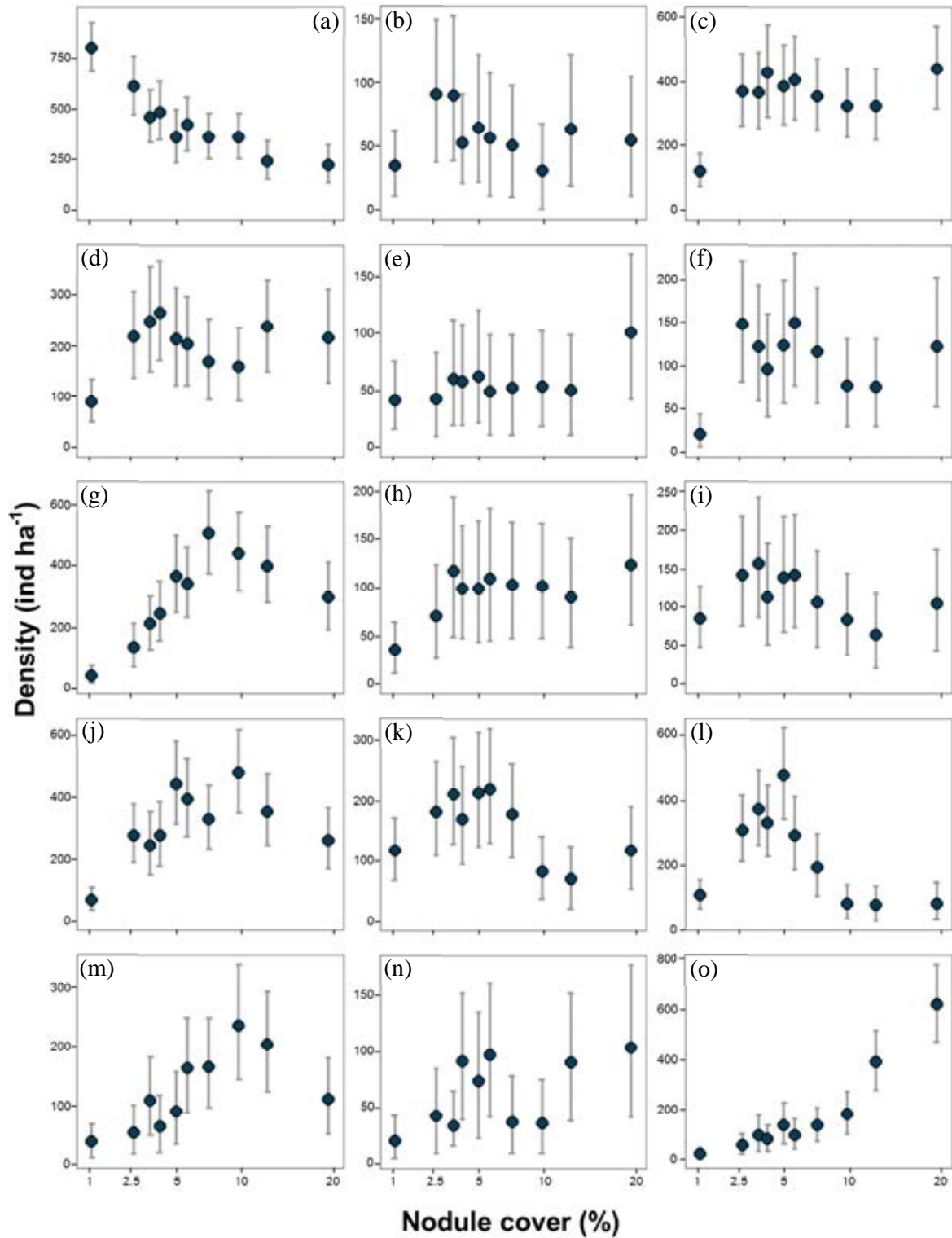
Figure B4. Variation in morphospecies density with nodule cover at the APEI6 seafloor. Data are mean density values of top-15 most abundant metazoan morphospecies as calculated from each nodule cover class bootstrap-like sample set. Error bars represent 95% confidence intervals. **(a)** Porifera msp-5. **(b)** *Cladorhiza* cf *mexicana*. **(c)** Polychaete msp-5. **(d)** Irregularia msp-1. **(e)** *Mastigoteuthis* sp. **(f)** *Ophiosphalma* sp. **(g)** Columnella msp (Bryozoa). **(h)** Smithsonius msp

(Bryozoa). **(i)** Aspidodiadematidae msp. **(j)** Actinia msp-18. **(k)** Actinia msp-22. **(l)** *Callozostron* cf *bayeri*. **(m)** *Calyptrophora* cf *persephone*. **(n)** *Bathygorgia* cf *profunda*. **(o)** *Lepidisis* msp.
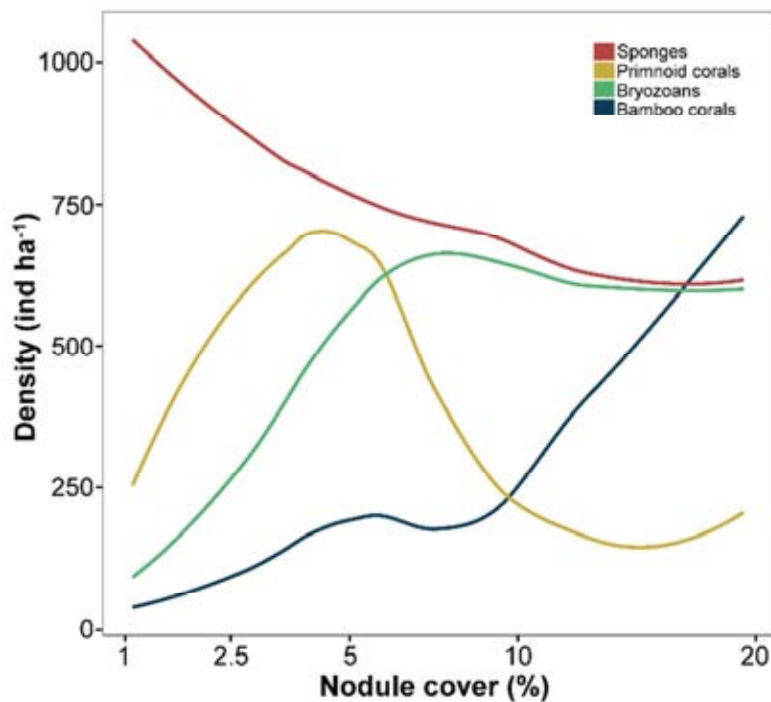
Figure B5. Variation in the density of selected metazoan taxonomic groups with nodule cover. Lines represent mean density values of each group as calculated from each nodule-cover class bootstrap-like sample set fitted by weighted least-squares, using a local polynomial regression.

Table B1. Spearman's rank correlations of all ecological parameters with nodule cover. Summary results of tests performed between mean density (ind m^{-2}) values of different metazoan groups as calculated from each nodule cover class bootstrap-like sample set and nodule cover variation, with detail of significant differences between nodule class 1 (mean cover = 1.1%) and the rest of classes (cover >2%). Distinct class 1: no overlap of class 1 confidence interval with any other class.

	Distinct class 1	Correlations	
		r_s	p-value
Functional group			
Deposit feeders	**yes**	-0.15	0.676
Predators and scavengers	no	0.28	0.425
Suspension feeders	**yes**	0.50	0.138
Taxonomic Phylum			
Annelida	**yes**	0.10	0.777
Bryozoa	**yes**	0.78	**0.008****
Cnidaria	**yes**	0.49	0.150
Arthropods: crustaceans	no	0.83	**0.003***
Echinodermata	**yes**	-0.25	0.489
Porifera	no	-0.84	**0.002***
Morphospecies			
Polychaete msp-5	**yes**	0.18	0.627
Columnella msp	**yes**	0.76	**0.011***
Smithsonius msp	no	0.50	0.138
Actinia msp-18	**yes**	0.47	0.174
Actinia msp-22	no	0.83	**0.003***
C. cf *persephone*	no	-0.36	0.310
B. cf *profunda*	no	0.55	0.098
Lepidisis msp	no	0.95	**0*****
C. cf *bayeri*	no	-0.60	0.067
Irregularia msp-1	no	-0.03	0.934
Aspidodiadematidae msp	no	-0.54	0.108
Ophiosphalma sp	no	-0.03	0.934
Porifera msp-5	no	-0.93	**0*****
*C.*cf *mexicana*	no	-0.24	0.511
Mastigoteuthis sp	no	0.44	0.200

Manuscript Details

Manuscript number	PROOCE_2018_141
Title	Megafaunal variation in the abyssal landscape of the Clarion Clipperton Zone
Article type	Full Length Article

Abstract

The potential for imminent polymetallic nodule mining in the Clarion Clipperton Fracture Zone (CCZ) has attracted considerable scientific and public attention. This concern stems from both the extremely large seafloor areas that may be impacted by mining, and the very limited knowledge of the faunistics and ecology of this region. The key environmental factors regulating local seafloor ecology are still very poorly understood. In this study, we focus on megafaunal ecology in the proposed conservation zone 'Area of Particular Environmental Interest 6'. We employ swathe bathymetric survey data to objectively define three key landscape types in the area (Flat, Ridge, Trough; water depth: 3950-4250 m) that are generally characteristic of the wider CCZ environment. We use direct seabed sampling to further characterise the sedimentary environment in each landscape type, detecting no statistically significant differences in particles size distributions or organic matter content. Additional seafloor environmental characteristics and data on both the metazoan and xenophyophore components of the megafauna were derived by extensive photographic survey from an autonomous underwater vehicle. Image data revealed that there were statistically significant differences in seafloor cover by nodules and in the occurrence of other hard substrata habitat between landscape types. Statistically significant differences in megafauna standing stock, functional structuring, diversity, and faunal composition were found between landscape types. Geomorphological variations presumably regulating local bottom water flows and the availability of nodule and xenophyophore test substrata between study areas may be the mechanism driving these assemblage differences. We also used these data to assess the influence of the sampling unit size choice on the estimation of ecological parameters. Sampling unit size evaluation supported our results, although each parameter exhibited a different sensitivity to this factor. All of these results are important to the appropriate management of potential mining activities in the CCZ and elsewhere in the deep ocean.

Keywords	polymetallic nodules; geomorphology; biodiversity; deep-sea mining; abyssal plain; AUV survey; NE Pacific; CCZ; APEI
Manuscript category	Interdisciplinary
Corresponding Author	Erik Simon-Lledo
Corresponding Author's Institution	National Oceanography Centre
Order of Authors	Erik Simon-Lledo, Jennifer Durden, Noelie Benoist, Timm Schoening, Rachel Jeffreys, Brian Bett, Veerle Huvenne, Daniel O.B. Jones
Suggested reviewers	Diva Amon, Lenaick Menot, Ann Vanreusel

Submission Files Included in this PDF

File Name [File Type]

Cover letter for APEI6_landsc.docx [Cover Letter]

Highlights_only.docx [Highlights]

APEI6_landsc_MN_esl.docx [Manuscript File]

To view all the submission files, including those not included in the PDF, click on the manuscript title on your EVISE Homepage, then click 'Download zip file'.

National Oceanography Centre

European Way

Southampton, SO14 3ZH

11th of June 2018

Dear Sir/Madam,

Would you please consider the attached manuscript "Megafaunal variation in the abyssal landscapes of the Clarion Clipperton Zone (CCZ)" for submission to Progress in Oceanography. We believe that the attached research paper addresses an important topic that is highly appropriate for PiO.

Our paper explores the influence of seafloor landscape on benthic megafauna communities in the abyssal Pacific. We targeted one of the proposed marine protected areas (Area of Particular Environmental Interest 6) set up by the International Seabed Authority to protect the environment from the harmful effects of potentially imminent polymetallic nodule mining. There is an urgent need for baseline ecological analyses such as the present study, since knowledge of the drivers structuring biological communities in the area is scarce, yet essential for effective regulation.

We analysed a large image dataset, covering ~15,000 m^2 of seafloor, which we demonstrate , through analysis of sampling effort, to be enough to provide good quality and stable estimates of key biological metrics. Our analysis detected clear differences in community structure, biodiversity levels, and fauna standing stock between characteristic landscape types, showing that local geomorphological variations at the landscape scale can play an important role in the structuring of the CCZ megabenthos. Changes in terrain have long been hypothesised to be important in the ecology of the abyss, but these effects have primarily been assessed in topographically prominent environments, such as canyons, ridges, and seamounts. Very few studies have assessed such patterns in abyssal plains, and this is the first to demonstrate that biodiversity can be modulated by terrain variations at the CCZ. The results have highly relevant conservational value. Differences found between formerly assumed homogenous abyssal landscape types flag the importance of taking geomorphological variations into consideration during the development of environmental policies at the CCZ.

Possible referees:

Dr. Lenaick Menot. Ifremer, Plouzané, France: lenaick.menot@ifremer.fr
Dr. Diva Amon, Natural History Museum, London, UK: divaamon@gmail.com
Prof. Dr. Ann Vanreusel, Ghent University, Belgium: ann.vanreusel@ugent.be

Authors remarks:

This is the first time that this manuscript has been submitted to any journal. All authors participated in the research and/or article preparation and have approved the final article. Authors declarations of interest: none. The funding sources of this article, listed in the main text, had no involvement in the study design, nor in the collection, analysis, or interpretation of data. We would like to use colour for figures in print.

Yours faithfully

Erik Simon-Lledó

Telephone: +44 7596414311

Email: esl1n13@soton.ac.uk

Highlights

- Used objective landscape classification based on AUV surveys to explore the influence of geomorphology in the structuring of abyssal megafauna

- Statistically significant differences in megafauna standing stock, functional structuring, diversity, and faunal composition were found between landscape types.

- Lower megafauna density and diversity were found in a bathymetric valley (Trough area), which can have important implications for mining exploitation

- Evaluation of the effect of the sample unit size supported our results and highlighted the importance of the choice of sampling unit in abyssal sampling, particularly at the CCZ.

Megafaunal variation in the abyssal landscape of the Clarion Clipperton Zone

Erik Simon-Lledó[1-2,*], Jennifer M. Durden[2-3], Noelie M.A. Benoist[1,2], Timm Schoening[4], Rachel M. Jeffreys[5], Brian J. Bett[1], Veerle A. I. Huvenne[1], Daniel O.B. Jones[1]

[1]National Oceanography Centre, University of Southampton, Waterfront Campus, European Way, SO14 3ZH, Southampton, UK
[2]Ocean and Earth Science, University of Southampton, National Oceanography Centre, Southampton, UK
[3]Present address: University of Hawaii at Manoa, Honolulu HI, USA, 96822.
[4]GEOMAR Helmholtz Centre for Ocean Research, Kiel, Germany
[5]School of Environmental Science, University of Liverpool, Liverpool, UK

*Corresponding author: e.simon-lledo@soton.ac.uk

1. Introduction

The likelihood of polymetallic nodule mining in the Clarion Clipperton Fracture Zone (CCZ) has attracted considerable scientific attention (Levin et al., 2016; Van Dover et al., 2017; Wedding et al., 2015). The potential impacts of mining are likely to extend over extremely large seafloor areas (Aleynik et al., 2017; Glover & Smith, 2003). Such disturbance may lead to major change in the benthic fauna (Jones et al., 2017) and full recovery might take thousands of years (Glasby et al., 1982). Sixteen nodule mining exploration contract areas (75,000 km^2 each) were granted in the CCZ between 2001 and 2014 by the International Seabed Authority (ISA) (Wedding et al., 2015). The ISA also allocated a series of nine Areas of Particular Environmental Interest (APEIs) beyond these claim areas, where exploitation is prohibited (ISA, 2012). The APEIs were designated to preserve source populations of species for future recolonization of disturbed areas (Lodge et al., 2014). However, the majority of these APEIs remain unstudied; it is not clear if their environmental conditions and faunas are similar to those of the mining claims (Glover et al., 2016a). As a result, improved knowledge of the drivers structuring biological communities in the CCZ is urgently needed to test the presumed functionality and current spatial arrangement of the APEIs system, and to re-assess the regional environmental plan (ISA, 2012).

The CCZ is generally considered as an extensive abyssal plain delimited by the topography of two WSW-ENE trending fracture zones, Clarion and Clipperton. There is a gradual increase in water depth from east (4000 m) to west (5000 m) owing to the sinking of older, cooler oceanic crust to the west (Pushcharovsky, 2006). However, slight variations in spreading rate appear to have shaped the CCZ seafloor into a series of bathymetric highs and lows with a characteristic spacing of 1 to 10 km, elongated perpendicular to fracture zones (Klitgord & Mammerickx, 1982; Olive et al., 2015). These horst and graben structures shape the CCZ seafloor as a succession of ridges, valleys, and intervening 'flat' zones. This topographic variation is thought to be generally characteristic of the abyssal environment worldwide (Harris et al., 2014). The very low influx of terrigenous sediments to the CCZ prevents the blanketing of this topography, as may occur on abyssal plains adjacent to continental margins (Smith & Demopoulos, 2003).

Abyssal plains represent some 70% of the world's seafloor (Harris et al., 2014) and are considered the largest ecosystems on Earth (Ramirez-Llodra et al., 2010). They are poorly explored but appear to have high species richness, including very many undescribed taxa (Smith et al., 2006). Despite their name, abyssal plains can have significant topography that influences the diversity and composition of deep-sea fauna (Durden et al., 2015; Leitner et al., 2017; Stefanoudis et al., 2016). This ecological variation appears to result from the interconnected effects of topographically-driven variation of local current dynamics (Thistle et al., 1991), sediment composition (Durden et al., 2015), and food supply (Smith and Demopoulos, 2003; Morris et al., 2016). However, habitat complexity derived from abyssal landscape geomorphology may have been

1

underappreciated in global estimations of ecological heterogeneity at the deep-sea floor (Durden et al., 2015; Morris et al., 2016); a factor that might be particularly significant to the ecology of the CCZ.

The CCZ appears to have one of the highest levels of deep-sea megafaunal (>1 cm length) species richness (Kamenskaya et al., 2013; Tilot et al., 2018). Morphospecies richness estimations from imagery data can rise above 200 taxa in local assessments (Amon et al., 2016). True species diversity and genetic biodiversity is expected to be much higher (Glover et al., 2015). Given their smaller body size, even higher local diversity is to be expected in the meio- and macrofaunal assemblages of the CCZ (De Smet et al., 2017; Pape et al., 2017). Epifauna, particularly suspension feeders, appear to have higher numerical densities in locations with higher nodule coverage (Vanreusel et al., 2016), with nodule-free areas having an higher proportion of deposit feeders, such as holothurians (Stoyanova, 2012). However, the precise role of nodules, and other local environmental factors, in the ecology of CCZ megafauna at the CCZ is still poorly understood. Faunal composition analyses are scarce, and most quantitative studies have been based on relatively small sampling unit areas (<1000 m^2) and low replication levels. Meaningful comparison across the CCZ is also hampered by a lack of standardization between studies.

Reliable estimation of ecological parameters relies on appropriate sampling of the populations under investigation. It is often these parameters that serve as the sole basis for conservation management decisions (Andrew & Mapstone, 1987; Magurran, 2004). Investigation of the pros and cons of different sampling strategies is commonplace in terrestrial and shallow-water marine ecology (Andrew & Mapstone, 1987; Buckland et al., 2001; Heck Jr et al., 1975) but rarely tackled in deep-sea studies, except for diversity estimators (Etter & Mullineaux, 2001; Grassle & Maciolek, 1992; Soetaert & Heip, 1990). In part, this lack of research stems from logistic constraints, however, the need is no less. In the CCZ, a key factor may be the very low numerical density of the megafauna, such that identifying an appropriate sampling unit size may be a particular issue (Benoist et al., submitted; Durden et al., 2016). Studies that demonstrate appropriate sampling to support their conclusions are key in ecology, not least those concerned with the regulation of mining activities (Durden et al., 2017a; Levin et al., 2016).

Our study assesses the ecology of the megafauna in the dominant landscape types of APEI6 in the eastern CCZ. We define the landscape types by objective analysis of the bathymetry, establish corresponding sedimentary environmental conditions by direct sampling, and further environmental characteristics and faunal data by extensive seafloor photography from an autonomous underwater vehicle (AUV). In this contribution we examine landscape-type-related variations in standing stock, diversity, and faunal composition and how these parameters, and their interpretation, might vary with the choice of sampling unit size.

2. Materials and methods

2.1. Study area

The CCZ basin floor is covered by extensive polymetallic nodule fields that add to the seabed heterogeneity and constitute a unique deep-sea habitat (Radziejewska, 2014). Seafloor nodule coverage can be extremely patchy and change drastically over tens of metres (Peukert et al., 2018). Surface sediment is mainly composed of Cenozoic pelagic clays and radiolarian oozes (ISA, 2010). The average carbonate compensation depth (CCD) is around 4500 m (Mewes et al. 2014), although much shallower to the east (~3500 m) than the

2

west (~5000 m) (Radziejewska, 2014). Bottom currents are generally weak (<10 cm s^{-1}), but direction shifts and periods of stronger flows are not infrequent (Aleynik et al., 2017). The supply of sinking food particles to the seafloor is extremely low (Lutz et al., 2007), although higher in the APEI6 area than in western areas (Veillette et al., 2007).
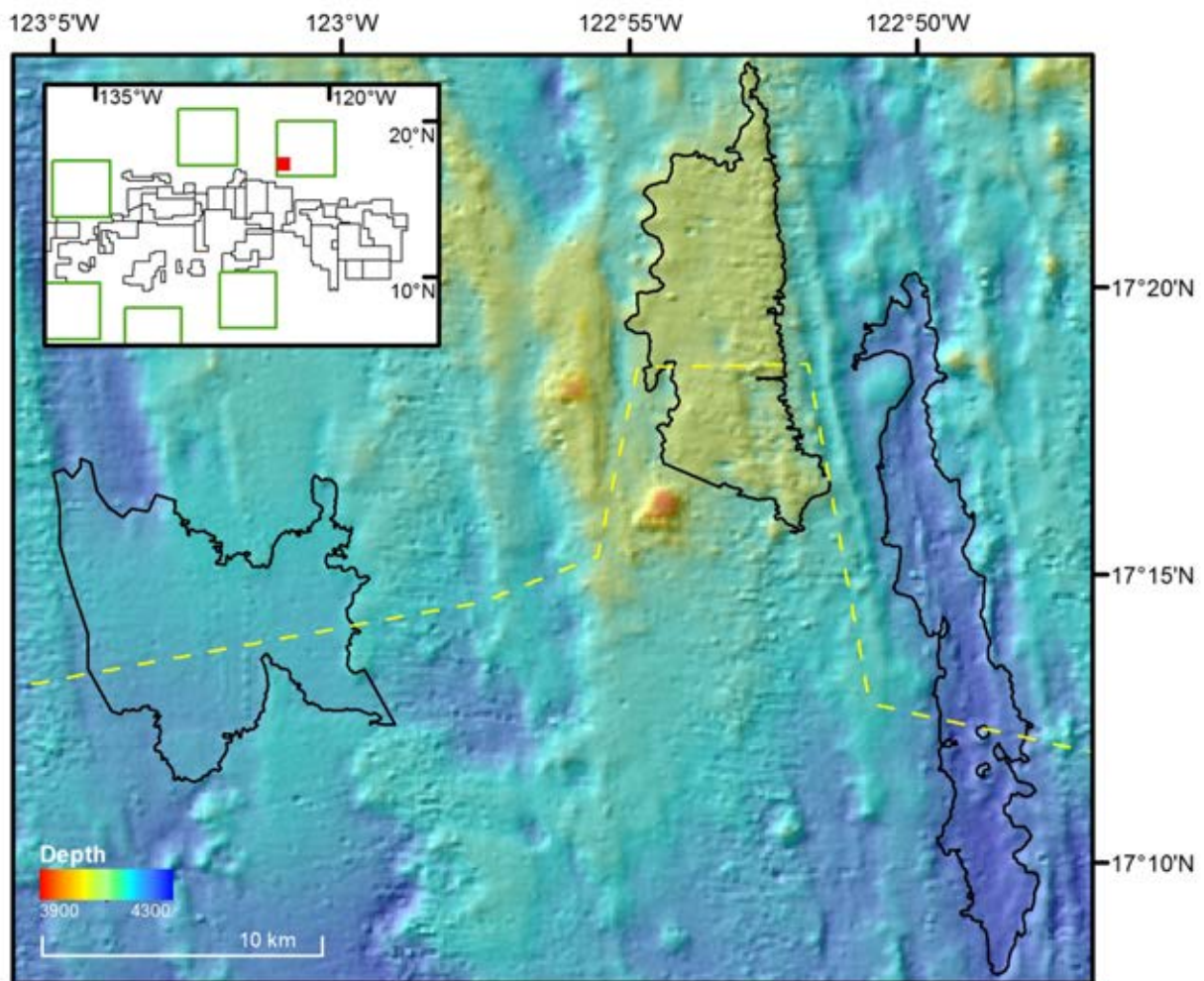
Fig. 1. Bathymetric survey chart of the study location within the APEI6 of the CCZ (North Pacific Ocean). Depth (in metres) is indicated by the colour bar. Landscape types mapped using objective classification depicted in dark lines. Yellow dashed line shows seafloor bathymetric profile depicted in Figure 2. A map of the eastern CCZ is inset, showing exploration licenced areas (black polygons), Areas of Particular Environmental Interest (green polygons), and study location (red square).

All results reported here relate to the APEI6 area, and were acquired during RRS *James Cook* cruise 120 (Jones, 2015). The survey represented a 5,500 km² rectangle of seafloor centred on 122° 55' W, 17° 16' N (Fig. 1), chosen to have similar topographic relief to mining contract areas in the central CCZ. Water depth ranged 3950-4250 m, and the seafloor landscape comprised a succession of crenulated ridges and shallow troughs oriented north-south between dispersed level-bottom (<3° slope) areas.

2.2.Survey design

3

2.2.1. Bathymetric mapping and landscape characterisation

Multibeam data were collected with the shipboard Simrad EM120 system (191 beams) and processed using CARIS HIPS and SIPS software (TeledyneCARIS; v8.0). The resultant digital elevation model (~100 m horizontal resolution) was used to calculate broad bathymetric position Index (bBPI) (Weiss, 2001) and terrain ruggedness index (TRI) (Wilson et al., 2007) using SAGA v. 2.1.4 software (Conrad et al., 2015). BPI was calculated using an inner radius of 500 m and an outer radius of 10,000 m, and TRI was calculated with a 500 m radius circular neighbourhood. These areas were selected to be representative of the landscape-scale geomorphological variation that was the target of this study. After visual inspection of the generated datasets, classification thresholds were set to map ridge (bBPI: 50 to 100; TRI: 0 to 150), trough (bBPI: -100 to -50; TRI: 0 to 150), and flat (bBPI: -100 to 50; TRI: 0 to 50) areas. Contours were drawn using ArcGIS v10 (ESRI, 2011) along threshold values of each dataset, and used to delimit representative polygons. Three polygons each representing a characteristic landscape type were chosen for stratified-random sampling: Flat area, Ridge area, and Trough area (Fig. 2). Data were projected in Universal Transverse Mercator projection, Zone 10N, using the World Geodetic System 1984 datum.
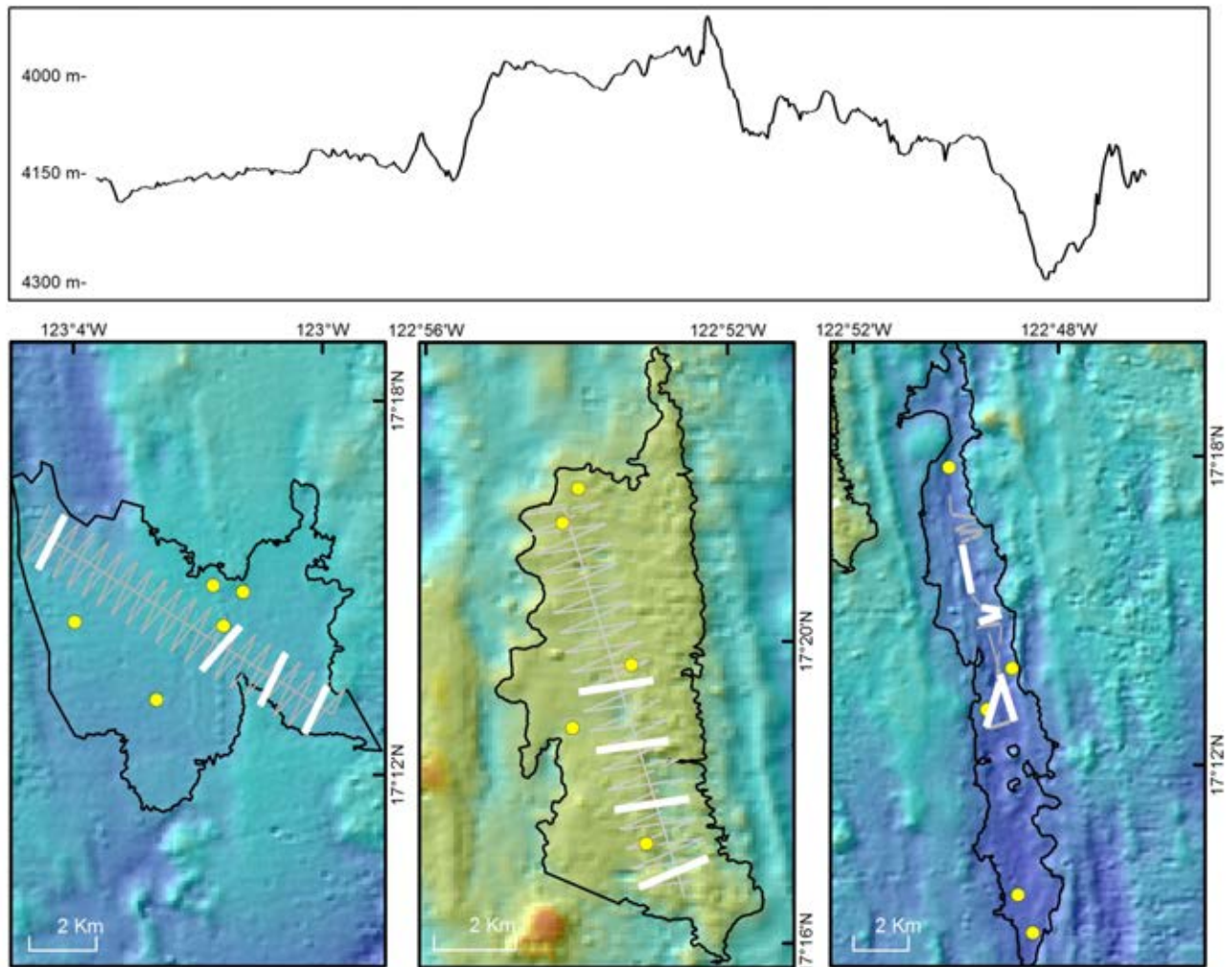
Fig. 2. Survey Landscape type study areas investigated at the APEI6. **A)** Seafloor bathymetric profile depicted as yellow-dashed line in Fig 1. **B to D:** Detail of sampling operations: grey lines indicate full AUV image survey tracks, thick white

lines highlight replicate sampling units selected for analysis, and yellow dots represent coring stations. Study areas surveyed: **B)** Flat area. **C)** Ridge area. **D)** Trough area.

2.2.2. Direct sampling

Five sediment sampling stations, with a minimum separation of 100 m, were randomly selected within each study area (Fig. 2.B-D). Two Megacore (Gage and Bett, 2005; 10cm internal diameter) samples were collected per station. Each sample was initially sliced and split by sediment depth. Sediment grain-size distributions were assessed from one core in 0-5 and 5-10 mm depth horizons, by laser diffraction using a Malvern Mastersizer 2000 after homogenisation (grains >2 mm removed), dispersal in 0.05% $(NaPO_3)_6$ solution, and mechanical agitation. Grain-size distributions obtained for the two horizons were averaged for presentation. The 0-10 mm horizon from the second core were assessed for sediment chemistry. Total carbon (TC) and total nitrogen (TN) contents were measured in duplicate (reproducibility <±5%) using a Carlo Erba NC 2500 CHN Elemental Analyser. Total organic carbon (TOC) was determined after de-carbonation of the samples using the acid HCl vapour method of (Yamamuro & Kayanne, 1995).

2.2.3. Photographic survey

Seafloor photographic images were collected using two digital cameras (FLIR *Grasshopper2*; 2448 x 2048 pixels), one mounted vertically, and one forward oblique facing on the autonomous underwater vehicle (AUV) Autosub6000 (Morris et al., 2014). The camera layout and the underwater navigation system were set as described in Morris et al. (2014). The AUV was programmed for a target altitude of 3 m above the seafloor, a speed of 1.2 m s^{-1}, and a photographic interval of 850 milliseconds. At the target altitude, individual vertical photographs imaged 1.71 m^2 of seabed.

In each area, a zig-zag survey design (Fig. 2.B-D), with random start point, was chosen to maximise sampling efficiency while minimising design-based bias in the spatial distribution of the replicate sampling units (Buckland et al., 2001; Strindberg & Buckland, 2004). A total of 40 sampling units, the straight line zig and zag sections, were surveyed in each area. Four sampling units were randomly selected in each area for subsequent analysis. Images taken as the vehicle changed course, i.e. junctions between sampling units, were discounted. In the remaining straight line sections, every second image was discounted to avoid overlap between consecutive images and the risk of double counting. To ensure consistency in specimen detection, images outside the altitude range 2-4 m were also discounted. The total seabed area analysed from each of the randomly selected sampling units was then standardised to c. 1320 m^2 (range 1321-1324 m^2) by random selection from the remaining constituent images, typically 715 photographs (range 555-781; SM, Table A.1). All images used for data generation were colour corrected as described by Morris et al. (2014).

2.3. Data analysis

2.3.1. Environmental assessment

Sediment grain size statistics were calculated using Gradistat v.8 software (Blott & Pye, 2001), applying the geometric method of moments (Krumbein, 1936). Mud content was calculated as the proportion of particles <63 µm. Carbonate content wet weight (% wt) was calculated from the difference between TC and TOC

(assuming all carbonate was $CaCO_3$). The ratio of total organic carbon to total nitrogen (C:N) was calculated as the molar ratio.

Nodule seafloor coverage (% cover) and total surface covered by nodules (m^2) were quantified from AUV imagery using the Compact-Morphology-based poly-metallic Nodule Delineation (CoMoNoD) method (Schoening et al., 2017). CoMoNoD attempts to detect all polymetallic nodules present in an image and calculates their areal extent (cm^2) based on an ellipsoidal shape projection, to correct for potential underestimation resulting from sediment cover. Only nodules ranging from 0.5 to 60 cm^2 (i.e. with maximum diameters of ~1 to ~10 cm) were considered for analysis to avoid inclusion of large non-nodule formations. Angular-shaped cobbles to large rocks and whale bones (min. diameter >10 cm) coated in ferromanganese crust were manually counted and measured. Average nodule cover (%) and total nodule area extent (m^2) were calculated across the selected images of each sampling unit.

2.3.2. Megafauna assessment

Images used for megafauna data generation were reviewed in random order to minimise time or sequence-related bias (Durden et al., 2016). Specimens (>10 mm) were identified to the lowest taxonomic level possible (morphospecies: msp), measured using the BIIGLE-DIAS software (Bielefeld Image Graphical Labeller and Explorer: Deep-sea Image Annotation System; (Langenkämper et al., 2017), and assigned to an "attached to hard substrata (i.e. nodules or rocks)" or "attached to sediment/unattached" life habit. To ensure consistency in identification, a megafauna morphospecies catalogue was developed and maintained in consultation with international taxonomic experts and by reference to the existing literature (Amon et al., 2017; Cummings et al., 2014; Dahlgren et al., 2016; Glover et al., 2016b). The likely feeding behaviour of each morphospecies was inferred from similar organisms described in the literature (i.e. Cummings et al., 2014; Iken et al., 2001). Individual metazoan specimen biovolume was estimated, as a proxy for biomass, from two body measurements using the generalised volumetric method described of Benoist et al. (submitted). Despite being comparable in size to metazoan morphospecies, xenophyophores were analysed separately since it is not possible to determine whether they are living from images (Hughes & Gooday, 2004).

A range of ecological parameters were calculated for each replicate sampling unit, including numerical density (ind m^{-2}) and proxy biomass density (ml m^{-2} ≈ g fresh wet weight m^{-2}). To examine the range of diversity characteristics, Hill's diversity numbers of order 0, 1, and 2 (Jost, 2006) were calculated as morphospecies richness (S), the exponential form of the Shannon index (exp H´), and the inverse form of Simpson's index (1/D), using the 'vegan' package implemented in R (Oksanen et al., 2007). Additionally, sample-based morphospecies rarefaction curves were fitted using the analytical method proposed by Colwell et al. (2012), using Estimate S v.9.1 software (Colwell, 2013), by randomly resampling sample data of each study area without replacement, while exp H´ and 1/D accumulation curves were calculated with replacement. K-dominance curves were also generated to explore dominance patterns (Clarke, 1990).

2.3.3. Statistical analyses

Generalized linear models (GLM) (Dobson & Barnett, 2008) were built to test whether statistically significant variation in environmental or biological parameters was apparent between study areas, using the 'car' package (Fox et al., 2016) implemented in R (R Core Team, 2017). Models were fitted with quasi-Poisson errors in non-negative integer metrics (i.e. density, S) with over-dispersion (Gardner et al., 1995), and with

normal errors applied to non-integer variables (i.e. mean grain size, exp H´, 1/D) (Freund & Littell, 1981). Differences in proportional metrics (i.e. nodule coverage, mud content, or functional group percentages) were tested with beta-regression models (Ferrari & Cribari-Neto, 2004) using the 'betareg' package (Cribari-Neto & Zeileis, 2010). When statistically significant effects were detected in these global test, simultaneous tests were applied to make multiple comparisons between individual study areas, using the 'multcomp' package in R (Hothorn et al., 2008). Homogeneity of variance and normality assumptions were verified by visual inspection of model histograms and QQ plots. Statistical significance was reported for $p < 0.05$.

Variations in community composition between study areas were explored using a range of abundance-based multivariate approaches. The Bray-Curtis dissimilarity measure, based on square-root transformed faunal density, as calculated using the 'vegan' package in R, was used throughout these analyses. Non-metric multidimensional scaling (nMDS) ordination was used to visualise variations ('vegan' package in R). A one-way permutational MANOVA (PERMANOVA) analysis (Anderson, 2001), with follow-up pair-wise tests, was used to test for statistically significant variations in assemblage composition between study areas, using PRIMER v.7 (Clarke & Gorley, 2015). A SIMPER (''similarity percentages'') analysis was performed to assess morphospecies contribution to between-group dissimilarity ('vegan' package in R).

2.3.4. Megafauna sampling effort evaluation

To assess the reliability of the biological survey developed in the present study, we investigated the effect of varying sampling unit size (seabed area or individuals covered per sample unit) on the accuracy (i.e. stabilization of mean value) and precision (i.e. coefficient of variation: CV) of different ecological parameters. Image data were first pooled within study area (i.e. across sampling units) and then randomly resampled 1000 times with or without replacement (depending on the target parameter and approach used: see below) into new sampling unit sets of increasing image number size. The mean (or median), the precision (CV), and the confidence intervals (95%) of each parameter were calculated at each sample unit size increase, together with the mean total seabed area and individuals represented by the images composing each subset.

Morphospecies rarefaction curves were fitted using the analytical method proposed by Colwell et al. (2012), using Estimate S v.9.1 software (Colwell, 2013), by randomly resampling image sets of increasing size without replacement. Accumulation curves were interpolated and extrapolated up to 3000 individuals sampled, to balance for differences in fauna densities. Additionally, curves were extrapolated up to 15,000 m^2 per study area (see SM-Fig S3). The autosimilarity approach proposed by Schneck and Melo (2010), as implemented in the seabed image case by Durden et al. (2016a), was applied to evaluate precision in assemblage description. At each sample size, Bray-Curtis dissimilarity was computed between two groups of images, each randomly selected without replacement and composed by half the total number of images of each set. Metazoan density, biomass density, and exp H´ and 1/D indexes were computed by bootstrapping image subsets resampled with replacement (Buckland et al., 2001). Custom R scripts and the 'vegan' package were used to process image data and calculate all ecological indices.

3. Results

3.1. Environmental assessment

414
415
416
417
418
419
420
421
422
423
424
425
426
427
428
429
430
431
432
433
434
435
436
437
438
439
440
441
442
443
444
445
446
447
448
449
450
451
452
453
454
455
456
457
458
459
460
461
462
463
464
465
466
467
468
469
470
471
472

Surface sediments (0-10 mm horizon) were dominated by radiolarian-bearing pelagic clay to fine silt particles (diameter <7.8 µm; 58-68% of particles), and medium to very coarse silt grains (diameter = 7.8-63 µm; 28-39% of particles). Mean and median particle size, and mud proportion showed no statistically significant variation between areas, though larger value ranges were evident among the Ridge area samples (Table 1). Subsurface sediments (>50 mm horizon) in the Ridge and Trough showed much greater variability in grain size distributions than those in the Flat area (SM, Fig. A.1; Table A.2). Relative proportions of TOC, TN, and CaCO$_3$ were almost homogenous across the study areas; no statistically significant differences were detected between study areas (Table 1).

The polymetallic nodules observed during the present study were of an ellipsoidal-flat shape with smooth surfaces. Mean nodule surface area was 2.5 cm^2, with most nodules <5 cm^2 (90%), and very few >10 cm^2 (1%). Nodules in the Flat were larger than in the other areas, though not significantly (Table 1). Average nodule cover was 6.4% and ranged from nodule-free to 38%. The highest mean nodule coverage was recorded in the Flat area (Table 1), although both the within-sampling unit and within-area deviations for this metric were high (SM, Table A.1). Nodule coverage did exhibit a statistically significantly difference between study areas (Table 1), with a statistically significant pair-wise difference between the Flat and Trough areas (Tukey, $p < 0.05$). Larger (>60 cm^2 in surface) hard substratum formations coated in ferromanganese crust were especially common in the Ridge area, where angular shaped cobbles, boulders, and whale bones were about ten times more abundant than in the other study areas (Table 1). However, the inclusion of these structures (total survey area surface <6 m^2) to the total hard-substratum availability of each sample unit was negligible, even in Ridge samples.

8

	Flat	Ridge	Trough	Error fit	F-value
Sample parameters					**($F_{2,14}$)**
Sediment mean grain size (µm)	8.1 (7.7 - 8.2)	9.5 (6.8 - 17.6)	9.2 (8 - 12.2)	G	0.34
Sediment mud content (%)	92.6 (91.7 - 93.8)	92.5 (79.9 - 95.7)	90.7 (85.6 - 93.2)	B	1.01
Sediment TOC (%)	0.42 (0.39 - 0.44)	0.41 (0.35 - 0.45)	0.44 (0.39 - 0.49)	B	0.8
Sediment C_{org} TN^{-1}	4.0 (3.8 - 4.3)	3.8 (3.6 - 4.0)	4.1 (3.7 - 4.5)	B	0.85
Sediment $CaCO_3$ (%)	0.33 (0.24 - 0.53)	0.48 (0.26 - 0.66)	0.36 (0.26 - 0.48)	B	0.5
Image parameters					**($F_{2,11}$)**
Nodule surface size (cm^2)	2.6 (2.3 - 2.9)	2.0 (1.7 - 2.3)	2.1 (1.6 - 2.6)	G	2.57
Nodule seabed cover (%)	10.1 (7.2 - 12.3)	6.3 (4.3 - 8.6)	3.8 (1.9 - 6.5)	B	**6.73****
Nodule seabed cover (m^2)	133.8 (95.4 - 162.6)	83.0 (56.4 - 113.8)	50.1 (24.5 - 86.4)	G	**4.82***
Other hard substrata (items ha^{-1})	62 (28 - 102)	682 (230 - 1132)	64 (30 - 102)	QP	**10.26****
Metazoan density (ind m^{-2})	0.49 (0.42 - 0.54)	0.47 (0.41 - 0.53)	0.32 (0.25 - 0.39)	QP	**5.23***
Metazoan biomass (g fwwt m^{-2})	1.6 (1.1 - 2.1)	2.9 (1.5 - 4.2)	2.1 (1.0 - 3.2)	G	0.79
Metazoan richness (S)	70.5 (67.2 - 74.0)	64.8 (61.0 - 68.5)	59.5 (50.5- 68.5)	QP	2.09
Metazoan exp(H')	29.7 (27.0 - 32.3)	28.3 (25.5 - 31.5)	23.4 (18.3 -28.4)	G	2.33
Metazoan 1/D	16.4 (14.2 -18.5)	16.4 (13.2 - 19.6)	9.7 (6.2 -13.2)	G	**4.66***
Metazoan OHS (ind m^{-2})	0.34 (0.29 - 0.38)	0.28 (0.23 - 0.35)	0.19 (0.13 - 0.25)	QP	**5.33***
Metazoan OHS (%)	69.3 (60.9 - 74.4)	60.0 (50.2 - 67.3)	57.2 (48.2 - 65.5)	B	2.49
Metazoan SF density (ind m^{-2})	0.39 (0.34 - 0.44)	0.34 (0.29 - 0.39)	0.25 (0.19 - 0.31)	QP	**4.25***
Metazoan SF (%)	79.8 (77.9 - 81.6)	73.6 (69.6 - 76.1)	77.2 (74.8 - 79.5)	B	**5.33***
Metazoan DF density (ind m^{-2})	0.07 (0.07 - 0.08)	0.10 (0.09 - 0.11)	0.05 (0.04 - 0.07)	QP	**13.90****
Metazoan DF (%)	15.9 (14.4 - 17.4)	21.6 (18.5 - 24.8)	17.2 (14.9 - 19.4)	B	**5.56***
Xenophyophore density (ind m^{-2})	2.22 (1.54 - 2.99)	4.09 (3.55 - 4.60)	1.33 (0.48 - 2.6)	QP	**5.94****
Xenophyophore OHS (ind m^{-2})	1.15 (0.75 - 1.64)	1.36 (1.01 - 1.71)	0.52 (0.15 - 1.14)	QP	2.22
Xenophyophore OHS (%)	50.7 (47.5 - 54.2)	32.8 (28.3 - 37.2)	32.7 (24.3 - 41.3)	B	**10.22****

Table 1. Environmental and biological features assessed for each landscape type of the APEI6 with detail on the general linear models (GLM) applied to explore variations of these parameters between study areas. **Sediment parameters:** measured from surface sediment (0-10 mm) and shown as: mean (minimum - maximum) obtained amongst all replicate Megacore samples (n=5) collected in each area. *Parameters*: particle size; mud content (particles <63 µm) percentage; percentages of total organic carbon (TOC) and $CaCO_3$; and molar C_{org}/Total nitrogen ratio. **Image parameters:** measured from seafloor imagery data and shown as: mean (95% confidence intervals: lower – upper) calculated amongst all replicate image samples (n=4) collected in each area. *Parameters*: seafloor percentage cover and total nodule area calculated using the CoMoNoD algorithm on seabed imagery (see text); density of non-nodule (>10 cm) hard substrata (boulders and whale bones); total density and proportion of metazoan and xenophyophore individuals (>10mm) split in different functional (SF: suspension feeders; DF: deposit feeders) and attachment-type (OHS: on hard substratum) categories; biomass (grams of fresh wet weight) density inferred using the generalised volumetric method (see text); and diversity: richness, exponential Shannon (exp H'), and inverse Simpson (1/D) indices.

Fig 3. Examples of metazoan megafauna photographed at the APEI6 seafloor during AUV survey. Scale bars representing 50 mm. **A)** Actiniaria msp-6**. B)** Actiniaria msp-13**. C)** *Bathygorgia cf*. *profunda*. **D)** *Abyssopathes* cf *lyra*. **E)** Left: *Chonelasma sp.*; right: *Hyalonema sp.* **F)** *Cladorhiza* cf *kensmithi*. **G)** *Bathystylodactylus* cf *echinus*. **H)** *Nematocarcinus* sp. **I)** Sabellida msp-1 (polychaete). **J)** Left: *Freyastera sp.*; right: *Caulophacus sp.* **K)** *Psychropotes* cf *longicauda* **L)** *Benthodytes* cf. *typica*. **M)** *Coryphaenoides* sp. **N)** *Typhlonus nasus* **O and P:** probable new *Mastigoteuthis sp.* same specimen photographed with different cameras. **O)** Vertical view **P)** Oblique view. Image taken ~1" prior to the vertical shot.

10

Phylum/Class	Group	Morphospecies	Flat		Ridge		Trough	
	(*)	(n)	OSS	OHS	OSS	OHS	OSS	OHS
Ctenophora	Tentaculata	2	1		1			
Porifera	Porifera	10	26	45	33	40	52	35
	Desmospongidae	7	42	126	53	119	174	342
	Hexactinelidae	9	8	19	19	4	17	9
Cnidaria	Scyphozoa	2	5				6	
	Aff. Anthozoa	1		4		7	1	5
	Actiniaria	13	49	306	39	242	36	93
	Alcyonacea	6	107	821	125	633	52	252
	Antipatharia	1		1		1		
	Ceriantharia	2	8	3	2	1	5	1
	Pennatulacea	1	2	1	1		1	
Bryozoa	Cheilostomatida	4	19	251	44	226	25	95
Annelida	Echiura	3	21		20		10	
	Polychaeta	5	63	152	60	173	34	104
Mollusca	Bivalvia	1	74		140		66	
	Gastropoda	2	8		1		3	
	Octopoda	1			1		1	
	Scaphopoda	1	19		7		8	
	Teuthoidea	1	29		29		22	
Arthropoda	Aff. Crustacea	-	33		36		38	
	Amphipoda	3	12		11		11	
	Cirripeda	2	2	23	2	14	3	7
	Copepoda	2	12		2		8	
	Decapoda	8	43		20		30	
	Isopoda	1	16		17		14	
	Peracarida	1	7		8		3	
Echinodermata	Asteroidea	5	14		4		4	
	Crinoidea	6	1	12	4	20	5	19
	Echinoidea	5	60		79		45	
	Holothuroidea	11	32		19		16	
	Ophiuroidea	4	78		161		38	
Chordata	Urochordata	2	3	6	1	1	3	7
	Osteichthyes	7	23		18		15	
TOTAL		**129**	**817**	**1770**	**957**	**1481**	**746**	**969**

Table 2. Total abundance and taxonomical classification of metazoan morphospecies groups sampled at each APEI6 study area. Abundances show how specimens were found: sessile attached to hard-substratum (OHS); sessile on sediment or mobile fauna (OSS). (*) "Group" level taxonomical classification is not hierarchical, ranges from Class to Family level, to simplify tabulation.

11

650
651
652
653
654
655
656
657
658
659
660
661
662
663
664
665
666
667
668
669
670
671
672
673
674
675
676
677
678
679
680
681
682
683
684
685
686
687
688
689
690
691
692
693
694
695
696
697
698
699
700
701
702
703
704
705
706
707
708

3.2. Megafauna assessment

3.2.1. Metazoan fauna

A total of 6740 megafauna individuals (>10 mm) were recorded in the 15,840 m^2 of seabed examined during the present study (Table 2). Megafauna were classified into 129 morphospecies and 11 higher taxonomic categories (i.e. Order, Family; Table 2). Rare taxa (≤ 3 records) represented a third of the total morphospecies richness. The fauna observed (Fig. 3) were predominantly cnidarians (25 msp; 0.18 ind m^{-2}, ~70% of which were Alcyonacea bamboo corals), sponges (27 msp; 0.07 ind m^{-2}), annelids (9 msp; 0.04 ind m^{-2}), bryozoans (4 msp; 0.04 ind m^{-2}), and echinoderms (32 msp; 0.04 ind m^{-2}). Mollusc, crustacean, fish, tunicate, and ctenophore morphospecies were also recorded at lower densities (<0.03 ind m^{-2}; Table 2). The metazoan fauna was primarily composed of suspension feeders (78%) and deposit feeders (16%), while predators and scavengers were scarce (4%). Almost 80% of suspension feeding individuals were found attached to polymetallic nodules or other hard substrata. The proportion of nodule-attached individuals was >70% of the total abundance in 37 morphospecies. These "nodule-dwelling" taxa constituted 70% of the total abundance, and 30% of the total richness recorded.

3.2.1.1. Patterns in faunal distribution

Mean metazoan density exhibited a statistically significantly difference between study areas (Table 1), with densities in Flat and Ridge areas higher than those in the Trough (Tukey, $p < 0.05$). We detected statistically significantly higher densities of suspension feeders in the Flat area compared to the Trough, and statistically significantly higher densities of deposit feeders in the Ridge than in the other study areas (Tukey, $p < 0.05$). Mean density and proportion of predators and scavengers was similar in all study areas (Table 1). Although the proportion of the fauna attached to nodules was not statistically significantly different between study areas (Table 1), the densities of nodule-attached individuals were statistically significantly higher in the Flat than in the Trough (Tukey, $p < 0.01$). The mean biomass density recorded across all sampling units was 1.22 g fwwt m^{-2} (in c. 1320 m^2 observed), with no statistically significant difference detected between study areas (Table 1).

Mean morphospecies richness (S) was higher in the Flat, though we found no statistically significant difference between study areas (Table 1). Sample-based morphospecies accumulation curves showed that this pattern was consistent at whole study areas sampling level (Fig. 4.A), and extrapolation of image-based curves predicted the same scenario even when triplicating the total sampling performed per study area (SM-Fig. A.2). Variations in diversity between study areas were more evident at progressively higher Hill's orders (q > 0). Mean exp H' and 1/D indices were higher in the Flat and the Ridge areas compared to the Trough, although these differences were statistically significant only in 1/D index (Table 1). These patterns were consistent at whole study areas sampling level (Fig. 4.B-C). We also detected a higher morphospecies dominance in the Trough area, and more even abundances in the Flat and Ridge areas (Fig. 5.A).
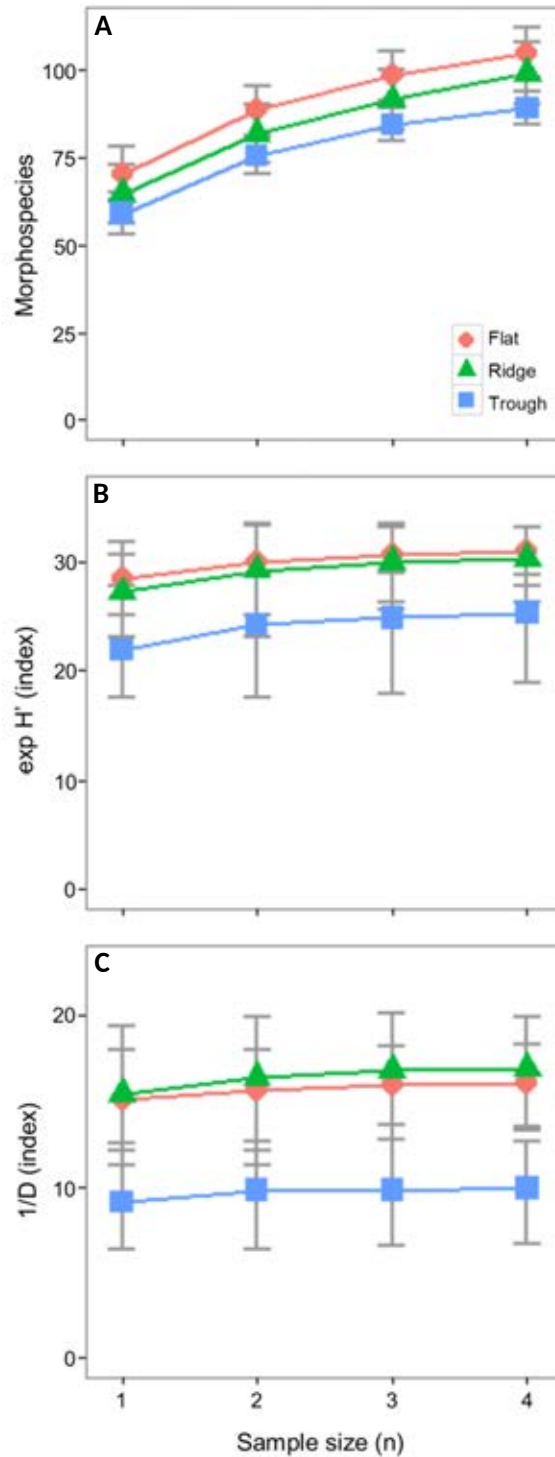
Fig. 4. Sample-based diversity accumulation curves calculated for each APEI6 study area. Fauna occurrences of each replicate sample were randomly resampled (with or without replacement) 1000 times at each sampling effort level (n=1-4). **A)** Species rarefaction calculated without replacement. **B)** Exponential Shannon index, calculated with replacement. **C)** Inverse Simpson index, calculated without replacement. Error bars represent 95% confidence intervals between runs.

13
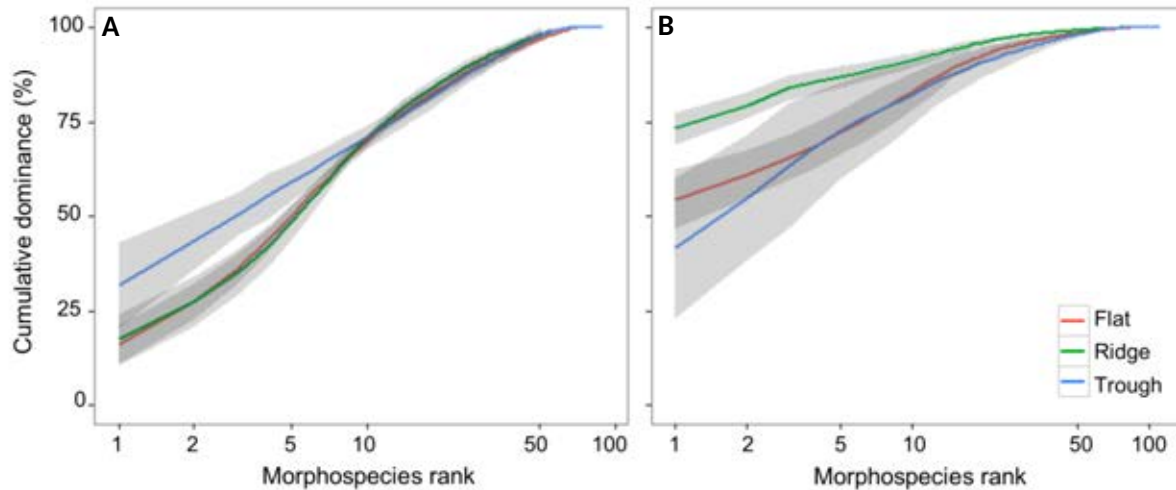
Fig. 5. Morphospecies k-dominance curves calculated for each APEI6 study area. Curve lines represent cumulative rank abundances calculated as the mean amongst the four replicate samples analysed for each area. Shadowing represents 95% confidence intervals. **A)** Curves calculated including only metazoan fauna. **B)** Curves calculated including metazoans and xenophyophores.

3.2.1.2. Variations in community composition

Cnidarians, sponges, bryozoans, and echinoderms showed the clearest variations in density between study areas (Fig. 6). In total, 54% of the morphospecies recorded were present in all three study areas, 22% were noted in only two areas, and 24% were detected in one area only area. Most (70%) of the single area records were singletons (SM, Fig. A.3) and the rest rare morphospecies ($\leq$ 5 occurrences). Nevertheless, a statistically significant difference in faunal composition was detected between the study areas (PERMANOVA, $R^2 = 0.39$, $p < 0.001$) (Fig. 7.A), with statistically significant differences apparent in paired comparisons between the Trough and the other study areas (pair-wise PERMANOVA, $R^2=0.36$-0.37, $p < 0.05$). SIMPER analysis showed that variations in the density of 10-15 morphospecies were responsible for 70% of the dissimilarity between study areas, but three morphospecies, a sponge (Porifera msp-5) and two soft corals (*Lepidisis* msp and *Callozostron* cf. *bayeri*), contributed most to the significant dissimilarities. Total density of *Porifera* msp-5 in the Trough (8.7 ind 100^{-1} m^{-2}) was four times higher than in the Ridge and Flat areas; total density of *Lepidisis* msp in the Flat (3.8 ind 100^{-1} m^{-2}) was four times higher than in the Ridge and 20 times higher than in the Trough areas; while total density of *C.* cf *bayeri* in the Ridge and the Flat (~2.5 ind 100^{-1} m^{-2}) was four times higher than in the Trough area.

14

827
828
829
830
831
832
833
834
835
836
837
838
839
840
841
842
843
844
845
846
847
848
849
850
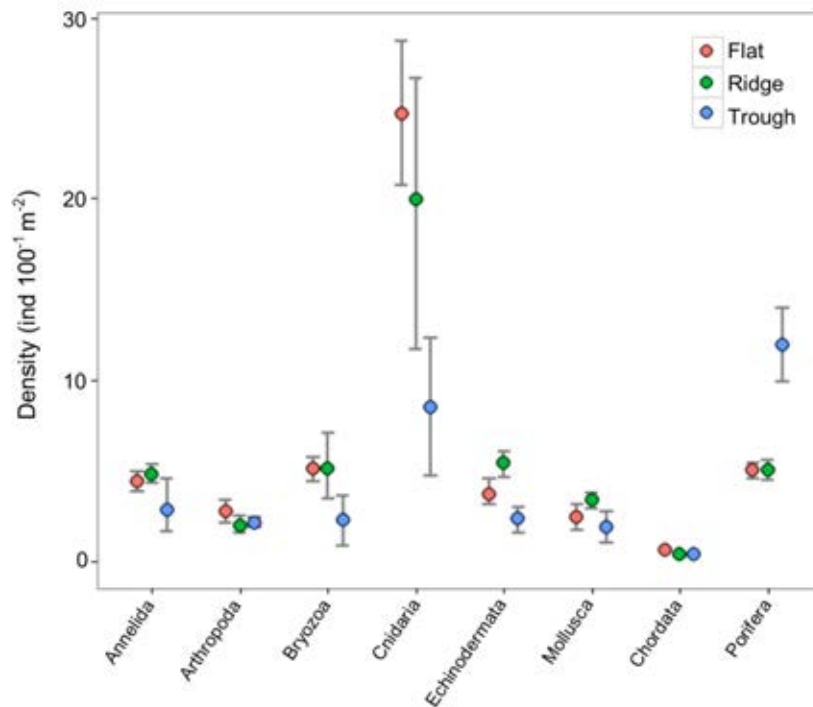
Fig. 6. Density variations of different metazoan taxonomic groups between APEI6 study areas. Points represent the mean density of each group calculated amongst the four replicate samples analysed for each area. Error bars represent 95% confidence intervals.
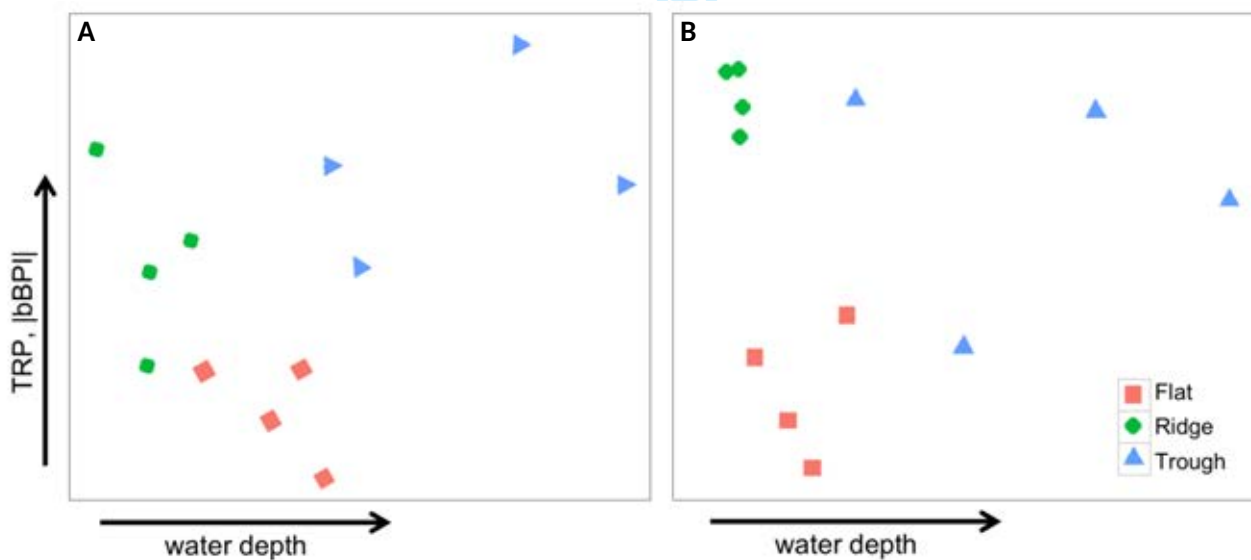
Fig. 7. Interpreted megafauna morphospecies composition nMDS for APEI6 samples. Two-dimensional representations of nMDS developed on Bray-Curtis resemblance matrix calculated from square-root transformed megafauna composition by abundance data. **A)** nMDS plot developed including only metazoan fauna. **B)** nMDS plot developed including metazoans and xenophyophores. Arrows indicating the (non-linear) trend in water depth and bathymetric derivatives suggested for each axis.

15

886
887
888
889
890
891
892
893
894
895
896
897
898
899
900
901
902
903
904
905
906
907
908
909
910
911
912
913
914
915
916
917
918
919
920
921
922
923
924
925
926
927
928
929
930
931
932
933
934
935
936
937
938
939
940
941
942
943
944

3.2.1.3. Sample unit size evaluation

Estimates of most of the ecological parameters assessed were consistent at the sample unit size used in the present study (c. 1320 m^2 of seabed) (Figs. 8-9). The maximum precision (CV) reached by each parameter with increasing sample unit size ranged from 0.02 to 0.30 (SM, Fig. A.4), yet increases in precision were relatively minor for most parameters with unit sizes >300 individuals (700-900 m^2), except for autosimilarity, which required much smaller sizes (>150 individuals; 300-450 m^2) to reach an almost constant precision rate (SM, Fig. A.5). Analysis of accuracy yield more variable results. Estimation of mean taxa richness required the largest unit size to stabilise (>500 individuals; 1000-1500 m^2) (Fig. 8.A-B), while fauna density required the smallest (>30 individuals; 50-100 m^2) (Fig. 9.A-B). Mean autosimilarity required unit sizes >500 individuals (1000-1500 m^2) to stabilise (Fig 9.C-F). At this size, mean within-sample similarity was >70% (i.e. two sub-samples of 250 individuals randomly generated from 500 individuals yield an average similarity >70%). Accuracy of biomass density estimates differed between study areas: sample unit sizes >500 individuals were required for stabilisation of median values in the Flat and Trough samples, while stabilisation in the Ridge occurred >250 individuals. Mean exp H' stabilized with unit sizes >350 individuals (700-1000 m^2) (Fig. 8.C-D), while mean 1/D stabilised with >200 individuals (400-600 m^2) (Fig. 8.E-F).

16

945
946
947
948
949
950
951
952
953
954
955
956
957
958
959
960
961
962
963
964
965
966
967
968
969
970
971
972
973
974
975
976
977
978
979
980
981
982
983
984
985
986
987
988
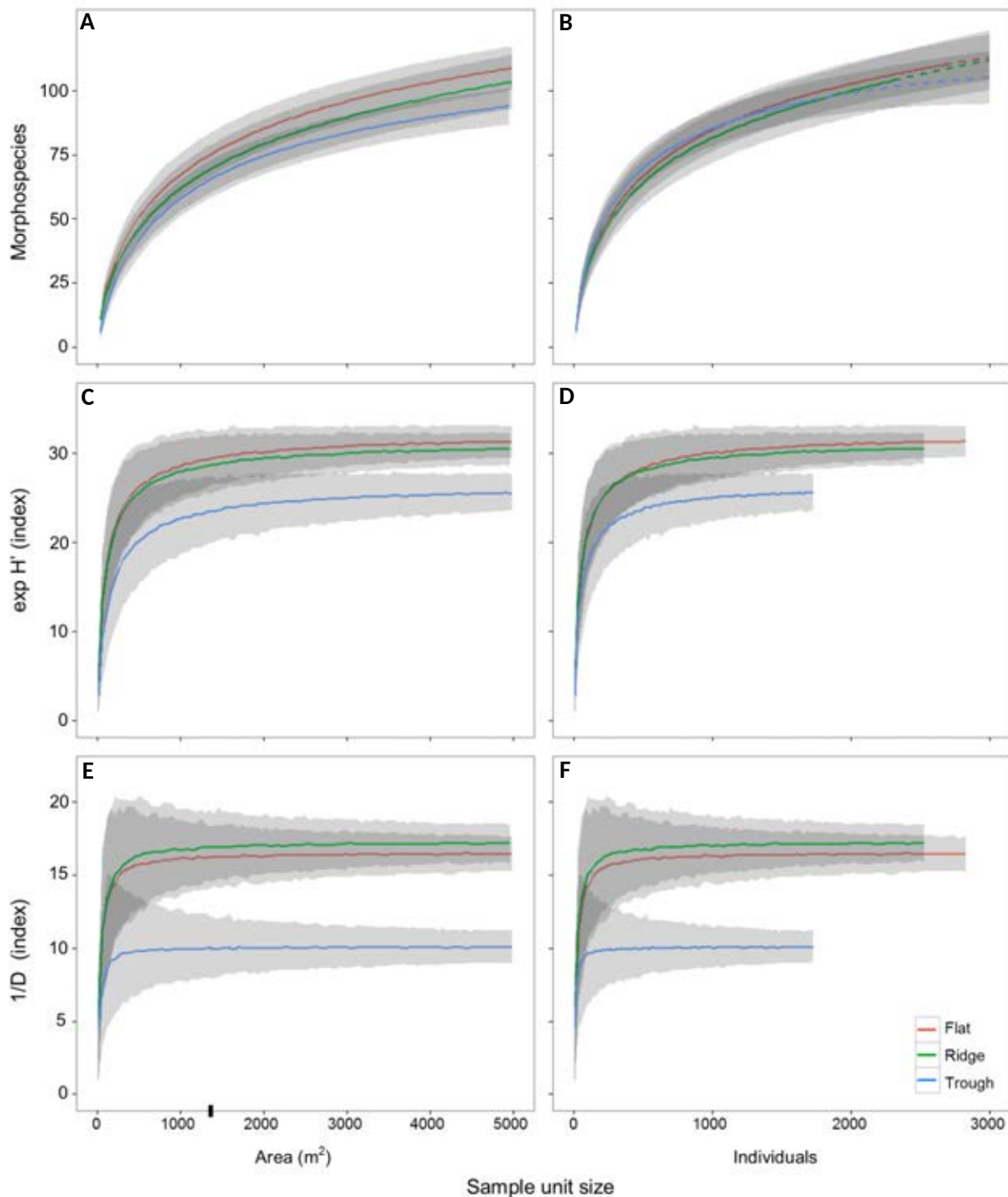
Fig. 8. Variation of the different metazoan community diversity indices used in the present study, as a function of the seabed area or number of individuals encompassed by the sample unit size. Lines represent mean values across the 1000 randomisations performed at each sample unit size increse, for each study area collated sample (n=3) (see methods). Shadowing representing 95% confidence intervals. Ticks on x-axis indicate the sampling unit size used in the present study (replicate sample areas = 1320 m²). **A and B:** Rarefied metzaoan morphospecies accumulation curves. **A)** Area-based accumulatiuon curves. **B)** Individual-based accumulation curves. Dashed lines represent sample extrapolation. **C and D:** Variation of metazoan exp H' diversity index. **E)** Area-based mean exp H'. **F)** Individual-based

989
990
991
992
993
994
995
996
997
998
999
1000
1001
1002
1003

17

mean exp H'. **E and F:** Variation of metazoan 1/D diversity index. **I)** Area-based mean 1/D. **J)** Individual-based mean 1/D.
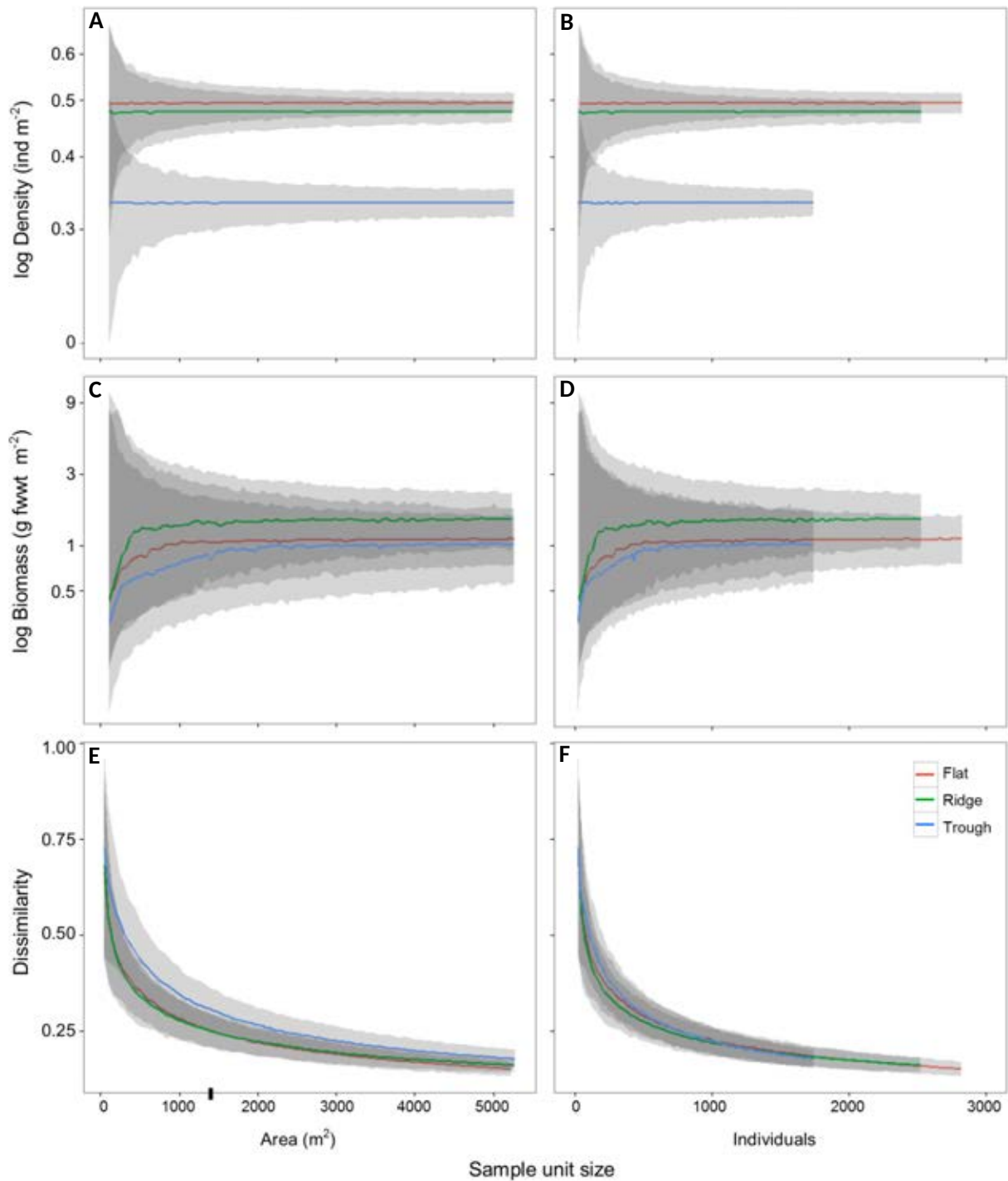
Fig. 9. Variation of the different metazoan community parameters used in the present study as a function of the seabed area or number of individuals encompassed by the sample unit size. Lines represent mean or median values across the 1000 randomisations performed at each sample unit size increse, for each study area collated sample (n=3) (see methods). Shadowing representing 95% confidence intervals. Ticks on x-axis indicate the sampling unit size used in the present study (replicate sample areas = 1320 m2). **A and B:** Variation of mean metazoa density. **A)** Area-based mean

18

density. **B)** Individual-based mean density.**C and D:** variation of median metazoan biovolume concentration. **A)** Area-based median biovolume. **H)** Individual-based mean biovolume. **E and F:** autosimilarity curves showing mean Bray-Curtis dissimilarity index calculated amongst pairs of metazoan samples. **E)** Area-based autosimilarity curves. **F)** Individual-based autosimilarity curves.

3.2.2. Xenophyophore fauna

Xenophyophore tests (Fig. 10) numerically dominated the megafauna recorded during the present study; being overall, six times more abundant than metazoans, and reaching a peak density of 17 ind m^{-2} in an image from the Ridge area. Mean xenophyophore density exhibited a statistically significantly difference between study areas (Table 1), with densities in the Ridge higher than those in the Trough (Tukey, $p < 0.01$). The recently described species *Aschemonella monile* (Gooday et al., 2017a) (Fig. 10.B) dominated the fauna, having mean densities of 3.27, 1.51, and 0.85 ind m^{-2} in the Ridge, Flat, and Trough areas respectively. The numerical dominance of xenophyophores has substantial impact on the perception of relative faunal diversity among the study areas (Fig. 5.B), inclusion of these foram taxa markedly increased rank 1 dominance (Berger-Parker index) in the Flat and Ridge areas, indicating a very substantial reduction in diversity in the Ridge area particularly.

Xenophyophores were classified in 23 morphospecies. Xenophyophore faunal composition exhibited statistically significant variation between study areas (PERMANOVA, $R^2 = 0.55$, $p < 0.001$), and statistically significant differences detected in all paired comparisons (pairwise PERMANOVA, $R^2 = 0.39$-0.61, $p < 0.05$). Joint analysis of xenophyophore and metazoan faunal composition yielded comparable results (Fig 7.B) to those obtained from the analysis of metazoan taxa only (Fig 7.A); statistically significant variations between study areas (PERMANOVA, $R^2 = 0.48$, $p < 0.001$) were led by statistically significant differences between the Trough and the other study areas (pairwise PERMANOVA, $R^2 = 0.37$-0.45, $p < 0.01$).
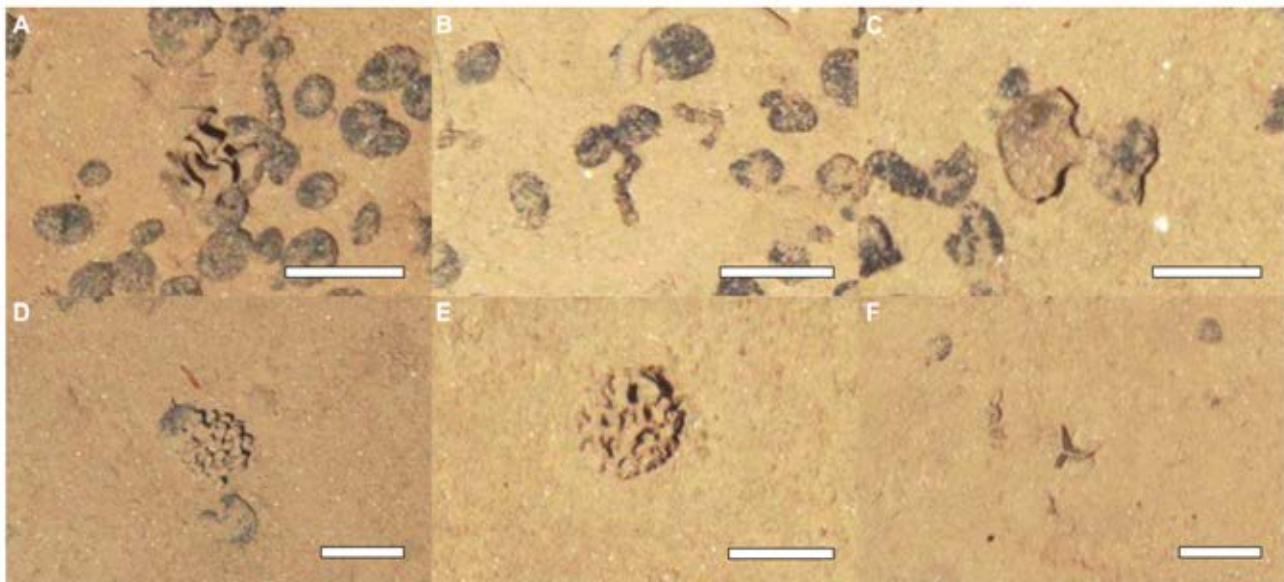
Fig. 10. Examples of xenophyophore megafauna photographed at the APEI6 seafloor during AUV survey. Scale bars representing 50 mm. **A)** *Reticulammina* msp. **B)** *Aschemonella monile.* **C)** Fan-shaped *Psammina* msp. **D)** Indeterminate Psamminid msp, possibly *Shinkaiya* or *Syringammina*. **E)** *Syringammina* cf *limosa.* **F)** Triradiate *Psammina* msp, possibly *P. multiloculata*.

1122
1123
1124
1125
1126
1127
1128
1129
1130
1131
1132
1133
1134
1135
1136
1137
1138
1139
1140
1141
1142
1143
1144
1145
1146
1147
1148
1149
1150
1151
1152
1153
1154
1155
1156
1157
1158
1159
1160
1161
1162
1163
1164
1165
1166
1167
1168
1169
1170
1171
1172
1173
1174
1175
1176
1177
1178
1179
1180

4. Discussion

4.1.Environmental setting at the APEI6

The high homogeneity in particle size and nutrient availability found across the APEI6 study areas suggests that these factors may be consistent over scales broader than the tens of kilometres between areas studied here. Our results were somewhat unexpected since variations in sediment grain-size distributions and particulate organic matter have commonly been reported between landscape types in previous assessments in the north Atlantic abyss (Durden et al., 2015; Morris et al., 2016), where bottom current speed ranges (Vangriesheim et al., 2001) are comparable to those expected at the APEI6, but sediments were coarser and more heterogeneous. Surface sediment particle sizes at the APEI6 were comparable in range to those found in eastern CCZ contract areas (Khripounoff et al., 2006; Mewes et al., 2014; Pape et al., 2017). Although sediments in these -more southerly- areas exhibit bimodal particle size distributions, being primarily composed of clays and fine silts (<6.3 μm), but with higher proportions of sands (>63 μm) than at the APEI6. Ranges of TOC (0.41-0.44%) and C:N ratios (3.8-4.1) were also comparable to those reported in eastern CCZ contract areas (Khripounoff et al., 2006; Mewes et al., 2014; Pape et al., 2017). This suggests that the sedimentary environment of the APEI6 may be generally representative of the environment found at a larger scale (i.e. eastern CCZ), although further exploration in other contract areas would be required to draw more precise conclusions in this regard.

Variations in nodule abundance could be indicative of environmental change between study areas. Locally stronger bottom-water currents reducing deposition rates are presumed to enhance nodule formation (Mewes et al., 2014; Skornyakova & Murdmaa, 1992). Higher nodule abundances in mild slopes and elevated seafloors, such as the Flat and the Ridge areas, have commonly been linked with low sedimentation rates (Frazer & Fisk, 1981; Mewes et al., 2014). Yet convergent channelling of bottom currents in bathymetric valleys, such as the Trough area, has also been suggested to limit deposition enhancing nodule growth (Peukert et al., 2018). The more irregular nodule coverage we observed in the Ridge (SM, Table 1) concurs with previous descriptions of hilltop environments at the CCZ (Jung et al., 2001; Margolis & Burns, 1976; Skornyakova & Murdmaa, 1992). In these, current circulation over rugged seafloor can generate scattered redistribution of surface materials (Jung et al., 2001; Nasr-Azadani & Meiburg, 2014; Peukert et al., 2018), which may have reduced the sediment blanketing of hard structures (i.e. rock fragments, whale bones) and trace fossils (Durden et al., 2017b) within the Ridge.

4.2.Sample unit size evaluation

Narrowing of the precision range with increasing sample unit size was apparent in all parameters (SM, Fig. A.5), as was expected from previous image-based assessments (Durden et al., 2016b), but the accuracy of each parameter (Figs. 8-9) showed a different sensitivity to this factor. The sample unit size we used in this study (c. 1320 m^2 of seafloor) was therefore sufficiently large for reliable estimation of fauna density, diversity of higher orders, and community dissimilarity, but was arguably too small for the assessment of taxa richness and biomass density patterns, as not all samples collected (SM, Table A.1) contained the minimum of 500 individuals suggested by our analysis for a reliable characterisation of these two parameters.

It is conceivable that the higher sensitivity to sample size was a "rarity-driven" effect. On the one hand, the low density combined with the high taxa richness we found at the APEI6 yield high rates of taxon rarity in our assessment. This is commonplace in abyssal sampling (Smith & Demopoulos, 2003), but has a negative effect on the accuracy of those diversity indices more sensitive to rare taxa, such as richness (Magurran, 2004; Soetaert & Heip, 1990). On the other hand, the high rarity of particularly large individuals appeared to restrict the accuracy of biomass density assessment, especially within the Flat and the Trough areas, were larger-sized fauna were even rarer. Predominance of the smaller taxa is common in low-productivity abyssal habitats (Rex et al., 2006; Smith et al., 2008a), yet large megafaunal species have an important ecological role in these environments (Billett et al., 2001; Ruhl et al., 2008), and these appear to require rather large sample unit sizes to be best characterised (i.e. 250-500 ind: this study). Higher rarity rates are therefore expected in abyssal megafauna surveys as an artefact of lower sample unit sizes, which can influence other parameters such as diversity or community composition analysis.

Our results underline that sampling unit evaluation is important for assessing the reliability of ecological patterns inferred from abyssal sampling. Minimum sample sizes for accurate estimation exhibited by different parameters were extremely variable (range: 30-500 individuals; 100-1500 m^2 of seafloor per sample unit). This means that with sampling units <400 m^2, most biological parameters estimated here would have been largely inaccurate and imprecise. For instance, it is likely that no variation in diversity nor community composition between areas might have been detected if transect size of this study had been set below 600 m^2, which would have biased the overall conclusions. This underlines the importance of appropriate tuning of the sampling unit size in abyssal ecology, especially at the CCZ, where these may have a paramount influence on conservation policy (Durden et al., 2017a; Levin et al., 2016). However, sample unit analyses have been commonly ignored in most assessments of megafauna at the CCZ (Stoyanova, 2012; Tilot et al., 2018; Vanreusel et al., 2016; Wang & Lu, 2002). This adds a level of difficulty to the already constrained comparability between studies in the region (Amon et al., 2016), and bounds the study of ecological patterns at the regional scale.

The use of different sampling devices and methods (i.e. definition of megafauna size, camera altitude, sampling unit size), is an ongoing issue for the comparability of image-based analyses (Durden et al., 2016b), especially at the CCZ (Amon et al., 2016). For example, megafauna assessments performed by Tilot et al. (2018) and Stoyanova (2012) using a different camera set-up reported densities ten times lower than those reported by Vanreusel et al. (2016) at the same contractor areas (IFREMER-2 and IOM-2, respectively). The application of improved imaging systems may have increased the apparent megafauna densities, influencing diversity estimations. This stresses the need for a standardization of both assessment method and morphotype taxonomy across the CCZ, to enable more reliable comparisons between the various APEI and claim areas, and simplify the detection of possible biogeographical boundaries across the CCZ.

4.3.Landscape ecology of metazoan megabenthos

Differences in megafauna density across the landscape types studied were predominately driven by variations in suspension feeder abundance (Table 1), particularly sessile cnidarians (Fig. 6). Potential topographically-enhanced bottom water current speeds have previously been suggested to promote the development of suspension feeding fauna in the abyss (Durden et al., 2015; Smith & Demopoulos, 2003; Thistle et al., 1985). Suspension feeders usually dominate the megabenthos in the CCZ and show higher abundances in areas with higher nodule density (Amon et al., 2016; Stoyanova, 2012; Vanreusel et al., 2016). Factors promoting higher nodule densities also enhance the development of suspension feeders (Vanreusel

21

et al., 2016); for example, in the present study most suspension feeders (80%) were attached to nodules. Suspension feeder density, and relative abundance, may therefore be related to both the availability of hard substrata and local enhancements in bottom water currents, and that the latter two factors may themselves be related. These factors suggest that low slopes or elevated topographies, as found at the Flat and Ridge areas, enhance suspension feeder densities increasing the overall metazoan standing stock of these areas, as compared to depressions, like the Trough area.

Variations in functional composition between study areas were driven by the distribution of deposit feeder fauna, suggesting enhanced resource availability for this group in the Ridge. This could indicate a higher food supply at the more elevated seafloor of the Ridge, owing to less particulate organic carbon loss during sinking (Smith et al., 2008a), but this is likely a small effect at abyssal depths for changes of few hundred meters (Lutz et al., 2007). Moreover, sediment TOC exhibited no statistically difference between study areas, nor was there a statistically significant difference in the C:N ratio. This suggests that, if there were variations in food supply for deposit feeders, these may either have occurred at a finer spatial scale (i.e. patch accumulations: Lampitt, 1985; Smith et al., 1996), or be related with the quality rather than the quantity of the available resource (Ginger et al., 2001).

Deposit feeder abundance was predominantly composed by ophiuroids (Table 2), and the density of these was both positively correlated with xenophyophore test abundance (r_s= 0.77-0.79, p < 0.01), as was the density of predator and scavenger fauna, although at a weaker level (r_s= 0.65, p < 0.05). Biological structures can be important in the generation of habitats in the deep-sea (Buhl-Mortensen et al., 2010). Such associations are common in the in the north-eastern Pacific abyss, for instance, sponge stalks can serve as microhabitats for species-rich assemblages of suspension-feeder epifauna (Beaulieu, 2001), or for the attachment of octopod egg clutches during brooding (Purser et al., 2016). Co-occurrence of xenophyophores and ophiuroids has been previously documented in eastern Pacific seamounts (Levin et al., 1986; Levin & Thomas, 1988). Levin (1991) suggested that xenophyophore tests represent a sTable A.ubstratum that can function as refuge from predators and or nursey habitat for juvenile mobile metazoans, like ophiuroids. Xenophyophore test substratum has shown to play a crucial role in the regulation of meiofauna and macrofauna communities at the CCZ (Gooday et al., 2017b), and our results suggest that these may also be important in the functional structuring of megafauna.

Heterogeneity diversity measures indicated clearly reduced diversity in the Trough relative to Flat and Ridge areas, markedly so in the case of 1/D index (Fig. 4.C). The dominance component of diversity was higher in the Trough (Fig. 5.A) unless xenophyophores were included (Fig. 5. B). The lower metazoan heterogeneity diversity of the Trough was caused by a general decrease in the density of most morphospecies, combined with a clearly higher abundance of the sponge *Porifera msp-5*, possibly better adapted to a presumably more disturbed environmental regime in this area. *Porifera msp-5* was amongst the smallest morphospecies we detected (mean diameter: 13.1 ± 3.1 mm; without elimination of individuals >10 mm: 8.8 ± 3.4 mm) and was predominantly found (>70%) encrusting nodules. A recent study revealed a similar dominance, also exhibited by a small nodule-encrusting sponge (*Plenaster craigi*) in the eastern CCZ (Lim et al., 2017). Our results highlight the importance of a standardized detection of small -and usually predominant- taxa for robust assessment of heterogeneity diversity in CCZ megafauna communities.

Previous CCZ megafauna studies related the presence of nodules with increased metazoan richness (Amon et al., 2016; Tilot et al., 2018; Vanreusel et al., 2016). Although we found no direct correlation between nodule availability and sample diversity (of any order), it is possible that the overall lower nodule availability of the Trough played an important role in the reduction of evenness we observed there, since most of the

22

APEI6 metazoan abundance was composed by nodule-dwelling taxa. However, the survey design applied in this study was optimised for the detection of patterns at a relatively broad scale (few kilometres), compared to the tens of meters at which nodule coverage variations usually occur at the CCZ (Peukert et al., 2018). Moreover, our sampling effort evaluation highlighted that two samples did not contain a sufficiently large specimen coverage (<500 ind) to reliably assess richness patterns, and that this may also have affected the estimation of richness in previous studies. Further analysis of the APEI6 dataset at a finer spatial scale (in prep.) shall further expand and contextualize the precise relation between nodules and both the richness and evenness components of megafauna diversity.

Statistically significant differences in megafaunal density, functional composition, evenness and taxon composition were variously apparent between the landscape types studied. Previous studies showed that even modest topographic elevation (i.e. hills) has substantive effect on abyssal megafaunal compositions (Durden et al., 2015; Leitner et al., 2017; Stefanoudis et al., 2016). However, in this study the assemblages of the Flat and Ridge (in previous studies: plain and hill areas, respectively) showed a higher similarity, as compared to the Trough area, where most taxa densities were somewhat reduced and the dominant morphospecies shifted from colonial bamboo corals to a small-encrusting sponge. The higher availability of nodule and xenophyophore-test substrata in the Ridge and the Flat possibly increase the heterogeneity of these areas, enhancing the development of a more even assemblage type. Variations in heterogeneity commonly regulate niche diversification processes (Tews et al., 2004), exerting a fundamental influence on the diversity and structure of deep-sea benthic communities (Levin et al., 2001). Thus, our results suggest that by regulating nodule and xenophyophore test availability -and presumably bottom current speeds- geomorphological variations play a crucial role in the structuring of the CCZ megabenthos at the landscape scale.

4.4. Ecological significance of megafaunal xenophyophores

Test densities were almost four times higher in Ridge samples than in the Trough, and almost twice as dense as within the Flat area. Previous studies have also described higher relative xenophyophore densities in sites with sloping topography and enhanced water motion (Levin & Thomas, 1988; Stefanoudis et al., 2016). The feeding modes and strategies of xenophyophores remain uncertain (Gooday et al., 1993; Laureillard et al., 2004), with passive particle-trapping, suspension or deposit feeding mechanisms noted (Kamenskaya et al., 2013; Levin & Gooday, 1992). Accepting our inability to distinguish living specimens, that *A. monile* specimens alone represent over 70% of all megafauna observed in the Ridge area suggests considerable ecological significance for this taxon, and the xenophyophores as a group. Note that our identification of 23 xenophyophore morphospecies is undoubtedly an underestimate of their true species diversity, particularly in the CCZ where these are exceptionally diverse (Gooday et al., 2017b; Kamenskaya et al., 2013).

Inclusion of xenophyophores substantially affected the assessment of biological diversity, particularly in respect to heterogeneity diversity. It is conceivable that this was a 'true body size' mismatch effect. For example, Levin and Gooday (1992) suggest a protoplasm volume of 1 to 0.01% of test volume. This means that the mean test biomass of *A. monile* at the APEI6 was possibly <1 mg fwwt ind^{-1} - provided its devoid of protoplasm test interior (Gooday et al., 2017a)- while the mean biomass of the smallest taxa recorded in the metazoan fraction ranged between 40-60 mg fwwt ind^{-1}. As smaller individuals are largely more abundant in the abyss (Smith et al., 2008a), it is likely that the inclusion of xenophyophores artificially reduced the heterogeneity diversity, given that ~ 1 mg fwwt sized individuals from other taxa were not possible detect

23

and hence not represented in analyses. Consequently, general interpretation of diversity is probably best limited to the metazoan only assessments.

5. Conclusions

This paper presents an ecological assessment of megabenthic faunal distribution in response to seafloor geomorphology at the CCZ. Differences in the megafaunal ecology between landscape types of the APEI6 manifested as changes in standing stock, functional structure, diversity, and community composition. This shows that local geomorphological variations can play an important role in the structuring of the CCZ megabenthos. Our assessment somewhat concurs with previously reported differences between abyssal hills and adjacent plains in North Atlantic megafauna (Durden et al., 2015), and in fish populations at the CCZ (Leitner et al., 2017). Yet we have added a level of abyssal landscape heterogeneity (troughs), where megafauna showed the clearest variations. Analyses of sampling effort support our results: the collected sample size enabled a stable estimation of key biological metrics, but also highlighted limitations in understanding of some parameters.

Benthic ecology has been suggested to be regionally controlled by a gradient of POC-flux to the seafloor at the CCZ (Smith et al., 2008b; Veillette et al., 2007). However, local environmental factors presumably regulated by local geomorphology, such as bottom water flows (Mewes et al., 2014), or the availability of nodule (Peukert et al., 2018) and xenophyophore test (this study) substrata may play a key role at the local level, possibly influencing habitat heterogeneity across the CCZ. This complexity needs to be reflected in both local (claim-scale) and regional (CCZ-scale) management plans (Durden et al., 2017a; Levin et al., 2016) and in the design of future monitoring strategies aimed to characterise and preserve biodiversity in the CCZ.

6. Acknowledgements

24

7. References

Aleynik, D., Inall, M.E., Dale, A., Vink, A., 2017. Impact of remotely generated eddies on plume dispersion at abyssal mining sites in the Pacific. *Scientific Reports*, 7, 16959.

Amon, D., Ziegler, A., Drazen, J., Grischenko, A., Leitner, A., Lindsay, D., Voight, J., Wicksten, M., Young, C., Smith, C., 2017. Megafauna of the UKSRL exploration contract area and eastern Clarion-Clipperton Zone in the Pacific Ocean: Annelida, Arthropoda, Bryozoa, Chordata, Ctenophora, Mollusca. *Biodiversity Data Journal*, 5, e14598.

Amon, D.J., Ziegler, A.F., Dahlgren, T.G., Glover, A.G., Goineau, A., Gooday, A.J., Wiklund, H., Smith, C.R., 2016. Insights into the abundance and diversity of abyssal megafauna in a polymetallic-nodule region in the eastern Clarion-Clipperton Zone. *Sci Rep*, 6, 30492.

Anderson, M.J., 2001. A new method for non-parametric multivariate analysis of variance. *Austral ecology*, 26, 32-46.

Andrew, N., Mapstone, B., 1987. Sampling and the description of spatial pattern in marine ecology. *Oceanography and marine biology*, 25, 39-90.

Beaulieu, S.E., 2001. Life on glass houses: sponge stalk communities in the deep sea. *Marine Biology*, 138, 803-817.

Benoist, N.M., Bett, B.J., Morris, K.J., Ruhl, H.A., submitted. A generalised method to estimate the biomass of photographically surveyed benthic megafauna. *in prep. for Limnology & Oceanography: Methods*.

Billett, D.S.M., Bett, B.J., Rice, A.L., Thurston, M.H., Galéron, J., Sibuet, M., Wolff, G.A., 2001. Long-term change in the megabenthos of the Porcupine Abyssal Plain (NE Atlantic). *Progress in Oceanography*, 50, 325-348.

Blott, S.J., Pye, K., 2001. GRADISTAT: a grain size distribution and statistics package for the analysis of unconsolidated sediments. *Earth Surface Processes and Landforms*, 26, 1237-1248.

Buckland, S.T., Anderson, D.R., Burnham, K.P., Laake, J.L., Borchers, D.L., Thomas, L., 2001. *Introduction to Distance Sampling: Estimating Abundance of Biological Populations*: Oxford University Press.

Buhl-Mortensen, L., Vanreusel, A., Gooday, A.J., Levin, L.A., Priede, I.G., Buhl-Mortensen, P., Gheerardyn, H., King, N.J., Raes, M., 2010. Biological structures as a source of habitat heterogeneity and biodiversity on the deep ocean margins. *Marine Ecology*, 31, 21-50.

Clarke, K.R., 1990. Comparisons of dominance curves. *Journal of Experimental Marine Biology and Ecology*, 138, 143-157.

Clarke, K.R., Gorley, R.N., 2015. *PRIMER v7: User Manual/Tutorial*. PRIMER-E. Plymouth.

Colwell, R., 2013. EstimateS: Statistical estimation of species richness and shared species from samples. Version 9. *User's Guide and Application published at: http://purloclcorg/estimates*.

Colwell, R.K., Chao, A., Gotelli, N.J., Lin, S.Y., Mao, C.X., Chazdon, R.L., Longino, J.T., 2012. Models and estimators linking individual-based and sample-based rarefaction, extrapolation and comparison of assemblages. *Journal of Plant Ecology*, 5, 3-21.

Conrad, O., Bechtel, B., Bock, M., Dietrich, H., Fischer, E., Gerlitz, L., Wehberg, J., Wichmann, V., Böhner, J., 2015. System for Automated Geoscientific Analyses (SAGA) v. 2.1.4. *Geosci. Model Dev.*, 8, 1991-2007.

Cribari-Neto, F., Zeileis, A., 2010. Beta Regression in R. *2010*, 34, 24.

Cummings, J., Menot, L., Gooday, A.J., Arbizu, P.M., Molodtsowa, T., Paterson, G., 2014. Atlas of Abyssal Megafaunal morphotypes of the Clipperton-Clarion Fracture Zone. International Seabed Authority. http://ccfzatlas.com, Access date: 3/3/2017.

Dahlgren, T.G., Wiklund, H., Rabone, M., Amon, D.J., Ikebe, C., Watling, L., Smith, C.R., Glover, A.G., 2016. Abyssal fauna of the UK-1 polymetallic nodule exploration area, Clarion-Clipperton Zone, central Pacific Ocean: Cnidaria. *Biodiversity Data Journal*, e9277.

De Smet, B., Pape, E., Riehl, T., Bonifácio, P., Colson, L., Vanreusel, A., 2017. The Community Structure of Deep-Sea Macrofauna Associated with Polymetallic Nodules in the Eastern Part of the Clarion-Clipperton Fracture Zone. *Frontiers in Marine Science*, 4.

25

Dobson, A.J., Barnett, A.G., 2008. *An Introduction to Generalized Linear Models, Third Edition*. Boca Raton, FL: Chapman & Hall/CRC Press.

Durden, J.M., Bett, B.J., Jones, D.O.B., Huvenne, V.A.I., Ruhl, H.A., 2015. Abyssal hills – hidden source of increased habitat heterogeneity, benthic megafaunal biomass and diversity in the deep sea. *Progress in Oceanography*, 137, 209-218.

Durden, J.M., Bett, B.J., Schoening, T., Morris, K.J., Nattkemper, T.W., Ruhl, H.A., 2016a. Comparison of image annotation data generated by multiple investigators for benthic ecology. *Marine Ecology Progress Series*, 552, 61-70.

Durden, J.M., Murphy, K., Jaeckel, A., Van Dover, C.L., Christiansen, S., Gjerde, K., Ortega, A., Jones, D.O.B., 2017a. A procedural framework for robust environmental management of deep-sea mining projects using a conceptual model. *Marine Policy*, 84, 193-201.

Durden, J.M., Schoening, T., Althaus, F., Friedman, A., Garcia, R., Glover, A.G., Greinert, J., Jacobsen Stout, N., Jones, D.O.B., Jordt, A., Kaeli, J., Köser, K., Kuhnz, L.A., Lindsay, D., Morris, K.J., Nattkemper, T.W., Osterloff, J., Ruhl, H.A., Singh, H., Tran, M., Bett, B.J., 2016b. Perspectives in visual imaging for marine biology and ecology: from acquisition to understanding. In R.N. Hughes, D.J. Hughes, I.P. Smith, A.C. Dale (Eds.), *Oceanography and Marine Biology: An Annual Review, Vol. 54* (pp. 1-72). Boca Raton, FL: CRC Press.

Durden, J.M., Simon-Lledo, E., Gooday, A.J., Jones, D.O.B., 2017b. Abundance and morphology of Paleodictyon nodosum, observed at the Clarion-Clipperton Zone. *Marine Biodiversity*, 47, 265-269.

Etter, R., Mullineaux, L., 2001. Deep-sea communities. *Marine Community Ecology. Sinauer Associates, Inc., Sunderland*, 367-393.

Ferrari, S., Cribari-Neto, F., 2004. Beta Regression for Modelling Rates and Proportions. *Journal of Applied Statistics*, 31, 799-815.

Fox, J., Weisberg, S., Adler, D., Bates, D., Baud-Bovy, G., Ellison, S., Firth, D., Friendly, M., Gorjanc, G., Graves, S., 2016. Package 'car'.

Frazer, J.Z., Fisk, M.B., 1981. Geological factors related to characteristics of sea-floor manganese nodule deposits. *Deep Sea Research Part A. Oceanographic Research Papers*, 28, 1533-1551.

Freund, R.J., Littell, R.C., 1981. *SAS for linear models: a guide to the ANOVA and GLM procedures*: Sas Institute Cary, North Carolina.

Gage, J.D., Bett, B.J., 2005. Deep-sea benthic sampling. In A. Eleftheriou, A. McIntyre (Eds.), *Methods for the study of marine benthos, 3rd ed* (pp. 273-325): Blackwell Science.

Gardner, W., Mulvey, E.P., Shaw, E.C., 1995. Regression analyses of counts and rates: Poisson, overdispersed Poisson, and negative binomial models. *Psychological bulletin*, 118, 392.

Ginger, M.L., Billett, D.S.M., Mackenzie, K.L., Konstandinos, K., Neto, R.R., K. Boardman, D., Santos, V.L.C.S., Horsfall, I.M., A. Wolff, G., 2001. Organic matter assimilation and selective feeding by holothurians in the deep sea: some observations and comments. *Progress in Oceanography*, 50, 407-421.

Glasby, G., Stoffers, P., Sioulas, A., Thijssen, T., Friedrich, G., 1982. Manganese nodule formation in the Pacific Ocean: a general theory. *Geo-marine letters*, 2, 47-53.

Glover, A., Dahlgren, T., Taboada, S., Paterson, G., Wiklund, H., Waeschenbach, A., Cobley, A., Martínez, P., Kaiser, S., Schnurr, S., Khodami, S., Raschka, U., Kersken, D., Stuckas, H., Menot, L., Bonifacio, P., Vanreusel, A., Macheriotou, L., Cunha, M., Hilário, A., Rodrigues, C., Colaço, A., Ribeiro, P., Błażewicz, M., Gooday, A., Jones, D., Billett, D., Goineau, A., Amon, D., Smith, C., Patel, T., McQuaid, K., Spickermann, R., Brager, S., 2016a. The London Workshop on the Biogeography and Connectivity of the Clarion-Clipperton Zone. *Research Ideas and Outcomes*, 2, e10528.

Glover, A., Dahlgren, T., Wiklund, H., Mohrbeck, I., Smith, C., 2015. An End-to-End DNA Taxonomy Methodology for Benthic Biodiversity Survey in the Clarion-Clipperton Zone, Central Pacific Abyss. *Journal of Marine Science and Engineering*, 4, 2.

Glover, A.G., Smith, C.R., 2003. The deep-sea floor ecosystem: current status and prospects of anthropogenic change by the year 2025. *Environmental Conservation*, 30, 219-241.

Glover, A.G., Wiklund, H., Rabone, M., Amon, D.J., Smith, C.R., O'Hara, T., Mah, C.L., Dahlgren, T.G., 2016b. Abyssal fauna of the UK-1 polymetallic nodule exploration claim, Clarion-Clipperton Zone, central Pacific Ocean: Echinodermata. *Biodiversity Data Journal*, e7251.

Gooday, A.J., Bett, B.J., Pratt, D.N., 1993. Direct observation of episodic growth in an abyssal xenophyophore (Protista). *Deep Sea Research Part I: Oceanographic Research Papers*, 40, 2131-2143.

Gooday, A.J., Holzmann, M., Caulle, C., Goineau, A., Jones, D.O.B., Kamenskaya, O., Simon-Lledó, E., Weber, A.A.T., Pawlowski, J., 2017a. New species of the xenophyophore genus Aschemonella (Rhizaria: Foraminifera) from areas of the abyssal eastern Pacific licensed for polymetallic nodule exploration. *Zoological Journal of the Linnean Society*, zlx052-zlx052.

Gooday, A.J., Holzmann, M., Caulle, C., Goineau, A., Kamenskaya, O., Weber, A.A.T., Pawlowski, J., 2017b. Giant protists (xenophyophores, Foraminifera) are exceptionally diverse in parts of the abyssal eastern Pacific licensed for polymetallic nodule exploration. *Biological Conservation*, 207, 106-116.

Grassle, J.F., Maciolek, N.J., 1992. Deep-Sea Species Richness: Regional and Local Diversity Estimates from Quantitative Bottom Samples. *The American Naturalist*, 139, 313-341.

Harris, P.T., Macmillan-Lawler, M., Rupp, J., Baker, E.K., 2014. Geomorphology of the oceans. *Marine Geology*, 352, 4-24.

Heck Jr, K.L., van Belle, G., Simberloff, D., 1975. Explicit calculation of the rarefaction diversity measurement and the determination of sufficient sample size. *Ecology*, 1459-1461.

Hothorn, T., Bretz, F., Westfall, P., 2008. Simultaneous Inference in General Parametric Models. *Biometrical Journal*, 50, 346-363.

Hughes, J.A., Gooday, A.J., 2004. Associations between living benthic foraminifera and dead tests of Syringammina fragilissima (Xenophyophorea) in the Darwin Mounds region (NE Atlantic). *Deep Sea Research Part I: Oceanographic Research Papers*, 51, 1741-1758.

Iken, K., Brey, T., Wand, U., Voigt, J., Junghans, P., 2001. Food web structure of the benthic community at the Porcupine Abyssal Plain (NE Atlantic): a stable isotope analysis. *Progress in Oceanography*, 50, 383-405.

International Seabed Authority, 2010. Development of geological models for the Clarion Clipperton Zone polymetallic nodule deposits. *ISA technical studies*, 6.

International Seabed Authority, 2012. Decision of the Council relating to an environmental management plan for the Clarion-Clipperton Zone. ISBA/18/C/22. Kingston, Jamaica.

Jones, D.O.B., 2015. RRS James Cook Cruise JC120 15 Apr-19 May 2015. Manzanillo to Manzanillo, Mexico. Managing Impacts of Deep-seA resource exploitation (MIDAS): Clarion-Clipperton Zone North Eastern Area of Particular Environmental Interest.

Jones, D.O.B., Kaiser, S., Sweetman, A.K., Smith, C.R., Menot, L., Vink, A., Trueblood, D., Greinert, J., Billett, D.S., Arbizu, P.M., Radziejewska, T., Singh, R., Ingole, B., Stratmann, T., Simon-Lledo, E., Durden, J.M., Clark, M.R., 2017. Biological responses to disturbance from simulated deep-sea polymetallic nodule mining. *PLoS One*, 12, e0171750.

Jost, L., 2006. Entropy and diversity. *Oikos*, 113, 363-375.

Jung, H.-S., Ko, Y.-T., Chi, S.-B., Moon, J.-W., 2001. Characteristics of Seafloor Morphology and Ferromanganese Nodule Occurrence in the Korea Deep-sea Environmental Study (KODES) Area, NE Equatorial Pacific. *Marine Georesources & Geotechnology*, 19, 167-180.

Kamenskaya, O.E., Melnik, V.F., Gooday, A.J., 2013. Giant protists (xenophyophores and komokiaceans) from the Clarion-Clipperton ferromanganese nodule field (eastern Pacific). *Biology Bulletin Reviews*, 3, 388-398.

Khripounoff, A., Caprais, J.-C., Crassous, P., Etoubleau, J., 2006. Geochemical and biological recovery of the disturbed seafloor in polymetallic nodule fields of the Clipperton-Clarion Fracture Zone (CCFZ) at 5,000-m depth. *Limnology and Oceanography*, 51, 2033-2041.

Klitgord, K.D., Mammerickx, J., 1982. Northern East Pacific Rise: magnetic anomaly and bathymetric framework. *Journal of Geophysical Research: Solid Earth*, 87, 6725-6750.

27

Krumbein, W.C., 1936. Application of logarithmic moments to size frequency distributions of sediments. *Journal of Sedimentary Research*, 6.

Lampitt, R.S., 1985. Evidence for the seasonal deposition of detritus to the deep-sea floor and its subsequent resuspension. *Deep Sea Research Part A. Oceanographic Research Papers*, 32, 885-897.

Langenkämper, D., Zurowietz, M., Schoening, T., Nattkemper, T.W., 2017. BIIGLE 2.0 - Browsing and Annotating Large Marine Image Collections. *Frontiers in Marine Science*, 4.

Laureillard, J., xe, janelle, L., Sibuet, M., 2004. Use of lipids to study the trophic ecology of deep-sea xenophyophores. *Marine Ecology Progress Series*, 270, 129-140.

Leitner, A.B., Neuheimer, A.B., Donlon, E., Smith, C.R., Drazen, J.C., 2017. Environmental and bathymetric influences on abyssal bait-attending communities of the Clarion Clipperton Zone. *Deep Sea Research Part I: Oceanographic Research Papers*, 125, 65-80.

Levin, L.A., 1991. Interactions Between Metazoans and Large, Agglutinating Protozoans: Implications for the Community Structure of Deep-Sea Benthos1. *American Zoologist*, 31, 886-900.

Levin, L.A., Demaster, D.J., McCann, L.D., Thomas, C.L., 1986. Effects of giant protozoans (Class Xenophyophorea) on deep-seamount benthos. *Marine Ecology-Progress Series*, 29, 99-104.

Levin, L.A., Etter, R.J., Rex, M.A., Gooday, A.J., Smith, C.R., Pineda, J., Stuart, C.T., Hessler, R.R., Pawson, D., 2001. Environmental influences on regional deep-sea species diversity. *Annual Review of Ecology and Systematics*, 51-93.

Levin, L.A., Gooday, A.J., 1992. Possible Roles for Xenophyophores in Deep-Sea Carbon Cycling. In G.T. Rowe, V. Pariente (Eds.), *Deep-Sea Food Chains and the Global Carbon Cycle* (pp. 93-104). Dordrecht: Springer Netherlands.

Levin, L.A., Mengerink, K., Gjerde, K.M., Rowden, A.A., Van Dover, C.L., Clark, M.R., Ramirez-Llodra, E., Currie, B., Smith, C.R., Sato, K.N., Gallo, N., Sweetman, A.K., Lily, H., Armstrong, C.W., Brider, J., 2016. Defining "serious harm" to the marine environment in the context of deep-seabed mining. *Marine Policy*, 74, 245-259.

Levin, L.A., Thomas, C.L., 1988. The ecology of xenophyophores (Protista) on eastern Pacific seamounts. *Deep Sea Research Part A. Oceanographic Research Papers*, 35, 2003-2027.

Lim, S.-C., Wiklund, H., Glover, A.G., Dahlgren, T.G., Tan, K.-S., 2017. A new genus and species of abyssal sponge commonly encrusting polymetallic nodules in the Clarion-Clipperton Zone, East Pacific Ocean. *Systematics and Biodiversity*, 15, 507-519.

Lodge, M., Johnson, D., Le Gurun, G., Wengler, M., Weaver, P., Gunn, V., 2014. Seabed mining: International Seabed Authority environmental management plan for the Clarion–Clipperton Zone. A partnership approach. *Marine Policy*, 49, 66-72.

Lutz, M.J., Caldeira, K., Dunbar, R.B., Behrenfeld, M.J., 2007. Seasonal rhythms of net primary production and particulate organic carbon flux to depth describe the efficiency of biological pump in the global ocean. *Journal of Geophysical Research*, 112.

Magurran, A.E., 2004. *Measuring biological diversity*: Blackwell Science Ltd., Blackwell Publishing (2004).

Margolis, S.V., Burns, R.G., 1976. Pacific Deep-Sea Manganese Nodules: Their Distribution, Composition, and Origin. *Annual Review of Earth and Planetary Sciences*, 4, 229-263.

Mewes, K., Mogollón, J.M., Picard, A., Rühlemann, C., Kuhn, T., Nöthen, K., Kasten, S., 2014. Impact of depositional and biogeochemical processes on small scale variations in nodule abundance in the Clarion-Clipperton Fracture Zone. *Deep Sea Research Part I: Oceanographic Research Papers*, 91, 125-141.

Morris, K.J., Bett, B.J., Durden, J.M., Benoist, N.M., Huvenne, V.A., Jones, D.O., Robert, K., Ichino, M.C., Wolff, G.A., Ruhl, H.A., 2016. Landscape-scale spatial heterogeneity in phytodetrital cover and megafauna biomass in the abyss links to modest topographic variation. *Sci Rep*, 6, 34080.

Morris, K.J., Bett, B.J., Durden, J.M., Huvenne, V.A.I., Milligan, R., Jones, D.O.B., McPhail, S., Robert, K., Bailey, D.M., Ruhl, H.A., 2014. A new method for ecological surveying of the abyss using autonomous underwater vehicle photography. *Limnology and Oceanography: Methods*, 12, 795-809.

Nasr-Azadani, M., Meiburg, E., 2014. Turbidity currents interacting with three-dimensional seafloor topography. *Journal of Fluid Mechanics*, 745, 409-443.

Oksanen, J., Kindt, R., Legendre, P., O'Hara, B., Stevens, M.H.H., Oksanen, M.J., Suggests, M., 2007. The vegan package. *Community ecology package*, 10.

Olive, J.-A., Behn, M.D., Ito, G., Buck, W.R., Escartín, J., Howell, S., 2015. Sensitivity of seafloor bathymetry to climate-driven fluctuations in mid-ocean ridge magma supply. *science*, 350, 310-313.

Pape, E., Bezerra, T.N., Hauquier, F., Vanreusel, A., 2017. Limited Spatial and Temporal Variability in Meiofauna and Nematode Communities at Distant but Environmentally Similar Sites in an Area of Interest for Deep-Sea Mining. *Frontiers in Marine Science*, 4.

Peukert, A., Schoening, T., Alevizos, E., Köser, K., Kwasnitschka, T., Greinert, J., 2018. Understanding Mn-nodule distribution and evaluation of related deep-sea mining impacts using AUV-based hydroacoustic and optical data. *Biogeosciences*, 15, 2525-2549.

Purser, A., Marcon, Y., Hoving, H.T., Vecchione, M., Piatkowski, U., Eason, D., Bluhm, H., Boetius, A., 2016. Association of deep-sea incirrate octopods with manganese crusts and nodule fields in the Pacific Ocean. *Curr Biol*, 26, R1268-R1269.

Pushcharovsky, Y.M., 2006. Tectonic types of the Pacific abyssal basins. *Geotectonics*, 40, 345-356.

R Core Team, 2017. R: A language and environment for statistical computing. Vienna, Austria: R Foundation for Statistical Computing.

Radziejewska, T., 2014. Characteristics of the Sub-equatorial North-Eastern Pacific Ocean's Abyss, with a Particular Reference to the Clarion-Clipperton Fracture Zone. *Meiobenthos in the Sub-equatorial Pacific Abyss: A Proxy in Anthropogenic Impact Evaluation* (pp. 13-28). Berlin, Heidelberg: Springer.

Ramirez-Llodra, E., Brandt, A., Danovaro, R., De Mol, B., Escobar, E., German, C.R., Levin, L.A., Martinez Arbizu, P., Menot, L., Buhl-Mortensen, P., Narayanaswamy, B.E., Smith, C.R., Tittensor, D.P., Tyler, P.A., Vanreusel, A., Vecchione, M., 2010. Deep, diverse and definitely different: unique attributes of the world's largest ecosystem. *Biogeosciences*, 7, 2851-2899.

Rex, M.A., Etter, R.J., Morris, J.S., Crouse, J., McClain, C.R., Johnson, N.A., Stuart, C.T., Deming, J.W., Thies, R., Avery, R., 2006. Global bathymetric patterns of standing stock and body size in the deep-sea benthos. *Marine Ecology Progress Series*, 317, 1-8.

Ruhl, H.A., Ellena, J.A., Smith, K.L., 2008. Connections between climate, food limitation, and carbon cycling in abyssal sediment communities. *Proceedings of the National Academy of Sciences*, 105, 17006-17011.

Schneck, F., Melo, A.S., 2010. Reliable sample sizes for estimating similarity among macroinvertebrate assemblages in tropical streams. *Annales de Limnologie - International Journal of Limnology*, 46, 93-100.

Schoening, T., Jones, D.O.B., Greinert, J., 2017. Compact-Morphology-based poly-metallic Nodule Delineation. *Scientific Reports*, 7.

Skornyakova, N.S., Murdmaa, I.O., 1992. Local variations in distribution and composition of ferromanganese nodules in the Clarion-Clipperton Nodule Province. *Marine Geology*, 103, 381-405.

Smith, C.R., De Leo, F.C., Bernardino, A.F., Sweetman, A.K., Arbizu, P.M., 2008a. Abyssal food limitation, ecosystem structure and climate change. *Trends Ecol Evol*, 23, 518-528.

Smith, C.R., Demopoulos, A.W.J., 2003. Ecology of the deep Pacific Ocean floor. In P.A. Tyler (Ed.), *Ecosystems of the World: Ecosystems of the Deep Ocean*, Vol. 28 (pp. 179-218). Amsterdam, the Netherlands: Elsevier.

Smith, C.R., Drazen, J., Mincks, S.L., 2006. Deep-sea biodiversity and biogeography: Perspectives from the abyss. *International Seabed Authority Seamount Biodiversity Symposium*.

Smith, C.R., Gaines, S., Friedlander, A., Morgan, C., Thurnherr, A., Mincks, S., Watling, L., Rogers, A., Clark, M., Baco-Taylor, A., 2008b. Preservation reference areas for nodule mining in the clarion-clipperton zone: rationale and recommendations to the International Seabed Authority. *Manoa*.

Smith, C.R., Hoover, D.J., Doan, S.E., Pope, R.H., Demaster, D.J., Dobbs, F.C., Altabet, M.A., 1996. Phytodetritus at the abyssal seafloor across 10° of latitude in the central equatorial Pacific. *Deep Sea Research Part II: Topical Studies in Oceanography*, 43, 1309-1338.

Soetaert, K., Heip, C., 1990. Sample-size dependence of diversity indices and the determination of sufficient sample size in a high-diversity deep-sea environment. *Marine Ecology Progress Series*, 59, 305-307.

Stefanoudis, P.V., Bett, B.J., Gooday, A.J., 2016. Abyssal hills: Influence of topography on benthic foraminiferal assemblages. *Progress in Oceanography*, 148, 44-55.

Stoyanova, V., 2012. Megafaunal Diversity Associated with Deep-sea Nodule-bearing Habitats in the Eastern Part of the Clarion-Clipperton Zone, NE Pacific. *International Multidisciplinary Scientific GeoConference: SGEM: Surveying Geology & mining Ecology Management*; *Sofia.*, 1, 645-651.

Strindberg, S., Buckland, S.T., 2004. Zigzag survey designs in line transect sampling. *Journal of Agricultural, Biological, and Environmental Statistics*, 9, 443-461.

Tews, J., Brose, U., Grimm, V., Tielbörger, K., Wichmann, M.C., Schwager, M., Jeltsch, F., 2004. Animal species diversity driven by habitat heterogeneity/diversity: the importance of keystone structures. *Journal of Biogeography*, 31, 79-92.

Thistle, D., Ertman, S.C., Fauchald, K., 1991. The fauna of the HEBBLE site: patterns in standing stock and sediment-dynamic effects. *Marine Geology*, 99, 413-422.

Thistle, D., Yingst, J.Y., Fauchald, K., 1985. A deep-sea benthic community exposed to strong near-bottom currents on the Scotian Rise (western Atlantic). *Marine Geology*, 66, 91-112.

Tilot, V., Ormond, R., Moreno Navas, J., Catalá, T.S., 2018. The Benthic Megafaunal Assemblages of the CCZ (Eastern Pacific) and an Approach to their Management in the Face of Threatened Anthropogenic Impacts. *Frontiers in Marine Science*, 5.

Van Dover, C.L., Ardron, J.A., Escobar, E., Gianni, M., Gjerde, K.M., Jaeckel, A., Jones, D.O.B., Levin, L.A., Niner, H.J., Pendleton, L., Smith, C.R., Thiele, T., Turner, P.J., Watling, L., Weaver, P.P.E., 2017. Biodiversity loss from deep-sea mining. *Nature Geoscience*, 10, 464.

Vangriesheim, A., Springer, B., Crassous, P., 2001. Temporal variability of near-bottom particle resuspension and dynamics at the Porcupine Abyssal Plain, Northeast Atlantic. *Progress in Oceanography*, 50, 123-145.

Vanreusel, A., Hilario, A., Ribeiro, P.A., Menot, L., Arbizu, P.M., 2016. Threatened by mining, polymetallic nodules are required to preserve abyssal epifauna. *Sci Rep*, 6, 26808.

Veillette, J., Sarrazin, J., Gooday, A.J., Galéron, J., Caprais, J.-C., Vangriesheim, A., Étoubleau, J., Christian, J.R., Kim Juniper, S., 2007. Ferromanganese nodule fauna in the Tropical North Pacific Ocean: Species richness, faunal cover and spatial distribution. *Deep Sea Research Part I: Oceanographic Research Papers*, 54, 1912-1935.

Wang, C., Lu, D., 2002. Application of deep ocean photo and video tow system in deep-sea megafaunal studies. *China Ocean Press*, 14, 74-81.

Wedding, L., Reiter, S., Smith, C., Gjerde, K., Kittinger, J., Friedlander, A., Gaines, S., Clark, M., Thurnherr, A., Hardy, S., 2015. Managing mining of the deep seabed. *science*, 349, 144-145.

Weiss, A., 2001. Topographic position and landforms analysis. *21st Annual ESRI User Conference*. San Diego, CA.

Wilson, M.F., O'Connell, B., Brown, C., Guinan, J.C., Grehan, A.J., 2007. Multiscale terrain analysis of multibeam bathymetry data for habitat mapping on the continental slope. *Marine Geodesy*, 30, 3-35.

Yamamuro, M., Kayanne, H., 1995. Rapid direct determination of organic carbon and nitrogen in carbonate-bearing sediments with a Yanaco MT-5 CHN analyzer. *Limnology and Oceanography*, 40, 1001-1005.

1771
1772
1773
1774
1775
1776
1777
1778
1779
1780
1781
1782
1783
1784
1785
1786
1787
1788
1789
1790
1791
1792
1793
1794
1795
1796
1797
1798
1799
1800
1801
1802
1803
1804
1805
1806
1807
1808
1809
1810
1811
1812
1813
1814
1815
1816
1817
1818
1819
1820
1821
1822
1823
1824
1825
1826
1827
1828
1829

31

Supplementary material: Appendix A

Table A.1. Summary metadata for each sampling unit analysed during the present study. Coordinates (latitude, longitude; in decimal degrees) indicate the central position of each sampling unit. Images (n) are the total number of images processed per transect. Average percentage of polymetallic nodule coverage (± St Dev) was calculated as the mean of the percentage coverages values obtained for each transect image using the CoMoNoD algorithm. Visual annotations: Total abundance of fauna (total counts >10 mm), total morphospecies richness, and percentage of fauna detected on hard substratum (OHS), separated into metazoan and xenophyophore taxa. Landscape types: FL= Flat, RI= Ridge, TR=Trough

Sampling unit	Centre latitude (°)	Centre longitude (°)	Images (n)	Seafloor area (m^2)	Nodule cover (%)	Metazoa			Xenophyophores		
						Abundance	Taxa	OHS (%)	Abundance	Taxa	OHS (%)
FL 3	17.262	-123.072	774	1322	12.3 (± 3.2)	745	68	75	1722	18	49
FL 33	17.233	-123.027	775	1321	5.4 (± 1.2)	532	76	72	2952	18	58
FL 26	17.225	-123.013	781	1323	10.5 (± 4.0)	634	71	72	2749	18	55
FL 39	17.217	-123.001	778	1321	12.4 (± 5.6)	677	67	56	4365	19	59
RI 2	17.282	-122.878	720	1324	9.1 (± 8.0)	537	63	65	5687	20	36
RI 9	17.297	-122.883	729	1322	5.5 (± 2.1)	552	67	61	4731	20	28
RI 15	17.310	-122.888	666	1323	3.6 (± 1.1)	629	59	47	4508	19	39
RI 21	17.323	-122.891	765	1321	6.2 (± 7.5)	720	70	69	6379	20	30
TR 15	17.264	-122.830	694	1324	1.7 (± 1.4)	382	54	60	1202	18	26
TR 18	17.248	-122.821	555	1322	8.0 (± 3.4)	506	72	43	4217	18	52
TR 25	17.223	-122.817	709	1324	3.2 (± 2.3)	546	65	67	1237	19	45
TR 29	17.220	-122.820	623	1323	1.8 (± 1.9)	280	47	56	419	18	37

32

Fig. A.1. Sediment grain-size distributions plots generated for different sediment horizons sampled at the APEI6 seafloor. Lines representing mean frequency across each of the five replicate megacore samples collected per landscape type. Shadowed areas representing maximum and minimum values per replicate set. Each core was initially sliced and split into nine different sediment depths (0-5, 5-10, 10-15, 15-20, 20-30, 30-50, 50-100, 100-150, and 150-200 mm). Sediment grain-size distributions at each horizon were measured independently by laser diffraction. Horizons 0-5, 5-10, 10-15, 15-20, 20-30, 30-50 were averaged into a 0-50 mm depth.
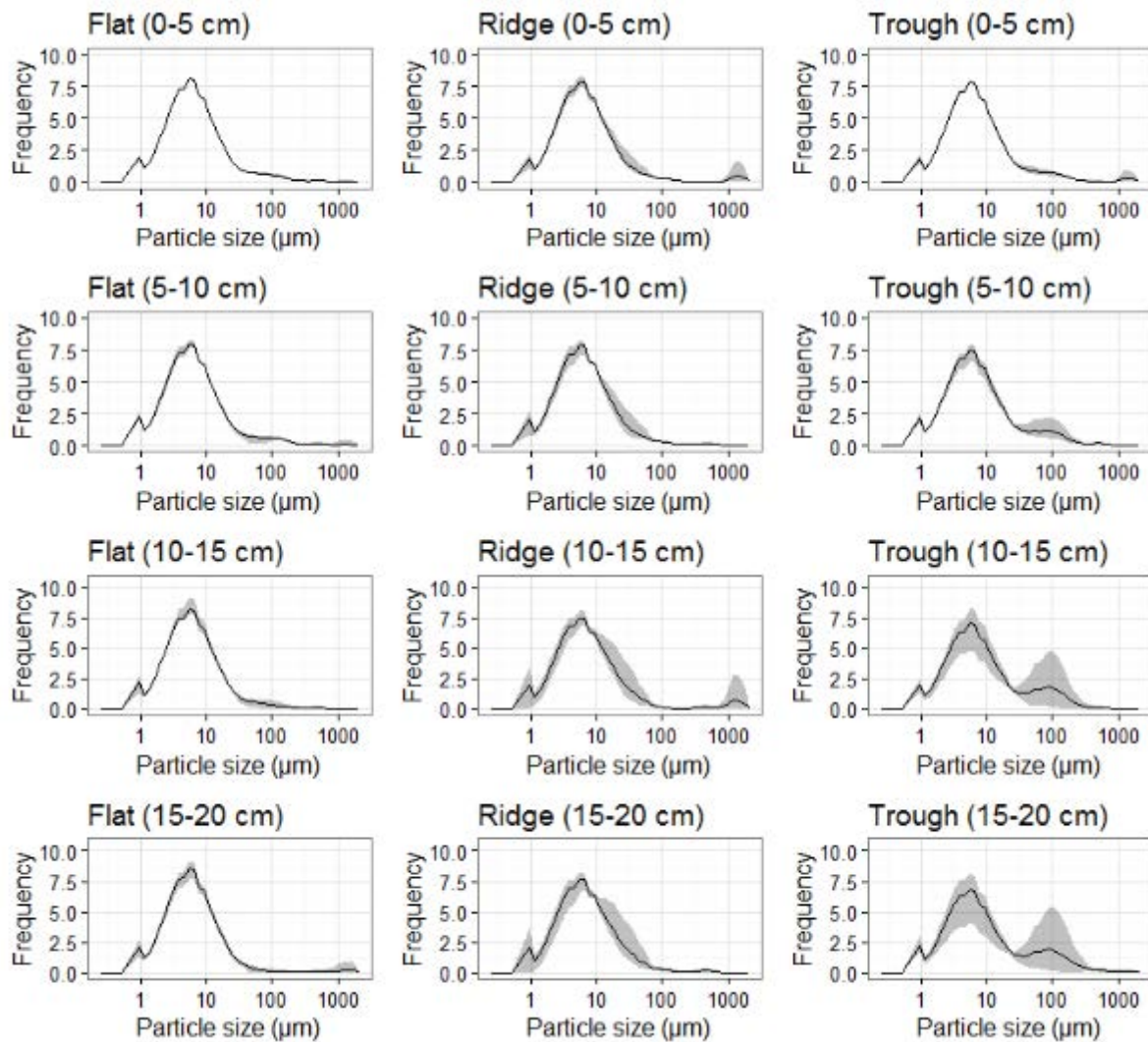
Table A.2. Particle size statistics calculated applying a geometric method of moments for different sediment horizons sampled at the APEI6 seafloor. Values representing maximum and minimum ranges across each of the five replicate megacore samples collected per landscape type. Each core was initially sliced and split into nine different sediment depths (0-5, 5-10, 10-15, 15-20, 20-30, 30-50, 50-100, 100-150, and 150-200 mm). Sediment grain-size distributions at each horizon were measured independently by laser diffraction. Horizons 0-5, 5-10, 10-15, 15-20, 20-30, 30-50 were averaged into a 0-50 mm depth, prior to the statistical processing.

Horizon	Statistic	Flat	Ridge	Trough
0 to 5 cm	Mean	7.15 - 7.61	6.71 - 9.21	7.60 - 8.50
	St dev	2.82 - 3.03	2.54 - 4.77	2.99 - 4.04
	Skewness	0.96 - 1.50	0.46 - 2.02	0.86 - 1.86
	Kurtosis	4.50 - 7.35	3.22 - 8.29	3.79 - 7.50
	Mode	7.19	7.19	7.19
	D_{50}	6.47 - 6.70	6.29 - 7.40	6.61 - 7.03
5 to 10 cm	Mean	6.50 - 8.52	6.56 - 8.72	7.49 - 11.16
	St dev	2.73 - 3.66	2.71 - 2.78	2.95 - 3.97
	Skewness	0.89 - 1.56	0.46 - 1.15	0.67 - 1.07
	Kurtosis	4.18 - 6.60	3.20 - 5.82	2.73 - 5.20
	Mode	7.19	7.19	7.19
	D_{50}	5.97 - 6.89	5.98 - 7.95	6.63 - 8.17
10 to 15 cm	Mean	6.06 - 7.24	6.33 - 11.67	6.47 - 20.08
	St dev	2.10 - 3.00	2.43 - 6.73	2.48 - 4.72
	Skewness	0.06 - 1.08	0.12 - 1.64	0.06 - 0.90
	Kurtosis	2.75 - 5.02	2.34 - 6.26	1.79 - 6.14
	Mode	7.19	7.19	7.19
	D_{50}	6.04 - 6.48	5.87 - 9.50	6.29 - 16.45
15 to 20 cm	Mean	5.77 - 8.55	6.07 - 10.61	6.35 - 20.15
	St dev	2.19 - 4.28	2.50 - 2.94	2.56 - 5.07
	Skewness	0.01 - 1.93	0.13 - 1.18	- 0.14 - 1.85
	Kurtosis	2.59 - 7.50	2.35 - 6.17	1.77 - 8.79
	Mode	7.19	7.19	7.19 - 115.00
	D_{50}	5.69 - 6.63	5.70 - 10.28	5.93 - 31.85

34

1989
1990
1991
1992
1993
1994
1995
1996
1997
1998
1999
2000
2001
2002
2003
2004
2005
2006
2007
2008
2009
2010
2011
2012
2013
2014
2015
2016
2017
2018
2019
2020
2021
2022
2023
2024
2025
2026
2027
2028
2029
2030
2031
2032
2033
2034
2035
2036
2037
2038
2039
2040
2041
2042
2043
2044
2045
2046
2047

Fig. A.2. Morphospecies rarefaction curves extrapolated to ~three times the area sampled at each landscape type for the present study. Triangles showing the total size of the sample analysed at each geomorphology. Expected richness with sample coverages of 15,000 m² show a lower richness at the Trough (~107 msp) compared to the Flat (~130 msp) and the Ridge (~134 msp) areas, but confidence intervals continued to overlap between curves. Whole geomorphological units sample size (5280 m²) covered 85-90% of the expected richness > 15,000 m².
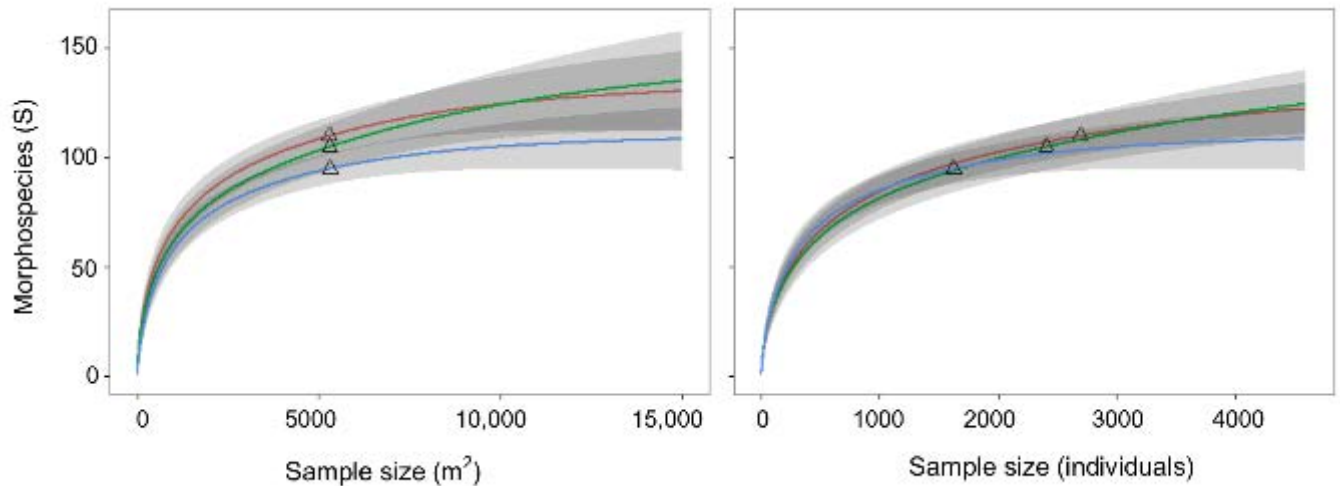
Fig. A.3. Metazoan morphospecies surveyed for the present study. Venn diagram showing the total number of metazoan taxa shared between each combination of landscape types of the APEI6. *In brackets*: singleton morphospecies.

35

2048
2049
2050
2051
2052
2053
2054
2055

Fig. A.4. Variations of the coefficient of variatio36n with increasing sample size calculated for the main ecological estimators used in the present study. Coefficients of variation were calculated as the standard deviation divided by the mean of each estimator at each different sampling effort (see methods), for2 the whole metazoan dataset collected for each landscape type of the APEI6.

2107
2108
2109
2110
2111
2112
2113
2114

Fig. A.5. Relative variations of the coefficient of variation with increasing sample size calculated for the main ecological estimators used in the present study. Coefficients of variation were calculated as the standard deviation divided by the mean of each estimator at each different sampling effort (see methods), for the whole metazoan dataset collected for each landscape type of the APEI6, and then divided by the minimum value exhibited in each along the sample size spectrum assessed.